

AUS Repository

Durability of Mortar and Epoxy Bonded Galvanized Steel Mesh Sheets to Concrete Surfaces

| | |
|---------------|---|
| Item Type | Thesis |
| Authors | Douier, Kais Aiman |
| Download date | 2026-03-16 05:19:43 |
| Link to Item | http://hdl.handle.net/11073/16435 |

DURABILITY OF MORTAR AND EPOXY BONDED GALVANIZED STEEL MESH
SHEETS TO CONCRETE SURFACES

by

Kais Aiman Douier

A Thesis Presented to the Faculty of the
American University of Sharjah
College of Engineering
in Partial Fulfillment
of the Requirements
for the Degree of
Master of Science in
Civil Engineering

Sharjah, United Arab Emirates

April 2019

Approval Signatures

We, the undersigned, approve the Master's Thesis of Kais Aiman Douier

Thesis Title: Durability of Mortar and Epoxy Bonded Galvanized Steel Mesh Sheets to Concrete Surfaces

Signature

Date of Signature

(dd/mm/yyyy)

Dr. Rami Haweeleh
Professor, Department of Civil Engineering
Thesis Advisor

Dr. Jamal Abdalla
Professor, Department of Civil Engineering
Thesis Co-Advisor

Dr. Mousa Attom
Professor, Department of Civil Engineering
Thesis Committee Member

Dr. Wael Abuzaid
Assistant Professor, Department of Mechanical Engineering
Thesis Committee Member

Dr. Irtishad U. Ahmad
Head, Department of Civil Engineering

Dr. Lotfi Romdhane
Associate Dean for Graduate Affairs and Research
College of Engineering

Dr. Naif Darwish
Acting Dean, College of Engineering

Dr. Mohamed El-Tarhuni
Vice Provost for Graduate Studies

Acknowledgment

I would like to express my gratitude and respect to my life and thesis advisors Dr. Rami Haweeleh and Dr. Jamal Abdalla, for their guidance and support throughout the entire period of working under their supervision. Moreover, I would like to extend a special thanks to Mr. Arshi Faridi, Mr. Waleed Nawaz, and Mr. Mohammad Ansari, for taking the time and putting in the effort to aid me in conducting all the lab tests needed to complete this thesis. I would also like to thank the American University of Sharjah for providing me a teaching assistantship during my graduate studies.

Dedication

This thesis is dedicated to my loving and supporting family that pushed me through the pain to achieve excellence.

Abstract

Over the last few decades, fiber-reinforced polymer (FRP) sheets and plates have been extensively used as external strengthening materials and proved to be quite effective in enhancing the flexure and shear strength of reinforced concrete (RC) beams. Recently, galvanized steel mesh (GSM) composite sheets have emerged as a promising strengthening material due to its desirable mechanical properties and light-weight. However, very limited studies have been conducted to investigate the durability of bond behavior of GSM sheets to concrete surfaces, especially when subjected to harsh environments. Therefore, the main aim of this study is to investigate the bond behavior of GSM sheets attached externally to concrete surfaces via epoxy adhesive (SME) or cement-based mortar (SMM). Both systems were subjected to sun light and saline water exposures for up to a 12 months period. This study will examine the degradation of flexural and bond strength in RC beams, flexural bond prisms, mechanical properties of coupon laminates, and single-lap shear pullout specimens strengthened with both systems. The test results showed that RC beams strengthened with SME laminates achieved an initial increase of 55% in its load carrying capacity and retained 99 and 95% of its strength after 360 days of saline water and sun light exposures, respectively. However, RC beams strengthened with SMM laminates achieved an initial increase of 50% in its load carrying capacity and retained 71 and 74% of its strength after 360 days of exposure in saline water and sun light, respectively. Thus, it could be concluded that SME strengthening system is the best strengthening system that experienced the least degradation in both exposures when compared with SMM strengthening systems. The outcomes from this research will aid in developing environmental factors (C_E) for each exposure and test method that could be used in the design and analysis of externally bonded RC beams in the UAE and countries with similar harsh environmental exposures.

Search Terms: Galvanized Steel Mesh (GSM), Carbon Fiber Reinforced Polymer (CFRP), Bond Behavior, RC beams, Durability.

Table of Contents

| | |
|--|----|
| Abstract | 6 |
| List of Figures | 10 |
| List of Tables | 13 |
| Chapter 1: Introduction | 15 |
| 1.1 Research Objectives | 17 |
| 1.2 Research Significance | 17 |
| Chapter 2: Literature Review | 19 |
| 2.1 Externally-Bonded Reinforcement (EBR) | 19 |
| 2.2 Carbon Fiber Reinforced Polymer (CFRP) | 19 |
| 2.3 Galvanized Steel Mesh (GSM) | 19 |
| 2.4 Durability Study | 22 |
| 2.4.1 Sun exposure..... | 22 |
| 2.4.2 Saline water exposure..... | 23 |
| 2.5 Testing Methods | 23 |
| 2.5.1 Reinforce concert (RC) beams. | 24 |
| 2.5.2 Small notched prisms..... | 24 |
| 2.4.3 Single-Lap shear tests..... | 25 |
| 2.5.4 Coupons test method. | 26 |
| 2.6 Polymers and adhesives | 27 |
| 2.6.1 Epoxy adhesive..... | 27 |
| 2.6.2 Cement-based mortar..... | 28 |
| Chapter 3: Experimental program..... | 29 |
| 3.1 Experimental Program..... | 29 |
| 3.2 Exposure Setup..... | 29 |
| 3.2.1 Lab exposure..... | 29 |
| 3.2.2 Sun exposure..... | 30 |

| | |
|--|----|
| 3.2.3. Saline water exposure..... | 30 |
| 3.3 Test Specimens And Setup..... | 31 |
| 3.3.1. Specimen designation..... | 31 |
| 3.3.1. Reinforced concrete specimens..... | 31 |
| 3.3.2. Coupons..... | 35 |
| 3.3.3. Flexural bond small prism..... | 36 |
| 3.3.4. Single-Lap shear prism..... | 37 |
| 3.4 Analytical Environmental Model (C_E)..... | 39 |
| 3.5 Materials Properties..... | 41 |
| 3.5.1. Concrete..... | 41 |
| 3.5.2. Steel..... | 42 |
| 3.5.3. Galvanized Steel Mesh..... | 42 |
| 3.5.4. Epoxy adhesive..... | 43 |
| 3.5.5. Cement-Based mortar..... | 44 |
| 3.5.6. CFRP sheet..... | 44 |
| 3.5.7. CFRP epoxy adhesive..... | 45 |
| 3.6 Analytical Prediction..... | 45 |
| 3.7 Form Work..... | 47 |
| 3.8 Material Installations..... | 48 |
| 3.8.1. Surface preparation..... | 48 |
| 3.8.2. SMM installation..... | 48 |
| 3.8.3. SME installation..... | 49 |
| 3.8.4. CFRP installation..... | 49 |
| Chapter 4: Experimental Results and Discussion..... | 51 |
| 4.1. RC Beams Control Un-Exposed Group..... | 51 |
| 4.2. RC Beams 180 Days Exposed Group..... | 54 |
| 4.2.1. RC beams after 180 days of saline exposure..... | 54 |

| | |
|--|-----|
| 4.2.2. RC beams after 180 days of sun exposure..... | 57 |
| 4.3. RC Beams 360 Days Exposed Group | 60 |
| 4.3.1. RC beams after 360 days of saline exposure..... | 60 |
| 4.3.2. RC beams after 360 days of sun exposure..... | 63 |
| 4.4. RC Beams Degradation..... | 66 |
| 4.4.1. RC beams ESR/LSR degradation model..... | 68 |
| 4.4.2. RC beams R_n degradation model..... | 69 |
| 4.4.3. RC beams R_b degradation model..... | 71 |
| 4.4.4. CFRP RC beams sun light exposure..... | 72 |
| 4.4.5. CFRP beams saline water exposure..... | 73 |
| 4.4.6. SME RC beams sun light exposure | 73 |
| 4.4.7. SME RC beams saline water exposure..... | 74 |
| 4.4.8. SMM RC beams sun light exposure..... | 74 |
| 4.4.9. SMM RC beams saline water exposure..... | 75 |
| 4.5. Flexure Prisms Results | 75 |
| 4.6. Coupon Results | 79 |
| 4.7. Pullout Results..... | 83 |
| 4.8. Proposed Environmental Factor for U.A.E. Harsh Environments | 86 |
| Chapter 5: Summary and conclusion | 88 |
| References..... | 90 |
| Appendix..... | 95 |
| Vita..... | 101 |

List of Figures

| | |
|---|----|
| Figure 1: Steel Chord [40] | 20 |
| Figure 2: Low-Density Galvanized Steel Mesh [41] | 20 |
| Figure 3: Medium-Density Galvanized Steel Mesh [41]..... | 20 |
| Figure 4: High-Density Galvanized Steel Mesh [41] | 21 |
| Figure 5: Sample RC beam | 24 |
| Figure 6: Sample flexural prism | 25 |
| Figure 7: Sample single-lap shear specimen..... | 26 |
| Figure 8: (a) epoxy SME coupon specimen, (b) mortar SMM coupon specimen | 27 |
| Figure 9: Lab Exposure..... | 29 |
| Figure 10: Sun Exposure..... | 30 |
| Figure 11: Saline water exposure..... | 30 |
| Figure 12: Specimen designation example | 31 |
| Figure 13: RC beam longitudinal view | 32 |
| Figure 14: Cross-sectional view of control RC beam..... | 33 |
| Figure 15: Control RC beams loading map | 33 |
| Figure 16: Strengthened RC beam loading map | 34 |
| Figure 17: (a) Cross section of CFRP strengthened RC beam, (b) Cross section of GSM strengthened RC beam | 34 |
| Figure 18: Sample coupons..... | 36 |
| Figure 19: Small beam longitudinal and cross-sectional view | 37 |
| Figure 20: Single-Lap shear prism..... | 38 |
| Figure 21: Sample expected strength for sun-exposed specimens..... | 39 |
| Figure 22: Sample expected strength for saline-exposed specimens..... | 39 |
| Figure 23: Stress-strain diagram [27] | 46 |
| Figure 24: Form Work | 48 |
| Figure 25: Surface grinding of RC beams | 48 |
| Figure 26: SMM installation..... | 49 |
| Figure 27: SME installation | 49 |
| Figure 28: CFRP installation | 50 |
| Figure 29: Summary results of load-deflection curve response for control un-exposed RC beams..... | 52 |

| | |
|---|----|
| Figure 30: Summary results of load-deflection curve response for RC beams after 180 days of saline exposure | 55 |
| Figure 31: Summary results of load-deflection curve response for RC beams after 180 days of sun exposure | 58 |
| Figure 32: Summary results of the load-deflection curve response for RC beams after 360 days of saline exposure | 61 |
| Figure 33: Summary results of the load-deflection curve response for RC beams after 360 days of sun exposure | 64 |
| Figure 34: Bar Graph of RC beams ESR/LSR degradation model..... | 68 |
| Figure 35: Line Chart of RC beams ESR/LSR degradation model | 69 |
| Figure 36: Bar Graph of RC beams Rn degradation model..... | 70 |
| Figure 37: Line Chart of RC beams Rn degradation model | 70 |
| Figure 38: Bar Graph of RC beams Rb degradation model..... | 71 |
| Figure 39: Line Chart of RC beams Rb degradation model | 72 |
| Figure 40: CFRP RC beams exposed to direct sun light | 72 |
| Figure 41: CFRP RC beams exposed to saline water | 73 |
| Figure 42: SME RC beams exposed to direct sun light | 73 |
| Figure 43: SME RC beams exposed to saline water..... | 74 |
| Figure 44: SMM RC beams exposed to direct sun light..... | 74 |
| Figure 45: SMM RC beams exposed to saline water..... | 75 |
| Figure 46: Bar graph of flexure prism RP degradation model..... | 77 |
| Figure 47: Line chart of flexure prism RP degradation model | 77 |
| Figure 48: Bar graph of coupon RC degradation model..... | 81 |
| Figure 49: Line chart of coupon RC degradation model | 81 |
| Figure 50: Bar graph of pullout RPO degradation model..... | 85 |
| Figure 51: Line chart of pullout RPO degradation model | 85 |
| Figure 52: Bar graph of CFRP RC beams in saline exposure..... | 95 |
| Figure 53: Line graph of CFRP RC beams in saline exposure | 95 |
| Figure 54: Bar graph of CFRP RC beams in sun exposure | 96 |
| Figure 55: Line graph of CFRP RC beams in sun exposure..... | 96 |
| Figure 56: Bar graph of SME RC beams in saline exposure | 97 |
| Figure 57: Line graph of SME RC beams in saline exposure..... | 97 |
| Figure 58: Bar graph of SME RC beams in sun exposure..... | 98 |

| | |
|--|-----|
| Figure 59: Line graph of SME RC beams in sun exposure | 98 |
| Figure 60: Bar graph of SMM RC beams in saline exposure | 99 |
| Figure 61: Line graph of SMM RC beams in saline exposure | 99 |
| Figure 62: Bar graph of SMM RC beams in sun exposure..... | 100 |
| Figure 63: Line graph of SMM RC beams in sun exposure | 100 |

List of Tables

| | |
|--|----|
| Table 1: Specimen designation summary | 31 |
| Table 2: RC. beams specimen designation | 32 |
| Table 3: Coupons specimen designation..... | 35 |
| Table 4: Flexure prism specimen designation | 36 |
| Table 5: Single-lap shear specimen designation | 38 |
| Table 6: Compressive strength of cubes and cylinders at 28 days | 41 |
| Table 7: Modulus of rupture for flexure beams | 42 |
| Table 8: Mechanical Properties of steel rebars | 42 |
| Table 9: GSM mechanical properties as reported by manufacturer [29]..... | 43 |
| Table 10: Geopolymer adhesive mechanical properties as reported by manufacturer [66] | 43 |
| Table 11: Cement-based mortar mechanical properties as reported by manufacturer [67]..... | 44 |
| Table 12: CFRP laminate mechanical properties as reported by manufacturer [68] .. | 44 |
| Table 13: V-Wrap 700 epoxy adhesive mechanical properties as reported by manufacturer [69]..... | 45 |
| Table 14: Predicted load carrying capacity..... | 47 |
| Table 15: Summary results of control un-exposed RC beams..... | 51 |
| Table 16: Sample failure mode of control un-exposed RC beams | 53 |
| Table 17: Summary results of RC beams after 180 days of saline exposure..... | 54 |
| Table 18: Sample failure mode of RC beams after 180 days of saline exposure | 56 |
| Table 19: Summary results of RC beams after 180 days of sun exposure | 57 |
| Table 20: Sample failure mode of RC beams after 180 days of sun exposure | 59 |
| Table 21: Summary results of RC beams after 360 days of saline exposure..... | 60 |
| Table 22: Sample failure mode of RC beams after 360 days of saline exposure | 62 |
| Table 23: Summary results of RC beams after 360 days of sun exposure | 63 |
| Table 24: Sample failure mode of RC beams after 360 days of sun exposure | 65 |
| Table 25: RC Beams degradation summary | 66 |
| Table 26: Flexure prism degradation summary | 76 |
| Table 27: Flexure prisms failure mode | 78 |
| Table 28: Coupon degradation summary | 79 |
| Table 29: Coupons failure mode..... | 82 |
| Table 30: Pullout degradation summary | 83 |
| Table 31: Pullout failure mode | 86 |

Table 32: Summary of the specimen's environmental factor87
Table 33: Recommended environmental factor (CE) in the UAE.....87

Chapter 1: Introduction

There has been an increase in the general interest of strengthening reinforced concrete (RC) structures that are deficient in flexural, shear and even torsional load capacities. The deficiency of these RC structures occurs due to deteriorations, oxidation of reinforcement steel, increase in the load on a specific structure, and finally poor maintenance [1-8]. Therefore, researchers proposed fiber reinforced polymers (FRP) laminates to be used as strengthening materials, such as carbon-fiber-reinforced-polymer (CFRP), and galvanized steel mesh (GSM). CFRP and GSM laminate have been used extensively in the past few years as external reinforcements to strengthen RC members such as columns, slabs, beams, and walls in several types of structures like industrial buildings, residential buildings, and bridges. These materials exhibited excellent performance and characteristics in external strengthening deficient RC members. Since both GSM and CFRP increase the load-carrying capacity, they improve the stiffness and strength of RC members [9-17].

Moreover, epoxy adhesive is one of the most commonly used to bond CFRP and GSM sheets to concrete surfaces. However, epoxy can sometimes be considered as a hazardous substance at elevated temperatures, mainly because it is flammable, and it also loses some of its strength turning into a soft polymer when exposed to high temperatures. Another epoxy drawback is that it emits dangerous fumes in the installation process or while combusting, and it cannot be applied as a bonding agent on wet surfaces [18-21]. All these reasons lead to the introduction of a new bonding agent using inorganic cement-based mortar, that can bond a steel fiber mesh to concrete surfaces. Comparison studies show that the cement-based mortar can be used as an adequate substitute of epoxy adhesives in low-density GSM sheets, or in other words, steel-mesh fiber strengthening system [22-30].

Regularly, while using CFRP strengthening systems, epoxy adhesive is used to bond the fibers to both the concrete surfaces and to each other, while the high-strength carbon fiber will mainly carry the tensile load applied on the system. However, attaching CFRP to concrete surfaces using cement mortar as a bonding agent is not practical and efficient, because carbon fiber's density is extremely high with approximately no spacing between the fibers. Therefore, the density of the carbon fibers would prevent the cement mortar bonding agent from penetrating the fibers through the

sheet, causing an early debonding phenomena which can significantly reduce the ultimate strength of the overall externally reinforced polymer system (EBR). However, due to the GSM sheets' low cords density, the system could be utilized with cement mortar as an adhesive in the strengthening system.

Additionally, GSM sheets are made of high strength galvanized cords, with a tensile strength greater than 2800 MPa, which are made of five high strength galvanized micro wires. Three of the wires are straight while the remaining two are wrapped around the three straight wires with a high torque angle, and these galvanized steel chords are attached to fiberglass micro mesh for installation purposes [31]. Generally, the GSM sheets are available in three different types that differ in their chord density. High-density steel mesh contains a chord density of 7.87 cords/cm, a medium density steel mesh contains 4.72 cords/cm, and the low-density steel mesh have a chord density of 3.15 cords/cm. Due to their high densities, both high and medium density steel mesh are attached to concrete surfaces with epoxy adhesive. Thus, cement-based mortar can be used to attach the low-density GSM sheets with a density of 3.15 cords/cm to concrete surfaces.

However, there is a gap in the literature on the performance and durability of GSM sheets that are attached with epoxy adhesive and cement-based mortar as bonding agents to RC beams in order to increase their flexural strength under harsh environmental exposures in UAE and similar GCC countries. But the CFRP external strengthening system starts showing degradation in its strength and performance when exposed to harsh environmental factors, such as humidity, extreme temperatures, saline water, ultraviolet radiations from the sun, and chemical exposures like chloride and alkaline [32,31].

The study is directed toward comparing the bond performance, strength, and behavior of low-density GSM sheets with a cord density of 3.15 cords/cm bonded by epoxy adhesive (SME) or cement-based mortar (SMM) and exposed to harsh environmental factors such as saline water and ultraviolet radiations from the sun. The extensive research conducted examined tensile single-lap shear pullout, flexural bond prisms, tensile coupon laminates, and finally RC beam specimens. Some of these specimens were externally strengthened with GSM sheets bonded with either mortar or epoxy adhesive. There are three exposures to be considered in this research: The first

is a lab-controlled environment simulating the control interior exposure, the second will take place in a saline water tank that simulates sea water, while the last exposure will be a sun exposure simulating an exterior exposure to ultraviolet radiations. The exposure periods will extend up to 12 months. The results of the tests will quantify the effect of exposure to different environmental elements in UAE on bond performance, and it will calculate the environmental factor (C_E) for each exposure and test method. Those environment factors could be used in line of ACI 440.2R-17 [34,35] guidelines to analyze and design strengthened RC members when subjected to UAE environmental exposures. The outcomes of this research project will improve the knowledge in this field area and will propose a set of recommendations on the usage of GSM composite sheets in strengthening RC members in UAE and similar GCC countries.

1.1 Research Objectives

The overall objective of this research is to investigate the bond behavior and durability of externally strengthened RC beams in flexure by using GSM sheets bonded with either cement-based mortar or epoxy adhesives and exposed to UAE harsh environments. The main objectives are:

1. To examine the practicality of utilizing GSM sheets as external strengthening materials bonded with either epoxy or mortar, when exposed to different sets of environmental exposures.
2. To examine the degradation in mechanical properties of GSM sheets such as the modulus of elasticity and tensile strength of laminates.
3. To examine the degradation in ductility, bond strength, and flexural strength of RC beams strengthened with both SME and SMM systems.
4. To compare the bond performance of SME and SMM systems with that of CFRP system when exposed to harsh environments.
5. To observe the different modes of failure for both SME and SMM strengthening systems exposed to harsh environments.

1.2. Research Significance

There is a lack of knowledge on the durability of externally strengthened RC beams with SME and SMM systems, especially when exposed to UAE harsh environment. Accordingly, the significance of this study is to acquire environmental

factors (C_E) of both strengthening systems for different test methods and environmental conditions. The results of this investigation could be implemented in strengthening design codes, such as ACI 440-2R-17 [34].

Chapter 2: Literature Review

A summary of several studies concerning CFRP, GSM, durability, and different testing methods will be reviewed and focused on in this section.

2.1. Externally-Bonded Reinforcement (EBR)

Steel and concrete structures could be strengthened using externally-bonded reinforcement (EBR) such as CFRP sheet, plates, or by using FRP near-surface mounting (NSM) rods [36]. Thus, developing new strengthening materials was the objective of many researchers and engineers. Their research aided in the development of carbon fiber reinforced polymer (CFRP) sheets. This composite material is unidirectional, which aids in strengthening RC and steel structures in shear and flexure.

2.2. Carbon Fiber Reinforced Polymer (CFRP)

CFRP materials are also used instead of steel cables, because of their low oxidation properties, but because carbon fiber's transverse properties have a significantly lower modulus of elasticity and strength relative to their longitudinal properties and it is very difficult to anchor them [37].

Tibhe and Rathi [38] conducted a study that examined the flexure strength of RC beams strengthened with CFRP sheets and plates. The study concluded that CFRP sheets and plates could be used to increase the moment capacity of an RC beams in the range from 40.0% to 101.8%.

Hosen et al. [39] have carried out an experiment that tested seven reinforced concrete beams. The CFRP laminates enhanced the flexure performance of RC beams, by increasing the RC beams' stiffness, ductility, and energy absorption capacity.

2.3. Galvanized Steel Mesh (GSM)

Another strengthening material utilized in externally bonded reinforcement systems is galvanized steel mesh (GSM). Five steel wires are used to form one steel cord, three wires of which are straight and the remaining two are twisted around them in a high torque angle as shown in Figure 1. The steel wires are coated with zinc or brass to protect against oxidation. When the wires are coated with zinc it's called galvanization [40].

GSM sheets are generally divided into three groups high, medium, and low-density steel mesh as shown in Figures 2-4 respectively. The density of the steel mesh is reported as cords per centimeter (cord/cm) [41].



Figure 1: Steel Chord [40]



Figure 2: Low-Density Galvanized Steel Mesh [41]



Figure 3: Medium-Density Galvanized Steel Mesh [41]



Figure 4: High-Density Galvanized Steel Mesh [41]

Galvanized steel mesh can be used to increase the flexure and shear capacity of RC beams in a similar fashion to CFRP systems. Moreover, the steel mesh can achieve the load-carrying capacity of RC beams up to 300%, and if GSM are installed with anchorage as a shear externally reinforced system it may increase the RC beam's shear capacity up to 200% [34]. Although steel reinforced polymer (SRP) systems such as GSM are slightly weaker than CFRP, their failure strain is higher than that of CFRP systems. Thus, the deflection and ductility of RC beams strengthened by GSM are greater than RC beams strengthened by CFRP [42].

Moreover, GSM sheets may be installed with mortar or epoxy separately or as a combined system. Napoli and Realfonzo [43] conducted a study to investigate the flexural performance of RC slabs strengthened with different SRP systems. The study tested 10 RC slabs strengthened by SRP system bonded with epoxy and steel reinforced grout system (SRG) bonded with the inorganic matrix. Their research concluded that SRP externally strengthening systems increased the flexural strength of slabs in a range from 27% to 106% when compared to the control un-strengthened slab.

According to Hawileh et al. [44], a study was conducted to test two types of Hardwire Steel-Fiber (HSF) sheets with different cord densities. The medium HSF cord density was 4.72 cord/cm, while the high HSF cord density was 7.87 cords/cm. seven RC beams were cast and strengthened with HSF using epoxy as an adhesive. Moreover, four-point bending tests were conducted to record the load-deflection response. However, the study showed that the high-density HSF strengthened specimens

increased their load-carrying capacity by 62% when compared to the control un-strengthened RC beam. While the medium density HSF strengthened specimens increased their load-carrying capacity by 29% when compared to the control un-strengthened specimens.

2.4. Durability Study

According to Ray and Rathore [45], the observation of systems behavior under harsh environment is called a durability study. In their research, the behavior of GSM sheet bonded with mortar and epoxy adhesives subjected to ultra-violet light (sun exposure) and saline water exposure was monitored over periods of time. The strengthening system's matrix, polymer, fiber, and interface/interphase may be degraded due to the harsh environment, and their rate and behavior of degradation depend on the type of environment presented.

2.4.1. Sun exposure. Sun exposure or ultra-violet (UV) radiation exposure is an important subject to research since some of the EBR systems are installed on the exterior face of a structure which may encounter sun exposure. The UV radiation energy is equivalent to the bond energy in the strengthening system, and UV wave length is between 290 and 400 nm [46]. Hydrogen abstractions are caused by UV exposure, resulting in free radicals. These free radicals and other reactions can cause lower molecular weights, loss of bearing capacities, and brittleness [47].

However, the EBR system starts degrading at its outer surface that is exposed to UV light. If the UV light only penetrates the outer surface, no major degradation will be observed but surface discoloration. If the UV light penetrates the outer surface and reaches the fiber mass, it may cause a degradation in the properties of the strengthening system [48].

Time of exposure and thickness of the system play a major role in the degradation process. It has been found that the degradation in the mechanical properties is highly dependent on the time of exposure to UV radiations and specimen thickness. A study of Kevlar 49 laminates under UV light radiation shows that a specimen of 0.13 mm thickness is affected by the radiation, and it retained 60% of its strength after 1000 hour of exposure, while specimen with a thickness of 0.25 mm and 0.5 mm didn't get affected by UV exposure and no degradation was observed [49]. Another study was conducted by exposing specimen for 14 years in an outdoor moderate climate to observe the mechanical degradation by subjecting the specimens to two tests pull-off, and peel

tests. The study concluded that the pull-off strength decreased by a range of 64 to 76% after 14 years. But it was still adequate adhesive properties, and the failure mode of the control specimen as well as the exposed specimen were similar and failed by substrate failure [50].

2.4.2. Saline water exposure. Another type of harsh environment exposure is sea water exposure or saline water exposure. The specimens are placed under saline water for periods of time to observe EBR system degradation and the effect of oxidation and rust on the specimens' overall strength. The degradation of EBR systems exposed to saline water occurs due to many reasons, such as diffusion through adhesives, or by absorption through pores deficiencies. The system may begin degrading once the water penetrates the interface. There are two types of degradation, the first happens when the adhesive itself degrades, while the second happens when the interface of adhesive degrades [51].

Nguyen et al. [46] conducted a study to observe the mechanical properties of steel and CFRP joints exposed to sea water at 20 °C and 50 °C for a duration of one year. In this study, specimens are exposed to a cyclic temperature with a high level of humidity up to 1000 hours. Moreover, the study concluded that specimens exposed to sea water showed a significant reduction in their overall stiffness and strength after 1 year of exposure, while those exposed to cyclic temperature and humidity reported a little reduction in their overall stiffness and strength after 1000 hour of exposure.

Another study conducted by Borrie et al. [52] to test the degradation of CFRP systems after being exposed to saline water, which contains 5% NaCl by weight. The exposure lasted up to 6 months at different thermal conditions, and with a static tensile sustained load. After the specimens were fatigue loaded, they encountered a static tensile loading till failure. The study concluded that more than 50% of the specimens tested observed a minimum of 10% decrease in their overall strength, while sheet laminate specimens observed a reduction in the range from 20% to 28% of their strength.

2.5. Testing Methods

There are many different testing methods that are differentiated through casting and manufacturing of different types of specimens. The variation of testing methods is due to that different aspect of load, strain, and stress capacity that needs to be observed.

Some of these methods are RC beams, small notched prisms, pull-out single shear prisms, and tensile coupon specimens.

2.5.1. Reinforce concert (RC) beams. Strengthened RC beam is usually tested to measure the flexural and shear strength of a system. Many of the studies mentioned before used RC beams as their test specimen. However, due to the large scale of this test, the results may vary slightly.

The fabrication of RC beams to fail in a certain mode plays a major role in a study conducted by Li. [53]. Also, the loading rate of the beam should be studied to give adequate results. When the loading rate for the RC specimen increase, the bearing capacity increases, the ductility decrease, and the stiffness decreases as well. However, the loading rate doesn't affect the failure mode, but it affects the distribution of cracks. The preferred loading rate for this test method is 2 mm/min.



Figure 5: Sample RC Beam

2.5.2. Small notched prisms. Small notched prisms, shown in Figure 6, or some time called small beam bond test is a simpler and cheaper method to test the bond behavior of EBR systems bonded to concrete surfaces. This method is mainly used to test the flexural capacity of a strengthening system and its debonding behavior. The preferred loading rate for this test method is 0.25 mm/min (0.01 in/min) [54].

There are many reasons for developing this method [54]:

1. To measure and evaluate the durability of EBR systems bond to concrete surfaces.
2. This method can yield more consistent results compared to large RC beams and single-lap pull out shear tests.

3. The test procedure is simpler and easier to perform.
4. To provide qualified results that can be understood easily.
5. To produce many replicated specimens and conduct larger studies in a more cost-efficient technique.



Figure 6: Sample Flexural Prism

2.4.3. Single-Lap shear tests. This testing method, shown in Figure 7, mainly used to evaluate the bond strength between the strengthening system and the concrete surface. The pull-out testing method is widely used in other studies [55,56] to measure the bond shear strength of EBR systems. However, this testing method needs extreme caution when preparing the specimen to be tested. It needs a certain setup that should be mounted on a tensile testing machine, and if the setup is slightly loose the results will vary significantly due to slip phenomena [55].

A comparison study was conducted to observe the difference between single-lap and double-lap shear tests. This study concluded that up until the peak load or when both sheets are still attached in the double-lap shear setup, both the single-lap and double-lap shear tests yielded similar results because load redistribution of the double-lap shear test was consistent with that of single-lap shear tests [56].

Another study was conducted to account for the eccentricity formed when using the single-lap shear test instead of double lap-shear test. Even though single-lap shear tests are easier to perform but the eccentricity that forms in the system may be a cause in varying test results of similar specimens. However, the study concluded that the

eccentricity effect is almost negligible when the bond length of strengthening material is stretched more than the effective bond length [56].

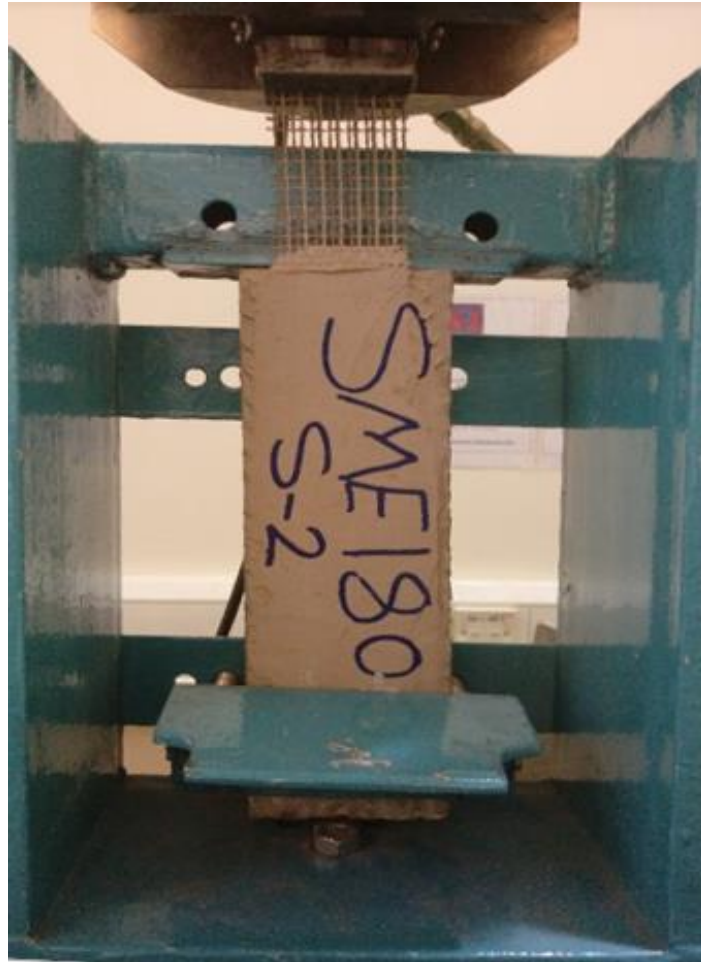


Figure 7: Sample Single-Lap Shear Specimen

2.5.4 Coupons test method. Coupon specimen, shown in Figure 8, is mainly used to calculate Yong's Modulus or modulus of elasticity. However, due to some inconsistent coupon fabrication and testing procedures, a variation in lab results may occur which may lead to inaccurate results. Thus, a study was conducted to uniform the testing procedure so that it minimizes result variance. The study recommends using the slope of the linear portion with stress intervals for different materials to determine Young's modulus, and it also recommends the use of AutoCAD and geometric equations to calculate the cross-sectional area of curved coupons [57].

One of the most important mechanical property is Young's Modulus. However, there are many different methods to calculate Young's modulus, and because these methods vary slightly, the results obtained are expected to vary [58].

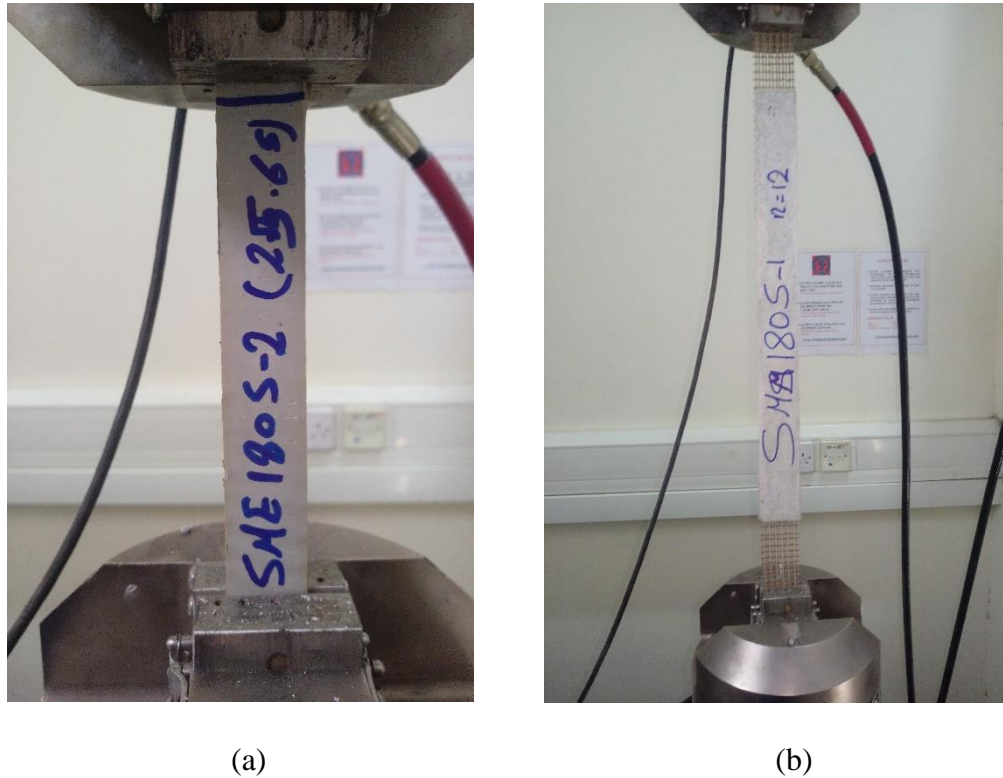


Figure 8: (a) Epoxy SME Coupon Specimen, (b) Mortar SMM Coupon Specimen

2.6. Polymers and Adhesives

The contact interface between concrete surfaces and strengthening sheets play a major role in the ultimate strength of EPR systems, due to debonding phenomena. This debonding phenomena is caused by reaching the ultimate shear stress of a strengthening system. Debonding will results in different failure mods such as adhesive failure, cohesive failure, and cover separation. Where adhesive failure occurs when the strengthening system detaches smoothly from its targeted concrete surface of contact, while cohesive failure occurs when the strengthening system detaches in a violent behavior taking some pieces of the concrete surface with it [59].

2.6.1. Epoxy adhesive. One of the most common adhesives used to bond FRP and GSM sheets to concrete surfaces is epoxy adhesive. It forms a strong bond with

concrete surfaces that can withstand large amount of shear stress. However, the strength of EBR systems depends majorly on the strength of the system's bond, and thus it depends majorly on the ability of epoxy to penetrate and wet the substrate [60]. Elevated levels of moisture content can affect the mechanical properties of the bond negatively, which can lead to a change in failure mode from cohesive failure to adhesive failure [61].

Moreover, epoxy adhesives are efficient bonding agents in NSM strengthening methods. On the other hand, the degradation of mechanical properties at high temperatures, toxic fumes, and flammability are disadvantages related to epoxy adhesives [62].

2.6.2. Cement-based mortar. Because epoxy adhesives struggle to withstand the load at high temperature, and the emission of toxic fumes in the installation process, cement mortar is considered as an adequate substitute to epoxy based adhesives. A study was conducted to measure the efficiency and compatibility of cementitious adhesive bond behavior, and to discover the advantages of NSM technique, and the study concluded that cement mortar adhesive used in NSM techniques is efficient and has a stronger bond than externally bonded CFRP systems [63].

Another study was conducted by Al-Abdwais [64] to measure the strength of the bond between the FRP and concrete surfaces at elevated temperature using mortar and epoxy adhesives. The study concluded that the performance of cementitious mortar is 1.8 times better than the performance of epoxy adhesives. Moreover, cement-based mortar exhibited strength at high temperatures reaching up to 255 °C, while epoxy-based adhesive failed at a temperature of 140 °C. Epoxy based adhesive's failure mode at high temperatures was due to slippage from softening of the adhesive, which results in an earlier loss of bond strength.

Although the mentioned literature summarizes bond strength and durability of GSM sheets. However, it also clearly shows the lack of knowledge in bond durability of GSM sheets bonded with mortar (SMM) or epoxy (SME), that are exposed to harsh environments in the UAE.

Chapter 3: Experimental program

3.1. Experimental Program

The specimens in this are divided into three groups of strengthening systems, GSM sheets bonded with epoxy (SME), GSM sheets bonded with mortar (SMM), and carbon fiber reinforced polymers (bonded with epoxy only). All experiments were conducted in three stages; the first stage of tests was conducted before exposure to serve as a benchmark for later comparison. The second group of testing was conducted after 6 months of harsh environmental exposures, such as direct sun light and saline water. Finally, the third group of tests was conducted after 12 months of exposure.

3.2. Exposure Setup

To test the bond durability of CFRP, SMM and SME specimens, the systems were placed in two harsh environmental exposures, ultraviolet radiation (sun exposure) and saline water exposure. The specimens were tested at three-time intervals, before exposure, after 6 months (180 days), and after 1 year (360 days).

3.2.1. Lab exposure. The control specimens are placed in a closed and temperature-controlled lab exposure as shown in Figure 9, so that they can be later compared to other exposures.



Figure 9: Lab Exposure

3.2.2. Sun exposure. The specimens are placed in an open space and oriented in such a way so that the strengthening systems will get the most sun exposure possible, as shown in Figure 10.



Figure 10: Sun Exposure

3.2.3. Saline water exposure. The specimens are placed in a water tank that is filled with saline water with a salt concentration of approximately 3% to mimic the seawater salinity, as shown in Figure 11.



Figure 11: Saline Water Exposure

3.3 Test Specimens and Setup

3.3.1. Specimen designation. All the specimens have been given a specific designation that is explained in Table 1 and Figure 12.

Table 1: Specimen designation summary

| Abb. | Meaning |
|------|--|
| CB | Control Beam (Unstrengthen) |
| C | Carbon Fiber Reinforced Polymer (CFRP) |
| SME | Steel Mesh Epoxy |
| SMM | Steel Mesh Mortar |
| S | Sun |
| W | Saline sea water. |

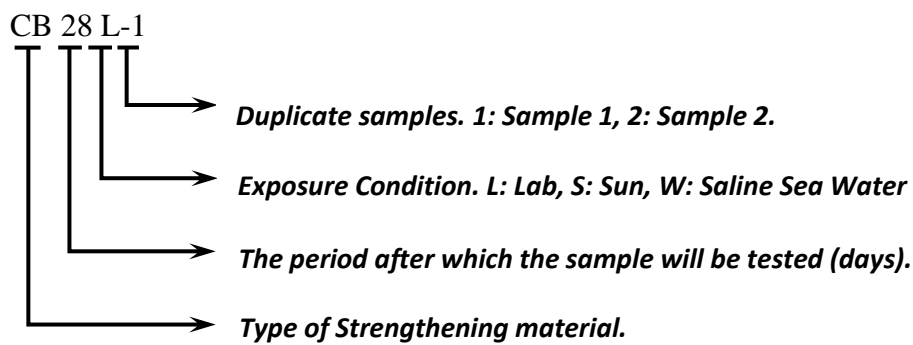


Figure 12: Specimen designation example

3.3.1. Reinforced concrete specimens. A total of 40 reinforced concrete (RC) beams are tested in this study. The 40 RC beams are divided into three strengthening groups, Carbon fiber, SME and SMM and a control group to serve as a benchmark for comparison. Each strengthening group consists of 10 specimens as summarized in the RC beams test matrix shown in Table 2.

Table 2: RC. beams specimen designation

| AUS Experimental Program (40 RC Beams) | | | | | |
|---|------------------------|---------------------|-------------|-------------------------|--------------------------|
| Exposure Condition | Exposure period | Control Beam | CFRP | Steel Mesh Epoxy | Steel Mesh Mortar |
| Laboratory Environment | 28 days | CB28L-1 | C28L-1 | SME28L-1 | SMM28L-1 |
| | | CB28L-2 | C28L-2 | SME28L-2 | SMM28L-2 |
| Direct Sun Light | 180 days | CB180S-1 | C180S-1 | SME180S-1 | SMM180S-1 |
| | | CB180S-2 | C180S-2 | SME180S-2 | SMM180S-2 |
| | 360 days | CB365S-1 | C365S-1 | SME365S-1 | SMM365S-1 |
| | | CB365S-2 | C365S-2 | SME365S-2 | SMM365S-2 |
| Saline Sea Water | 180 days | CB180W-1 | C180W-1 | SME180W-1 | SMM180W-1 |
| | | CB180W-2 | C180W-2 | SME180W-2 | SMM180W-2 |
| | 360 days | CB365W-1 | C365W-1 | SME365W-1 | SMM365W-1 |
| | | CB365W-2 | C365W-2 | SME365W-2 | SMM365W-2 |

These beams are reinforced with 2 \varnothing 8 mm top bars, and 2 \varnothing 12 mm bottom flexural reinforcement bars. Moreover, the beams are also reinforced with \varnothing 8 mm stirrups placed 120 mm center to center. The stirrups distribution and the cross-sectional view of the typical un-strengthened RC beams are shown in Figure 13 and 14, respectively.

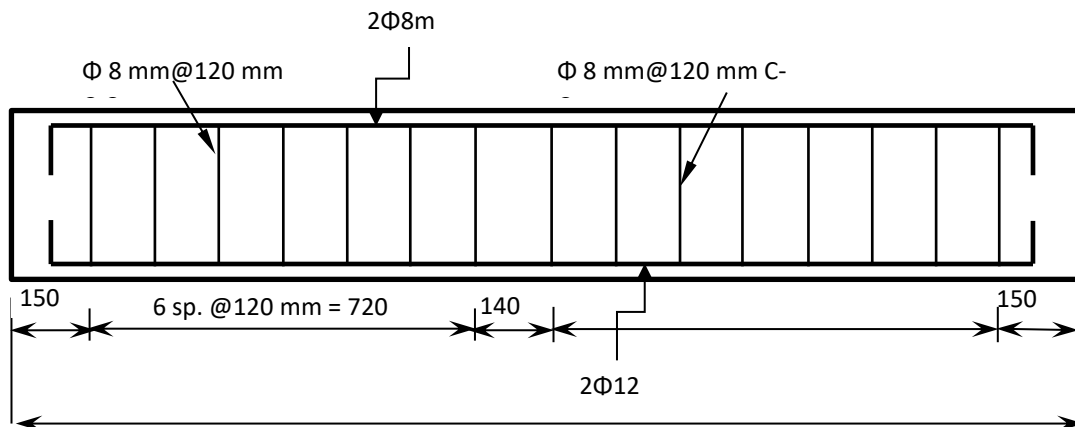


Figure 13: RC beam longitudinal view

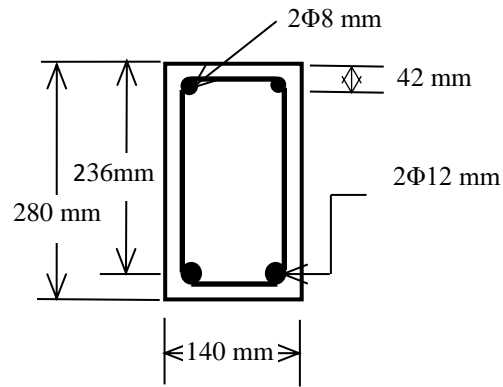


Figure 14: Cross-sectional view of control RC beam

The RC beams are 2000 mm long spanned at 1700 mm while testing and the two loads are placed 250 mm away from mid-span as shown in Figure 15. The four-point bending test will be conducted using the universal test machine (UTM) with a maximum capacity of 2000 kN. The loading rate of testing RC beams is chosen to be 2 mm/min.

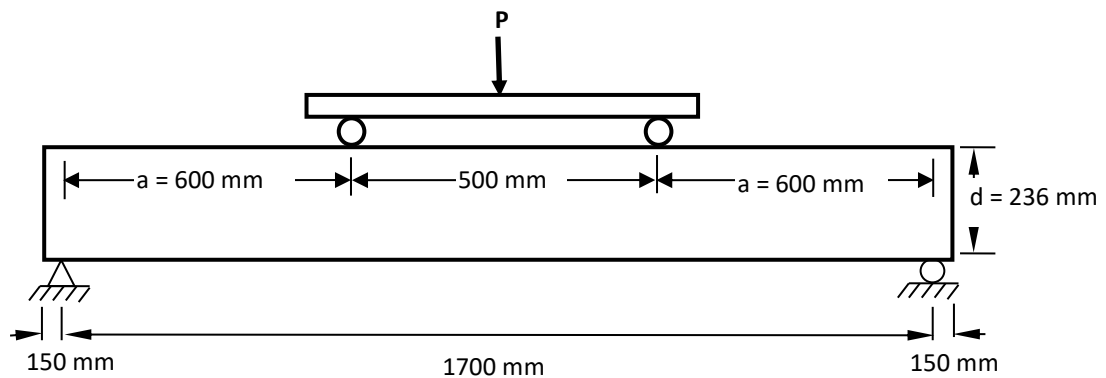


Figure 15: Control RC beams loading map

The specimens (SMM and SME) are spanned over 1600 mm and strengthened with the 2 layers of GSM that are 110 mm wide. While CFRP specimens are strengthened with 1 layer of CFRP that are also 110 mm wide. The loading map and the cross-sectional view of the typically strengthened RC beams are shown in Figures 16 and 17, respectively.

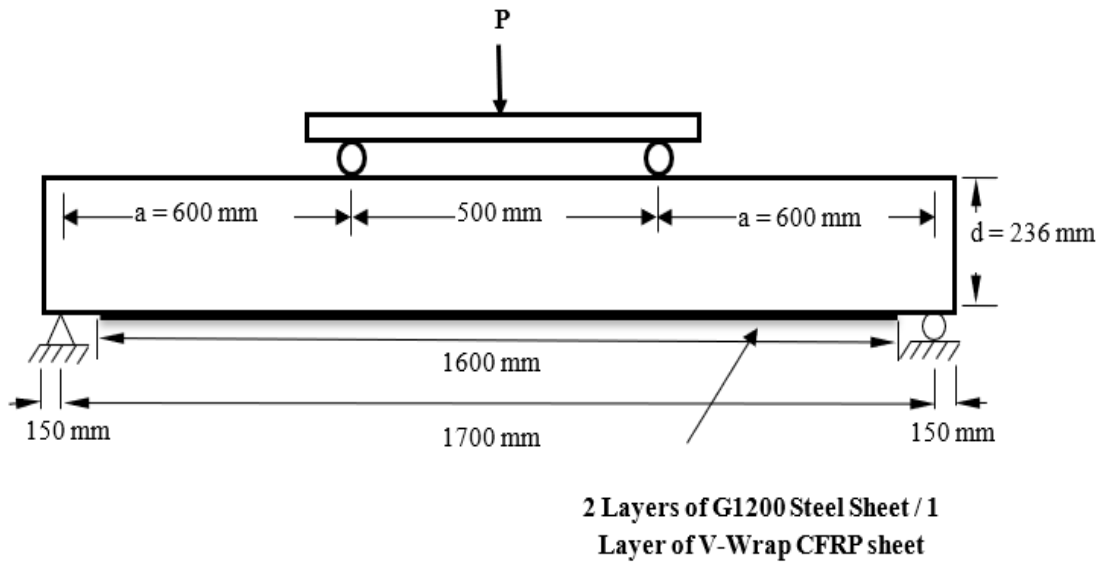


Figure 16: Strengthened RC beam loading map

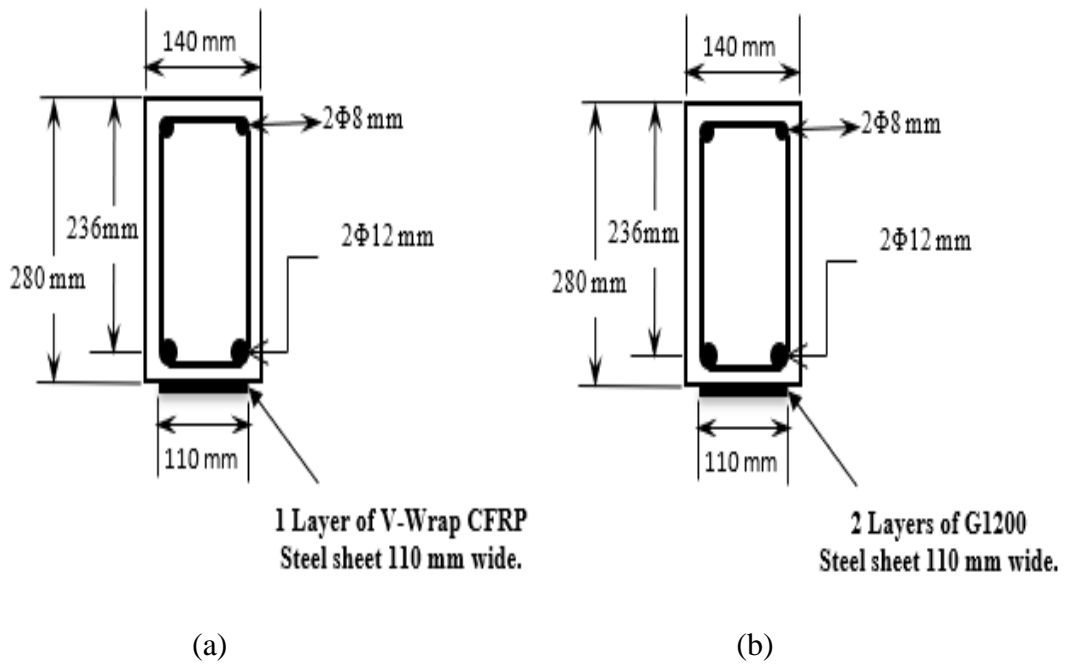


Figure 17: (a) Cross section of CFRP strengthened RC beam, (b) Cross section of GSM strengthened RC beam

3.3.2. Coupons. A total of 30 coupons are tested in this study. The coupons specimens are into three strengthening groups, CFRP, SME, and SMM. Each group of strengthening system consists of 10 specimens as summarized in the coupons test matrix shown in Table 3.

Table 3: Coupons specimen designation

| AUS Experimental Program (30 Coupons) | | | | |
|--|------------------------|-------------|-------------------------------|--------------------------------|
| Exposure Condition | Exposure period | CFRP | Steel Mesh Epoxy (SME) | Steel Mesh Mortar (SMM) |
| Laboratory Environment | 28 days | C28L-1 | SME28L-1 | SMM28L-1 |
| | | C28L-2 | SME28L-2 | SMM28L-2 |
| Direct Sun Light | 180 days | C180S -1 | SME180S -1 | SMM180S -1 |
| | | C180S-2 | SME180S-2 | SMM180S-2 |
| | 360 days | C365S-1 | SME365S-1 | SMM365S-1 |
| | | C365S-2 | SME365S-2 | SMM365S-2 |
| Saline Sea Water | 180 days | C180W-1 | SME180W-1 | SMM180W-1 |
| | | C180W-2 | SME180W-2 | SMM180W-2 |
| | 360 days | C365W-1 | SME365W-1 | SMM365W-1 |
| | | C365W-2 | SME365W-2 | SMM365W-2 |

The CFRP and SME coupons were designed to have an approximate width of 25 mm, total length of 250 mm, gauge length of 150 mm, and thicknesses will vary from 1 to 2.5 mm for CFRP and SME specimens respectively. However, the SMM coupons were manufactured to have a total of 12 galvanized cords. The specimens were tested in a standard tensile testing machine with a loading rate of 2 mm/min according to ASTM D3039 guidelines [65]. Figure 18 shows of CFRP, SME, and SMM coupons before testing.

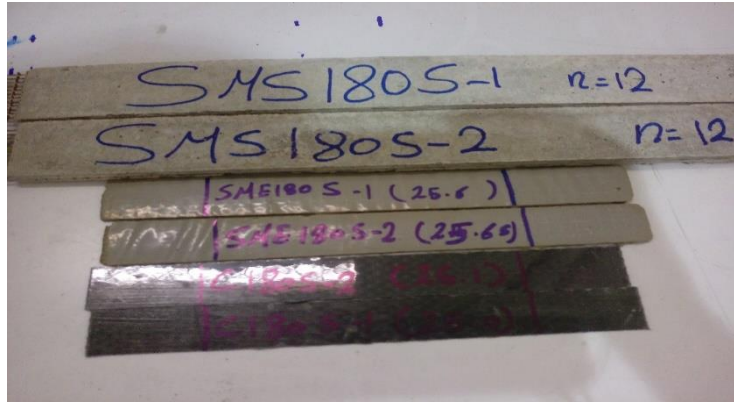


Figure 18: Sample coupons

3.3.3. Flexural bond small prism. A total of 18 flexural bond prisms are tested in this study. The flexural bond specimens were divided into three strengthening groups, CFRP, SME and SMM. Each group of strengthening system consists of 6 specimens that were tested at 28 day and 540 days, as summarized in the flexural prisms test matrix shown in Table 4.

Table 4: Flexure prism specimen designation

| <i>AUS Experimental Program (16 Flexure Prisms)</i> | | | | |
|---|------------------------|-------------|-------------------------------|--------------------------------|
| <i>Exposure Condition</i> | <i>Exposure period</i> | <i>CFRP</i> | <i>Steel Mesh Epoxy (SME)</i> | <i>Steel Mesh Mortar (SMM)</i> |
| <i>Laboratory Environment</i> | 28 days | C28L-1 | SME28L-1 | SMM28L-1 |
| | | C28L-2 | SME28L-2 | SMM28L-2 |
| <i>Direct Sun Light</i> | 540 days | C540S-1 | SME540S-1 | SMM540S-1 |
| | | C540S-2 | SME540S-2 | SMM540S-2 |
| <i>Saline Sea Water</i> | 540 days | C540W-1 | SME540W-1 | SMM540W-1 |
| | | C540W-2 | SME540W-2 | SMM540W-2 |

The flexural bond small prisms are designed to have a cross-sectional dimension of 100 mm by 100 mm, a total length of 500 mm and a free span of 300 mm. It also has a 50 mm deep saw cut with a width of 3 mm located at prism mid-span, as shown in Figure 19. The specimens were tested with a three-point flexural loading test, and with a loading rate of 0.25 mm/min [54]. The shear stress is calculated with the help of Equation (1).

$$\tau = \frac{3*P*L}{5*h*w*S} \quad (1)$$

Where τ is the shear stress to be calculated, P is the failure load obtained from the test, L is the clear span of the specimen (300 mm), h is the height of the specimen (100 mm), w is the width of the strengthening sheet (25 mm), and finally S is the length of the strengthening system.

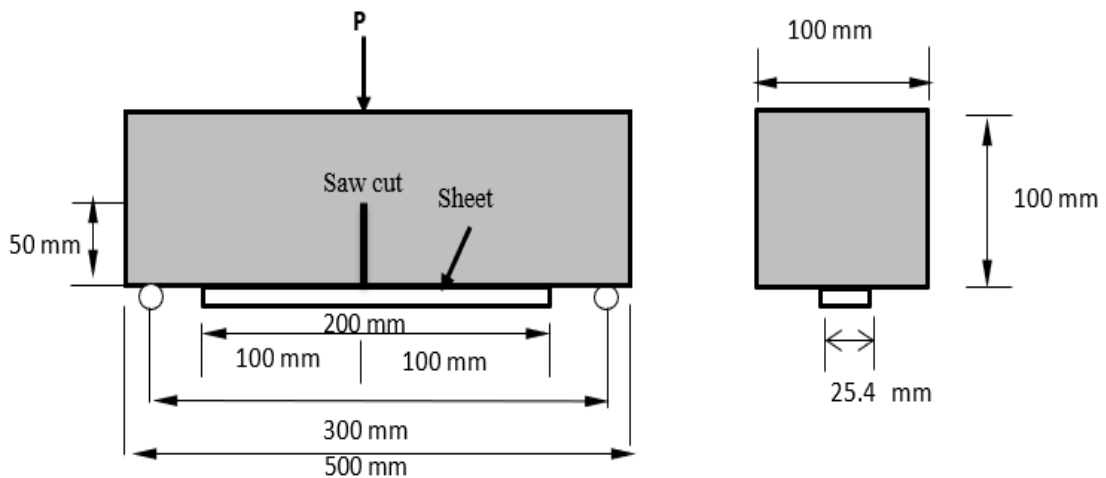


Figure 19: Small beam longitudinal and cross-sectional view

3.3.4. Single-Lap shear prism. A total of 30 single-lap shear specimens are tested in this study. The single-lap shear specimens were divided into two strengthening groups, CFRP, SME and SMM. Each group of strengthening system consists of 10 specimens as summarized in the test matrix shown in Table 5.

Table 5: Single-lap shear specimen designation

| AUS Experimental Program (30 Single-Lap shear prisms) | | | | |
|--|------------------------|-------------|-------------------------|--------------------------|
| Exposure Condition | Exposure period | CFRP | Steel Mesh Epoxy | Steel Mesh Mortar |
| Laboratory Environment | 28 days | C28L-1 | SME28L-1 | SMM28L-1 |
| | | C28L-2 | SME28L-2 | SMM28L-2 |
| Direct Sun Light | 180 days | C180S -1 | SME180S -1 | SMM180S -1 |
| | | C180S-2 | SME180S-2 | SMM180S-2 |
| | 360 days | C365S-1 | SME365S-1 | SMM365S-1 |
| | | C365S-2 | SME365S-2 | SMM365S-2 |
| Saline Sea Water | 180 days | C180W-1 | SME180W-1 | SMM180W-1 |
| | | C180W-2 | SME180W-2 | SMM180W-2 |
| | 360 days | C365W-1 | SME365W-1 | SMM365W-1 |
| | | C365W-2 | SME365W-2 | SMM365W-2 |

The single-lap shear prism is designed to have a cross-sectional area of 75 mm by 75 mm and strengthened by a 300 mm long and 50 mm wide GSM sheet as shown in Figure 20.

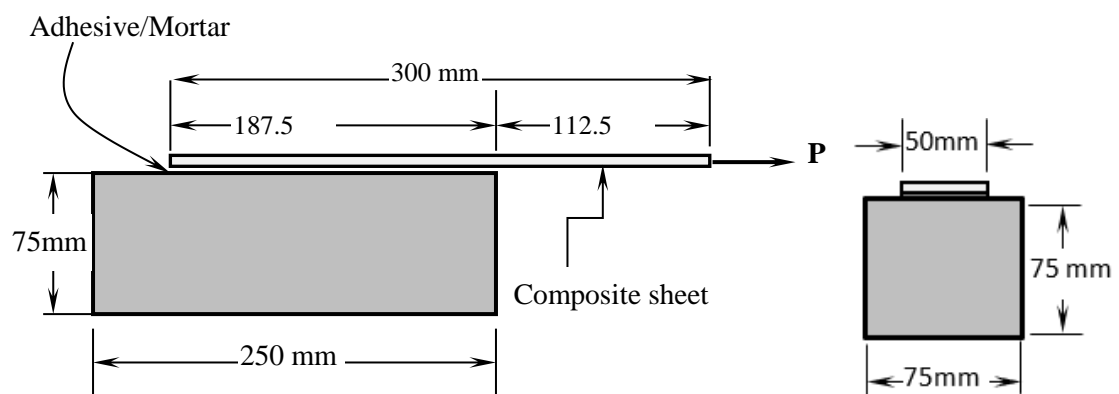


Figure 20: Single-Lap shear prism

3.4. Analytical Environmental Model (C_E)

Several equations are formulated and used to analyze the tests' raw data. These equations could be used to accurately measure the degradation that the RC beams encountered during their exposure time periods. These equations were formulated with the help of Figures 21 and 22, where it illustrates the definition of variables by offering a simplified version of the residual strength of strengthened and un-strengthened specimens that were either exposed or not exposed to harsh environments.

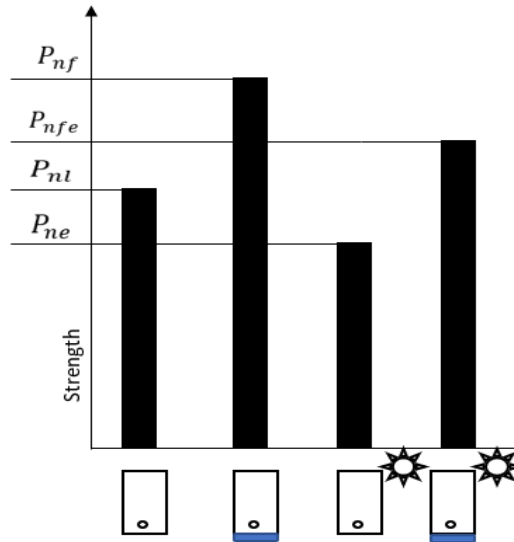


Figure 21: Sample expected strength for sun-exposed specimens

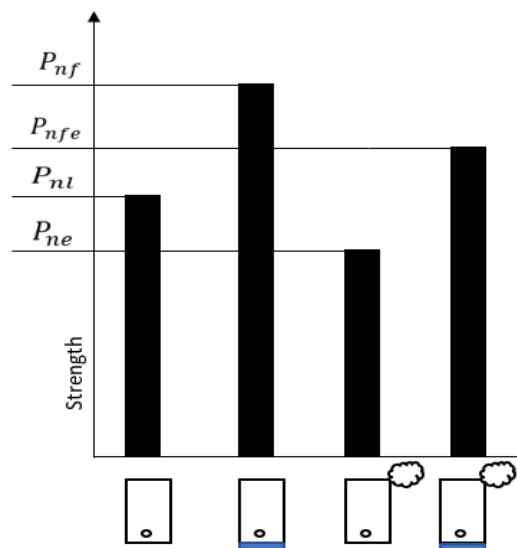


Figure 22: Sample expected strength for saline-exposed specimens

(LSR) is the lab strengthening ratio, (ESR) is the exposed strengthening ratio as shown in Equations (2 and 3) [66].

$$LSR = \frac{P_{nf}}{P_{nl}} \quad (2)$$

$$ESR = \frac{P_{nfe}}{P_{ne}} \quad (3)$$

where, P_{nl} is the ultimate load of control lab specimens, P_{nf} is the ultimate load of strengthened lab specimens, P_{nfe} is the ultimate load of exposed strengthened specimens, and finally P_{ne} is the ultimate load of exposed control lab specimens.

(R_n) is the retention ratio of the different RC beams strengthening systems described in Equation (4), where this equation takes into the consideration the degradation ratio of strengthened specimens over the degradation of un-strengthened specimens. Thus, Equation (4) considers the degradation of concrete, reinforcement steel and the strengthening system attached to the RC beams [66].

$$R_n = \frac{P_{nfe} / P_{ne}}{P_{nf} / P_{nl}} \quad (4)$$

(R_b) is the bond retention ratio for RC beams described in Equation (5), where this equation takes into consideration the strength of exposed specimens strengthening systems over the strength of unexposed specimens strengthening systems. Thus, Equation (5) considers the degradation of the strengthening system alone by eliminating the degradation of reinforcement steel and concrete in the RC beam [66].

$$R_b = \frac{P_{nfe} - P_{ne}}{P_{nf} - P_{nl}} \quad (5)$$

(R_c) is the coupon specimens retention ratio, (R_{po}) is the pull-out specimens retention ratio, and (R_p) is the flexural prism retention ratio. All three equations are simply obtained by dividing the ultimate load of exposed strengthened specimens over the ultimate load of strengthened lab specimens [66].

$$R_c = \frac{P_{nfe}}{P_{nf}} \quad (6)$$

$$R_{po} = \frac{P_{nfe}}{P_{nf}} \quad (7)$$

$$R_p = \frac{P_{nfe}}{P_{nf}} \quad (8)$$

It is common to report the stress and modulus of elasticity of CFRP per unit width. However, for GSM sheets bonded with cement-based mortar, these values must be reported per cord, and that is achieved by using the following equations.

$$\sigma = \frac{P}{nb} \quad (9)$$

$$\varepsilon = \frac{P}{nbE_f} \quad (10)$$

where (σ) is the stress in GSM sheet, (ε) is the strain in GSM sheet, (b) is the area of a single cord, and (n) is the number of cords in the investigated sheet [67].

3.5. Materials Properties

3.5.1. Concrete. The concrete used to cast all the specimens in this research was designed to have an approximate compressive strength of 40 MPa at 28 days. Table 6 shows the average compressive strength of tested cubes and cylinders.

Table 6: Compressive strength of cubes and cylinders at 28 days

| Sample | Dimensions (mm) | Compressive Strength (MPa) | Average (MPa) |
|------------|--------------------------|----------------------------|---------------|
| Cube 1 | 150 x 150 x 150 | 55.52 | 56.08 |
| Cube 2 | 150 x 150 x 150 | 56.64 | |
| Cylinder 1 | Dia. = 150, High= 300 | 41.3 | 38.9 |
| Cylinder 2 | Dia. = 150, High= 300 | 36.5 | |

Also, the concrete modulus of rupture for flexure beams was calculated and averaged to be 3.962 MPa. Table 7 shows the average modulus of rupture for flexure beams.

Table 7: Modulus of rupture for flexure beams

| Sample | Dimensions (mm) | Failure Load and Avg. (kN) | | Modulus of Rupture (MPa) | |
|-------------------|--------------------|-------------------------------|------|-----------------------------|-------|
| | | | | | |
| Flexure Beam 1 | 100 x 100 x 500 | 9.18 | 8.81 | 4.131 | 3.962 |
| Flexure Beam 2 | 100 x 100 x 500 | 8.43 | | 3.794 | |

3.5.2. Steel. Three steel rebars have been tested. The average modulus of elasticity was observed to be 199.9 GPa, while the average yield strength and tensile strength were 590.4 MPa and 640 MPa, respectively. Table 8 shows the tested mechanical properties of all steel specimens.

Table 8: Mechanical Properties of steel rebars

| Specimen number | F_y (MPa) | E (GPa) |
|-----------------|-------------|-----------|
| 1 | 588.5 | 199.988 |
| 2 | 587.4 | 199.971 |
| 3 | 595.05 | 200.000 |
| Average | 590.4 | 199.9 |

3.5.3. Galvanized Steel Mesh. High-strength galvanized steel mesh (GSM) sheets are made of galvanized steel cords that are bonded to a fiberglass mesh. The GSM sheets come in three different densities high, medium, and low density. However, this research focuses on the use of low-density steel mesh (GEO STEEL G1200) that has a density of 3.15 cords/cm. these high strengths galvanized steel chords are made of five galvanized steel wires, three of them are aligned parallel to each other and the remaining two will be wrapped around them in a high torque angle. The area of one wire is 0.1076 mm^2 , thus making the area of one cord to be 0.538 mm^2 . The tensile strength of the sheet, the tensile strength per unit width, elastic modulus, and the rupture

strain happens to be 3000 MPa, 4.72 kN/cm, 190 GPa, and 2% respectively as summarized in Table 9 [31].

Table 9: GSM mechanical properties as reported by manufacturer [31]

| GSM Sheet | |
|-------------------------------------|-------|
| Area of one cord (mm ²) | 0.538 |
| No. of cords/cm | 3.19 |
| Fiber density (g/cm ³) | 7.955 |
| Equivalent thickness (mm) | 0.169 |
| Tensile strength (MPa) | 3000 |
| Elastic Modulus (GPa) | 190 |
| Strain at failure (%) | 2 |

3.5.4. Epoxy adhesive. The epoxy adhesive used to bond GSM sheets to concrete surfaces was chosen to be GeoLite Gel which consists of two parts, part A and part B. The mixing ratio of these two parts is 3 parts of A to 1 part of B. after mixing these parts and epoxy adhesive will form with a flexural modulus of elasticity greater than 2.5 GPa and will have a bond strength greater than 14 MPa, as shown in Table 10 [68].

Table 10: Geoeopoly adhesive mechanical properties as reported by manufacturer [68]

| Epoxy Adhesive | |
|-----------------------------------|------|
| Tensile strength (MPa) | 14 |
| Glass transition temperature (°C) | 60 |
| Flexure elastic modulus (MPa) | 2500 |

3.5.5. Cement-Based mortar. GeoLite geo-mortar is a thixotropic geo-mortar with a crystalline reaction geo-binder base, which is prepared by mixing 25 kg with approximately 5 liters of water. The geo-mortar will have a strength greater than 2 MPa at 28 days, and an excellent reaction to fire (A1) as shown in Table 11 [69].

Table 11: Cement-based mortar mechanical properties as reported by manufacturer [69]

| Cement-based mortar | |
|----------------------------|----|
| Tensile strength (MPa) | 10 |
| Adhesive bond (MPa) | 2 |
| Reaction to fire | A1 |

3.5.6. CFRP sheet. V-Wrap C200H is a unidirectional high strength carbon fiber fabric, that could be used as a strengthening system for load carrying deficient structure. The C200H V-Wrap CFRP has an elastic modulus of 73,770 MPa, and a tensile strength of 1,034 MPa, as shown in Table 12 [70].

Table 12: CFRP laminate mechanical properties as reported by manufacturer [70]

| CFRP sheet | |
|----------------------------|----------------|
| Primary fiber direction | unidirectional |
| Weight (g/m ²) | 600 |
| Equivalent thickness (mm) | 1.02 |
| Tensile strength (MPa) | 1,034 |
| Elastic Modulus (MPa) | 73,770 |
| Strain at failure (%) | 2.1 |

3.5.7. CFRP epoxy adhesive. The epoxy adhesive used to bond CFRP sheets to concrete surfaces was chosen to be V-Wrap 700, which consists of two parts, part A and part B. The mixing ratio of these two parts is 3 parts of A to 1 part of B. after mixing these parts and epoxy adhesive will form with a flexural modulus of elasticity greater than 3 GPa and will have a bond strength greater than 72 MPa, as shown in Table 13 [71].

Table 13: V-Wrap 700 epoxy adhesive mechanical properties as reported by manufacturer [71]

| Epoxy Adhesive | |
|-----------------------------------|------|
| Tensile strength (MPa) | 72.4 |
| Glass transition temperature (°C) | 82 |
| Flexure elastic modulus (MPa) | 3120 |

3.6. Analytical Prediction

A set of equations are considered during the analytical prediction of the moment capacity of each strengthening system (CFRP, SMM, and SME). the beams are designed to fail by concrete crushing as advised by ACI 440-2R-17 code [32]. The equivalent flexural reinforcement ratio for all systems designed to be 0.00791 using Equation (11).

$$\rho_{eq} = \rho_s + n\rho_f = \frac{A_s}{bd} + \frac{E_f}{E_s} \frac{A_f}{bd} = \frac{226}{140 \times 236} + \frac{190}{200} \frac{110 \times 0.169}{140 \times 236} \times 2 = 0.00791 \quad (11)$$

ρ_s : Steel reinforcement ratio

ρ_f : Fiber reinforcement ratio

n: Number of layers

The flexural strength is obtained through Excel sheets, that are designed and verified by the ACI code. The equations used in these Excel sheets are based on force equilibrium and strain compatibility as shown below in Figure 23 and Equation (12) [27].

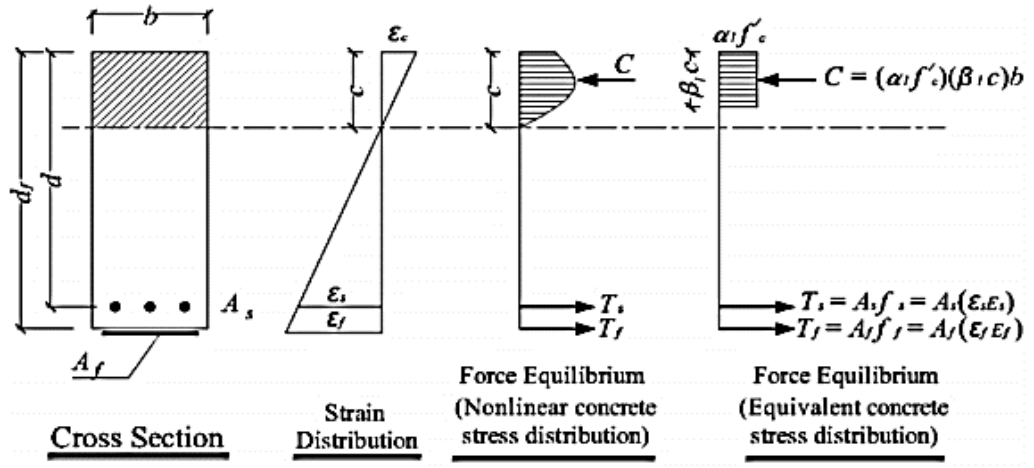


Figure 23: Stress-strain diagram [27]

$$M_n = C_E [A_s f_y \left(d - \frac{\beta_1 c}{2} \right) + \varphi A_{hs} f_{hsf,e} \left(h - \frac{\beta_1 c}{2} \right)] \quad (12)$$

C_E : is the environmental reduction factor of RC beam

M_n : is the maximum bending moment capacity of RC beam

A_s : is the net area of steel reinforcement

h : is the height of the section

f_y : is the yield strength of steel reinforcement

d : is the depth of the section

c : is the distance from the neutral axis to extreme compression fiber

β_1 : is the ratio that relates the depth of the equivalent rectangular concrete stress block to the neutral axis

φ : is a reduction factor for strength of 0.85

A_{hs} : is the area of external GSM sheet reinforcement

$f_{hsf,e}$: is the effective stress in the GSM sheet

The effective stress $f_{hsf,e}$ is calculated by using Equations (13) and (14). These equations are used to check the failure mode of the section. In this case debonding failure governs [27].

$$\epsilon_{hsf,d} = 0.41 \sqrt{\frac{f'_c}{nE_{hsf}t_{hsf}}} \leq 0.9\epsilon_{hsf,u} \quad (13)$$

$$\epsilon_{hsf,fe} = \epsilon_{cu} \left(\frac{d_f - c}{c} \right) - \epsilon_{bi} \leq 0.9\epsilon_{hsf,d} \quad (14)$$

$\epsilon_{hsf,d}$: is debonding strain in the GSM sheet

$\epsilon_{hsf,e}$: is the effective strain in GSM sheet attained at failure

f'_c : is the compressive stress in concrete

n : is the number of GSM layers

E_{hsf} : is the GSM sheet Elastic modulus

t_{hsf} : is the GSM sheet thickness

$\epsilon_{hsf,u}$: is the rupture strain of GSM sheet

The predicted load carrying capacity of strengthened beams are summarized in Table 14.

Table 14: Predicted load carrying capacity

| Specimen | Pu (kN) | ρ_{eq} | % Increase |
|--------------------------|------------|-------------|------------|
| Control | 90.79 | - | - |
| two sheets (110mm) G1200 | 141.46 | 0.79 | 55.81 |
| one sheet (100mm) G3300 | 139.57 | 0.79 | 53.73 |
| one sheet (140 mm) G2000 | 146.88 | 0.78 | 61.78 |
| one sheet (100mm) V-wrap | 140.46 | 0.79 | 54.71 |

3.7. Form Work

The Formwork was created by forming plywood into a designed length of 2000 mm and width of 140 mm as shown in Figure 24.



Figure 24: Form Work

3.8. Material Installations

3.8.1. Surface preparation. For all the strengthening system the same surface preparation method, where the surface of the concrete RC beam is strengthened and well cleaned with a brush. Since it is critical that the surface is not when installing adhesives, as shown in Figure 25.



Figure 25: Surface grinding of RC beams

3.8.2. SMM installation. Two layers of GSM sheets are placed on the bottom side of the RC beam. Each layer is installed by placing a thin base of cement-based mortar and then placing the first layer of GSM sheets, and repeating the same process for the second layer as shown in Figure 26.



Figure 26: SMM installation

3.8.3. SME installation. The installation of SME system is a similar method for SMM system. However, instead of applying mortar, epoxy adhesive is used as shown in Figure 27.



Figure 27: SME installation

3.8.4. CFRP installation. one layer of V-Wrap CFRP sheet is placed on the bottom side of RC beam. Each layer is installed by placing a thin base of epoxy adhesive is placed and then the CFRP sheets, which are soaked in the same epoxy adhesive, is placed on the RC beam, as shown in Figure 28.



Figure 28: CFRP installation

Chapter 4: Experimental Results and Discussion

4.1. RC Beams Control Un-Exposed Group

This group of RC beams has a total of eight specimens that were tested after 28 days of curing and zero days of exposure to environmental factors. Moreover, this group is divided in two 4 sub-groups, each of them contains two specimens. The first group contains two control (CB) un-strengthened specimens, which achieved an average of 86.5 kN ultimate load and a normal concrete crushing with steel yielding failure mode, while the second group contains two carbon fiber (C) reinforced specimens, which achieved an average of 126.9 kN ultimate load and an adhesive debonding with steel yielding failure mode. The third group has two steel mesh bonded with epoxy (SME) specimens, which achieved an average of 134.3 kN ultimate load and a cohesive cover separation action with steel yielding failure mode. However, the last group has two steel mesh bonded with mortar (SMM) specimens, which achieved an average of 129.6 kN ultimate load and an adhesive debonding with steel yielding failure mode. Table 15 summarizes the results of RC beams control un-exposed group, as well as the failure mode of each specimen.

Table 15: Summary results of control un-exposed RC beams

| Specimen | P_y (kN) | P_u (kN) | δ_y (mm) | δ_u (mm) | δ_f (mm) | Ductility index | | Failure mode |
|----------------|---------------|---------------|--------------------|--------------------|--------------------|---------------------|---------------------|---------------|
| | | | | | | δ_f/δ_u | δ_f/δ_y | |
| CB28L-1 | 73.20 | 87.40 | 5.40 | 12.70 | 19.00 | 1.50 | 3.52 | SY+CC (Flex.) |
| CB28L-2 | 71.50 | 85.60 | 5.10 | 11.90 | 18.30 | 1.53 | 3.58 | SY+CC (Flex.) |
| Average | 72.35 | 86.50 | 5.25 | 12.30 | 18.65 | 1.52 | 3.55 | |
| C28L-1 | 103.10 | 128.50 | 7.90 | 10.90 | 11.27 | 1.03 | 1.43 | SY+Deb. |
| C28L-2 | 105.20 | 125.30 | 7.43 | 10.85 | 10.90 | 1.01 | 1.47 | SY+Deb. |
| Average | 104.15 | 126.90 | 7.67 | 10.88 | 11.09 | 1.02 | 1.45 | |
| SME28L-1 | 110.38 | 130.70 | 7.10 | 10.45 | 10.79 | 1.03 | 1.52 | SY+Cov.S |
| SME28L-2 | 121.90 | 137.90 | 7.97 | 11.72 | 14.77 | 1.26 | 1.85 | SY+Cov.S |
| Average | 108.64 | 134.30 | 7.54 | 11.09 | 12.78 | 1.15 | 1.69 | |
| SMM28L-1 | 82.60 | 132.40 | 5.39 | 11.79 | 12.70 | 1.08 | 2.35 | SY+Deb. |
| SMM28L-2 | 78.00 | 126.80 | 6.62 | 6.62 | 12.10 | 1.83 | 1.83 | SY+Deb. |
| Average | 80.30 | 129.60 | 6.01 | 9.21 | 12.40 | 1.45 | 2.09 | |

Where, P_y is the yielding load, P_u is the ultimate load, δ_y is the yielding deflections, δ_u is the ultimate deflections, δ_f is the failure deflections. Moreover, SY stands for steel

yielding, CC stands for concrete crushing, Cov.S stands for cover separation, Deb stands for debonding.

Figure 29 shows the load-deflection response of RC beams control un-exposed group. Thus, it can be observed that the SME strengthening system tested in this group showed the maximum increase in load carrying capacity over the other strengthening system, since it achieved almost 55% increase in its load carrying capacity when compared to the control un-strengthened beam. However, CFRP and SMM achieved only 46% and 49% increase in their load carrying capacity respectively.

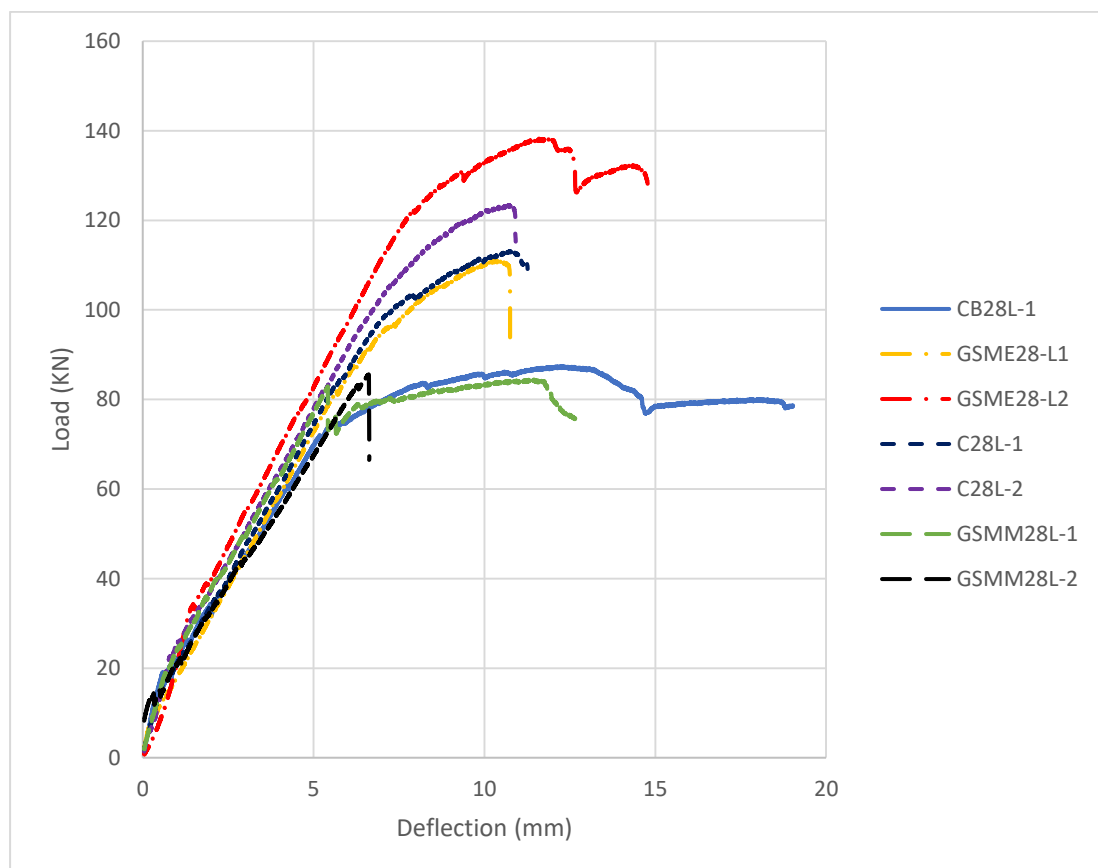





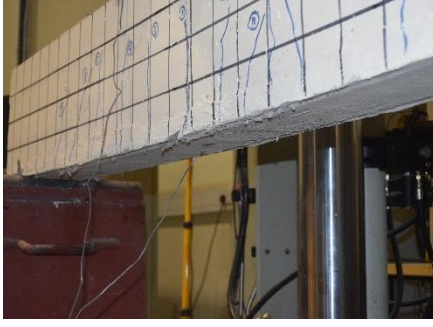




Figure 29: Summary results of load-deflection curve response for control un-exposed RC beams

Table 16 shows the failure mode of the same experimental group. Strengthening systems such as SMM and CFRP had a debonding failure mode which indicates a weak bond strength, while the SME strengthening system had a cover separation failure mode which indicates a strong bond strength between the interface and the substrate.

Table 16: Sample failure mode of control un-exposed RC beams

| Specimen | Before Failure | After Failure |
|--|---|--|
| CB28L-1 “Concrete crushing failure” |  |  |
| C28L-2 “Debonding failure” |  |  |
| SMM28L-1 “Debonding failure” |  |  |
| SME28L-1 “Cover separation failure” |  |  |

4.2. RC Beams 180 Days Exposed Group

4.2.1. RC beams after 180 days of saline exposure. This group of RC beams has a total of eight specimens that were tested after 28 days of curing and 180 days of saline water exposure. Moreover, this group is divided in two 4 sub-groups, each of them contains two specimens. The first group contains two control (CB) un-strengthened specimens, which achieved an average of 101.0 kN ultimate load and a normal concrete crushing with steel yielding failure mode. While the second group contains two carbon fiber (C) reinforced specimens, which achieved an average of 135.25 kN ultimate load and an adhesive debonding with steel yielding failure mode. The third group has two steel mesh bonded with epoxy (SME) specimens, which achieved an average of 145.5 kN ultimate load and a cohesive cover separation action with steel yielding failure mode. However, the last group has two steel mesh bonded with mortar (SMM) specimens, which achieved an average of 146.93 kN ultimate load and an adhesive debonding with steel yielding failure mode, as shown in Table 17, which summarizes the results of RC beams after 180 days of saline exposure, as well as the failure mode of each specimen.

Table 17: Summary results of RC beams after 180 days of saline exposure

| Specimen | P_y (kN) | P_u (kN) | δ_y (mm) | δ_u (mm) | δ_f (mm) | Ductility index | | Failure mode |
|----------------|---------------|---------------|--------------------|--------------------|--------------------|---------------------|---------------------|----------------|
| | | | | | | δ_f/δ_u | δ_f/δ_y | |
| CB180W-1 | 90.30 | 101.20 | 6.50 | 15.60 | 18.00 | 1.15 | 2.77 | SY+CC (Flex.)* |
| CB180W-2 | 84.10 | 100.80 | 6.10 | 15.90 | 17.30 | 1.09 | 2.84 | SY+CC (Flex.)* |
| Average | 87.20 | 101.00 | 6.30 | 15.75 | 17.65 | 1.12 | 2.80 | |
| C180W-1 | 117.40 | 136.10 | 8.30 | 10.10 | 10.30 | 1.02 | 1.24 | SY+Deb.* |
| C180W-2 | 122.40 | 134.40 | 8.80 | 11.15 | 11.40 | 1.02 | 1.30 | SY+Deb.* |
| Average | 119.90 | 135.25 | 8.55 | 10.63 | 10.85 | 1.02 | 1.27 | |
| SME180W-1 | 118.20 | 141.90 | 7.60 | 13.20 | 13.50 | 1.02 | 1.78 | SY+Cov.S* |
| SME180W-2 | 122.10 | 149.10 | 8.00 | 13.70 | 14.10 | 1.03 | 1.76 | SY+Cov.S* |
| Average | 120.15 | 145.50 | 7.80 | 13.45 | 13.80 | 1.03 | 1.77 | |
| SMM180W-1 | 120.10 | 144.80 | 8.10 | 14.10 | 14.20 | 1.01 | 1.75 | SY+Deb.* |
| SMM180W-2 | 125.30 | 149.05 | 7.90 | 12.90 | 13.10 | 1.02 | 1.66 | SY+Deb.* |
| Average | 122.70 | 146.93 | 8.00 | 13.50 | 13.65 | 1.01 | 1.71 | |

P_y : Yielding Load, P_u : Ultimate Load, δ_y : Yielding Deflections, δ_u : Ultimate Deflections, δ_f : Failure Deflections. * SY: Steel yielding, CC: Concrete crushing, Cov.S: Cover separation, Deb: Debonding.

Figure 30 shows the load-deflection response of RC beams after 180 days of saline exposure group. Thus, it can be observed that the SMM strengthening system tested in this group showed the maximum increase in load carrying capacity over the other strengthening system, since it achieved almost 45% increase in its load carrying capacity when compared to the control un-strengthened beam. However, CFRP and SME achieved only 34% and 44% increase in their load carrying capacity respectively.

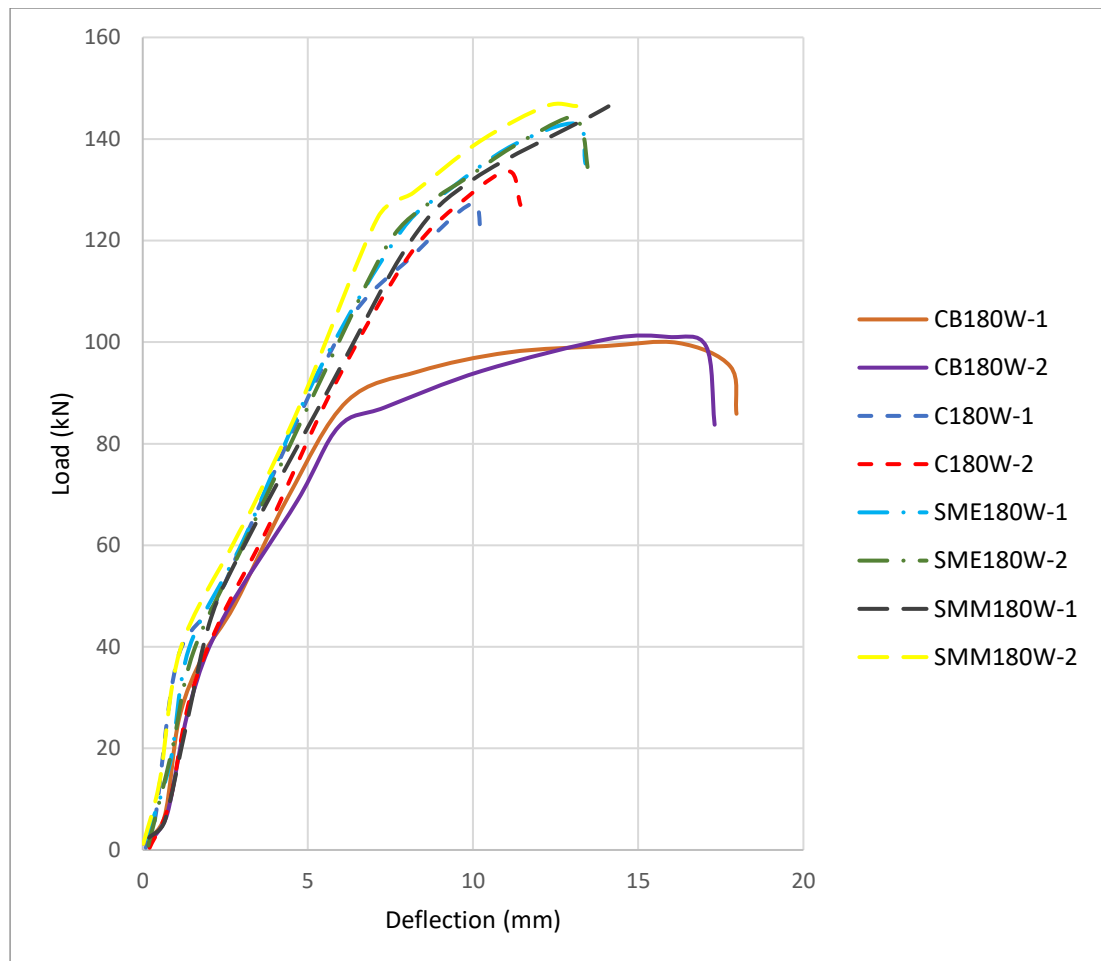



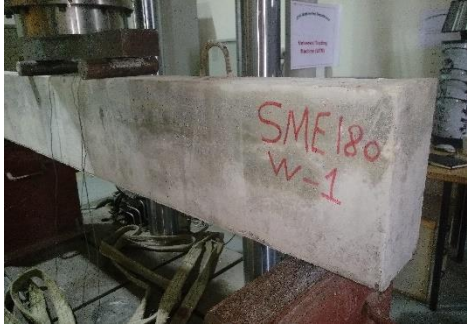



Figure 30: Summary results of load-deflection curve response for RC beams after 180 days of saline exposure

Table 18 shows the failure mode of the same experimental group. Strengthening systems such as SMM and CFRP had a debonding failure mode which indicates a weak bond strength, while the SME strengthening system had a cover separation failure mode which indicates a strong bond strength between the interface and the substrate.

Table 18: Sample failure mode of RC beams after 180 days of saline exposure

| Specimen | Before Failure | After Failure |
|---|--|---|
| <p>CB180W-1 “Concrete crushing failure”</p> |  <p>A photograph of a concrete beam specimen labeled 'CB180 W-1' in red marker. The beam is positioned horizontally in a testing machine, showing a smooth surface with some minor surface cracks.</p> |  <p>A photograph of the same concrete beam specimen after failure. The top surface is severely crushed and fragmented, with exposed aggregate and a jagged, broken appearance.</p> |
| <p>C180W-1 “Debonding failure”</p> |  <p>A photograph of a concrete beam specimen labeled 'C180 W-1' in red marker. The beam is positioned horizontally in a testing machine, showing a smooth surface with some minor surface cracks.</p> |  <p>A photograph of the same concrete beam specimen after failure. The top surface is severely debonded, with a large portion of the concrete layer missing, exposing the internal structure.</p> |
| <p>SMM180W-1 “Debonding failure”</p> |  <p>A photograph of a concrete beam specimen labeled 'SMM180 W-1' in red marker. The beam is positioned horizontally in a testing machine, showing a smooth surface with some minor surface cracks.</p> |  <p>A photograph of the same concrete beam specimen after failure. The top surface is severely debonded, with a large portion of the concrete layer missing, exposing the internal structure.</p> |
| <p>SME180W-1 “Cover separation failure”</p> |  <p>A photograph of a concrete beam specimen labeled 'SME180 W-1' in red marker. The beam is positioned horizontally in a testing machine, showing a smooth surface with some minor surface cracks.</p> |  <p>A photograph of the same concrete beam specimen after failure. The top surface is severely separated, with a large portion of the concrete cover missing, exposing the internal structure.</p> |

4.2.2. RC beams after 180 days of sun exposure. This group of RC beams has a total of eight specimens that were tested after 28 days of curing and 180 days of sun exposure. Moreover, this group is divided in two 4 sub-groups, each of them contains two specimens. The first group contains two control (CB) un-strengthened specimens, which achieved an average of 98.2 kN ultimate load and a normal concrete crushing with steel yielding failure mode. While the second group contains two carbon fiber (C) reinforced specimens, which achieved an average of 138.0 kN ultimate load and an adhesive debonding with steel yielding failure mode. The third group has two steel mesh bonded with epoxy (SME) specimens, which achieved an average of 135.4 kN ultimate load and an adhesive debonding with steel yielding failure mode. However, the last group has two steel mesh bonded with mortar (SMM) specimens, which achieved an average of 131.9 kN ultimate load and an adhesive debonding with steel yielding failure mode. Table 19 summarizes the results of RC beams after 180 days of sun exposure, as well as the failure mode of each specimen.

Table 19: Summary results of RC beams after 180 days of sun exposure

| Specimen | P_y (kN) | P_u (kN) | δ_y (mm) | δ_u (mm) | δ_f (mm) | Ductility index | | Failure mode |
|----------------|---------------|---------------|--------------------|--------------------|--------------------|---------------------|---------------------|----------------|
| | | | | | | δ_f/δ_u | δ_f/δ_y | |
| CB180S-1 | 88.10 | 98.90 | 6.20 | 13.00 | 22.40 | 1.72 | 3.61 | SY+CC (Flex.)* |
| CB180S-2 | 86.20 | 97.40 | 6.60 | 13.50 | 24.70 | 1.83 | 3.74 | SY+CC (Flex.)* |
| Average | 87.15 | 98.15 | 6.40 | 13.25 | 23.55 | 1.78 | 3.68 | |
| C180S-1 | 120.10 | 130.70 | 8.20 | 11.40 | 11.60 | 1.02 | 1.41 | SY+Deb.* |
| C180S-2 | 125.20 | 145.30 | 9.10 | 13.10 | 13.30 | 1.02 | 1.46 | SY+Deb.* |
| Average | 122.65 | 138.00 | 8.65 | 12.25 | 12.45 | 1.02 | 1.44 | |
| SME180S-1 | 117.50 | 135.10 | 7.80 | 9.10 | 10.10 | 1.11 | 1.29 | SY+Deb.* |
| SME180S-2 | 119.20 | 135.60 | 8.30 | 12.30 | 12.50 | 1.02 | 1.51 | SY+Deb.* |
| Average | 118.35 | 135.35 | 8.05 | 10.70 | 11.30 | 1.06 | 1.40 | |
| SMM180S-1 | 113.40 | 134.50 | 7.80 | 11.60 | 11.70 | 1.01 | 1.50 | SY+Deb.* |
| SMM180S-2 | 100.30 | 129.20 | 7.10 | 9.90 | 9.80 | 0.99 | 1.38 | SY+Deb.* |
| Average | 106.85 | 131.85 | 7.45 | 10.75 | 10.75 | 1.00 | 1.44 | |

P_y : Yielding Load, P_u : Ultimate Load, δ_y : Yielding Deflections, δ_u : Ultimate Deflections, δ_f : Failure Deflections* SY: Steel yielding, CC: Concrete crushing, Cov.S: Cover separation, Deb: Debonding.

Figure 31 shows the load-deflection response of RC beams after 180 days of sun exposure group. Thus, it can be observed that the CFRP strengthening system tested

in this group showed the maximum increase in load carrying capacity over the other strengthening system, since it achieved almost 40.6% increase in its load carrying capacity when compared to the control un-strengthened beam. However, SME and SMM achieved only 37% and 31% increase in their load carrying capacity respectively.

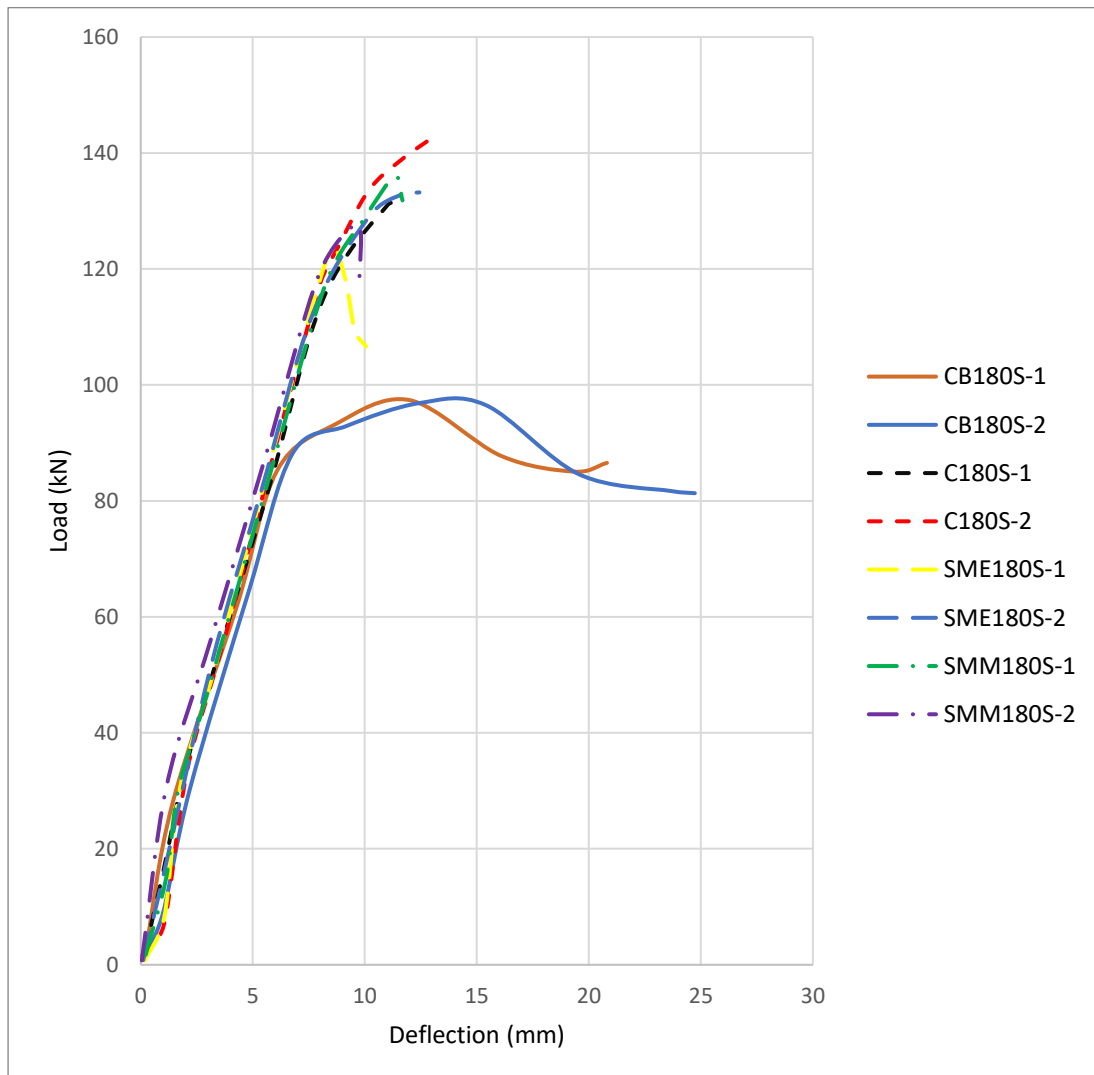






Figure 31: Summary results of load-deflection curve response for RC beams after 180 days of sun exposure

Table 20 show the failure mode of the same experimental group. All strengthening systems in this group of RC beams had a debonding failure mode which indicates a weakened bond strength.

Table 20: Sample failure mode of RC beams after 180 days of sun exposure

| Specimen | Before Failure | After Failure |
|---|---|--|
| <p>CB180S-1 “Concrete crushing failure”</p> |  <p>Photograph of specimen CB180S-1 before failure. The beam is supported on two points and has 'CB180 S-1' handwritten in blue on its side.</p> |  <p>Photograph of specimen CB180S-1 after failure. The beam shows significant concrete crushing and vertical cracking under load.</p> |
| <p>C180S-2 “debonding failure”</p> |  <p>Photograph of specimen C180S-2 before failure. The beam is supported on two points and has 'C180 S-2' handwritten in red on its side.</p> |  <p>Photograph of specimen C180S-2 after failure. The beam shows debonding of the concrete surface, with 'C180 S-2' handwritten in red on its side.</p> |
| <p>SMM180S-1 “debonding failure”</p> |  <p>Photograph of specimen SMM180S-1 before failure. The beam is supported on two points and has 'SMM 180S-1' handwritten in blue on its side.</p> |  <p>Photograph of specimen SMM180S-1 after failure. The beam shows debonding of the concrete surface, with 'SMM 180S-1' handwritten in blue on its side.</p> |
| <p>SME180S-1 “debonding failure”</p> |  <p>Photograph of specimen SME180S-1 before failure. The beam is supported on two points and has 'SME 180S-1' handwritten in red on its side.</p> |  <p>Photograph of specimen SME180S-1 after failure. The beam shows a large area of concrete debonding and spalling, with 'SME 180S-1' handwritten in red on its side.</p> |

4.3. RC Beams 360 Days Exposed Group

4.3.1. RC beams after 360 days of saline exposure. This group of RC beams has a total of eight specimens that were tested after 28 days of curing and 360 days of saline water exposure. Moreover, this group is divided in two 4 sub-groups, each of them contains two specimens. The first group contains two control (CB) un-strengthened specimens, which achieved an average of 110.61 kN ultimate load and a normal concrete crushing with steel yielding failure mode. While the second group contains two carbon fiber (C) reinforced specimens, which achieved an average of 141.0 kN ultimate load and an adhesive debonding with steel yielding failure mode. The third group has two steel mesh bonded with epoxy (SME) specimens, which achieved an average of 157.8 kN ultimate and a cohesive cover separation action with steel yielding failure mode. However, the last group has two steel mesh bonded with mortar (SMM) specimens, which achieved an average of 141.3 kN ultimate load and a cohesive cover separation action with steel yielding failure mode. Table 21 summarizes the results of RC beams after 360 days of saline exposure, as well as the failure mode of each specimen.

Table 21: Summary results of RC beams after 360 days of saline exposure

| Specimen | P_y (kN) | P_u (kN) | δ_y (mm) | δ_u (mm) | δ_f (mm) | Ductility index | | Failure mode |
|----------------|---------------|---------------|--------------------|--------------------|--------------------|---------------------|---------------------|----------------|
| | | | | | | δ_f/δ_u | δ_f/δ_y | |
| CB360W-1 | 89.15 | 108.83 | 6.16 | 20.16 | 20.36 | 1.01 | 3.31 | SY+CC (Flex.)* |
| CB360W-2 | 78.71 | 112.39 | 6.12 | 23.47 | 24.07 | 1.03 | 3.93 | SY+CC (Flex.)* |
| Average | 83.93 | 110.61 | 6.14 | 21.82 | 22.22 | 1.02 | 3.62 | |
| C360W-1 | 127.71 | 140.62 | 8.53 | 11.52 | 11.57 | 1.00 | 1.36 | SY+Deb.* |
| C360W-2 | 126.71 | 141.39 | 9.23 | 11.87 | 12.19 | 1.03 | 1.32 | SY+Deb.* |
| Average | 127.21 | 141.01 | 8.88 | 11.70 | 11.88 | 1.02 | 1.34 | |
| SME360W-1 | 128.46 | 154.00 | 8.38 | 13.43 | 14.23 | 1.06 | 1.70 | SY+Cov.S* |
| SME360W-2 | 136.32 | 161.63 | 9.53 | 14.20 | 14.92 | 1.05 | 1.57 | SY+Cov.S* |
| Average | 132.39 | 157.82 | 8.96 | 13.82 | 14.58 | 1.06 | 1.63 | |
| SMM360W-1 | 114.00 | 140.43 | 8.33 | 13.58 | 13.58 | 1.00 | 1.63 | SY+Cov.S* |
| SMM360W-2 | 119.92 | 142.15 | 8.05 | 12.41 | 12.90 | 1.04 | 1.60 | SY+Cov.S* |
| Average | 116.96 | 141.29 | 8.19 | 13.00 | 13.24 | 1.02 | 1.62 | |

P_y : Yielding Load, P_u : Ultimate Load, δ_y : Yielding Deflections, δ_u : Ultimate Deflections, δ_f : Failure Deflections. * SY: Steel yielding, CC: Concrete crushing, Cov.S: Cover separation, Deb: Debonding.

Figure 32 shows the load-deflection response of RC beams after 360 days of saline exposure group. Thus, it can be observed that the SME strengthening system tested in this group showed the maximum increase in load carrying capacity over the other strengthening system, since it achieved almost 43% increase in its load carrying capacity when compared to the control un-strengthened beam. However, CFRP and SMM achieved similarly to each other a 28% increase in their load carrying capacity.

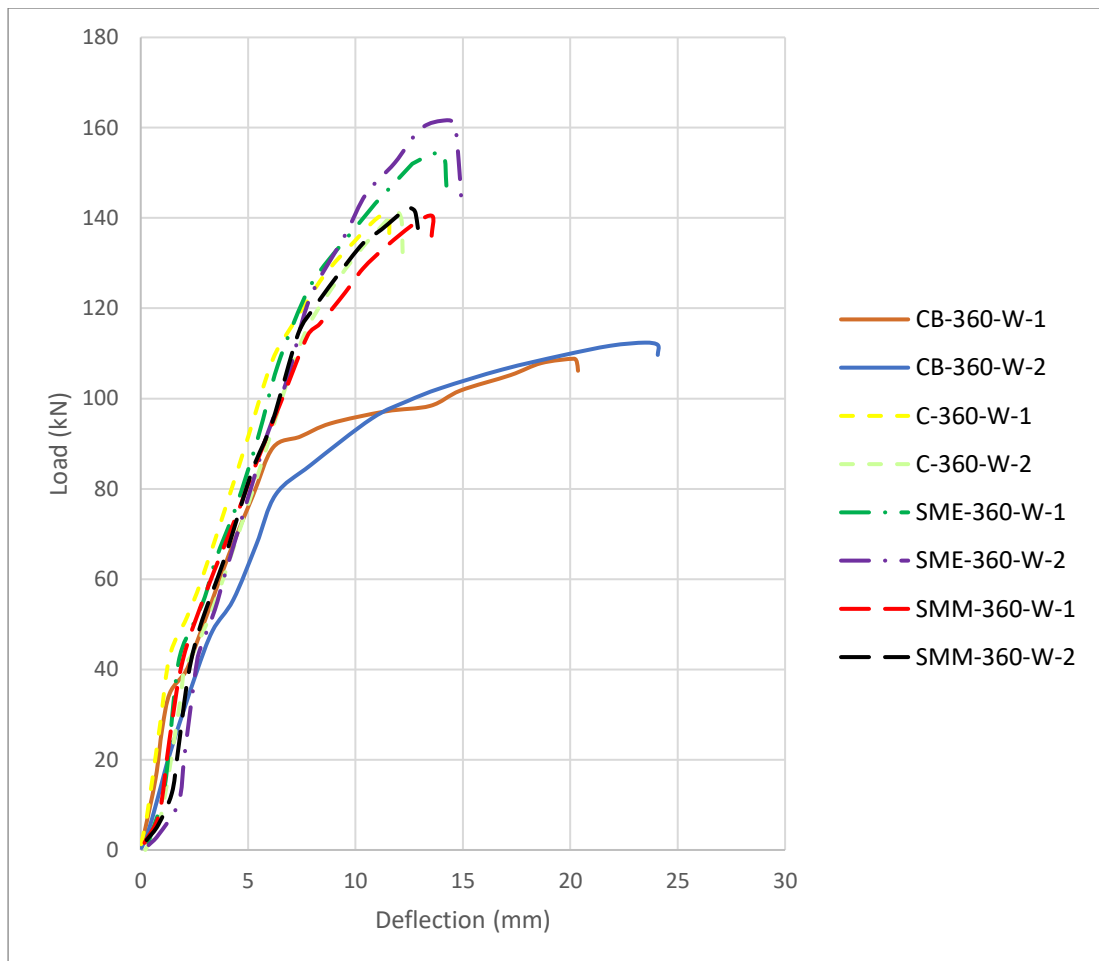







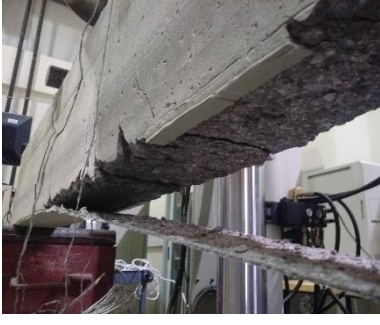


Figure 32: Summary results of the load-deflection curve response for RC beams after 360 days of saline exposure

Table 22 shows the failure mode of the same experimental group. Strengthening system such as CFRP had a debonding failure mode which indicates a weak bond strength, while SME and SMM strengthening systems had a cover separation failure mode which indicates a strong bond strength between the interface and the substrate.

Table 22: Sample failure mode of RC beams after 360 days of saline exposure

| Specimen | Before Failure | After Failure |
|---|---|---|
| <p>CB360W-1 “Concrete crushing failure”</p> |  |  |
| <p>C360W-1 “Debonding failure”</p> |  |  |
| <p>SMM360W-1 “Cover separation failure”</p> |  |  |
| <p>SME360W-1 “Cover separation failure”</p> |  |  |

4.3.2. RC beams after 360 days of sun exposure. This group of RC beams has a total of eight specimens that were tested after 28 days of curing and 360 days of sun exposure. Moreover, this group is divided in two 4 sub-groups, each of them contains two specimens. The first group contains two control (CB) un-strengthened specimens, which achieved an average of 99.1 kN ultimate load and a normal concrete crushing with steel yielding failure mode. While the second group contains two carbon fiber (C) reinforced specimens, which achieved an average of 135.4 kN ultimate load and a cohesive cover separation action with steel yielding failure mode. The third group has two steel mesh bonded with epoxy (SME) specimens, which achieved an average of 144.5 kN ultimate load and an adhesive debonding with steel yielding failure mode. However, the last group has two steel mesh bonded with mortar (SMM) specimens, which achieved an average of 130.9 kN ultimate load and a cohesive cover separation action with steel yielding failure mode. Table 23 summarizes the results of RC beams after 360 days of sun exposure, as well as the failure mode of each specimen.

Table 23: Summary results of RC beams after 360 days of sun exposure

| Specimen | P_y (kN) | P_u (kN) | δ_y (mm) | δ_u (mm) | δ_f (mm) | Ductility index | | Failure mode |
|----------------|---------------|---------------|--------------------|--------------------|--------------------|---------------------|---------------------|----------------|
| | | | | | | δ_f/δ_u | δ_f/δ_y | |
| CB360S-1 | 87.05 | 99.30 | 8.22 | 18.51 | 25.80 | 1.39 | 3.14 | SY+CC (Flex.)* |
| CB360S-2 | 83.91 | 98.84 | 7.81 | 15.85 | 22.51 | 1.42 | 2.88 | SY+CC (Flex.)* |
| Average | 85.48 | 99.07 | 8.02 | 17.18 | 24.16 | 1.41 | 3.01 | |
| C360S-1 | 126.42 | 139.48 | 10.53 | 13.28 | 13.35 | 1.01 | 1.27 | SY+Cov.S* |
| C360S-2 | 129.00 | 131.24 | 10.02 | 13.93 | 14.02 | 1.01 | 1.40 | SY+Cov.S* |
| Average | 127.71 | 135.36 | 10.28 | 13.61 | 13.69 | 1.01 | 1.33 | |
| SME360S-1 | 113.40 | 143.41 | 7.80 | 11.60 | 11.70 | 1.01 | 1.50 | SY+Deb.* |
| SME360S-2 | 104.48 | 145.50 | 7.90 | 9.71 | 12.35 | 1.27 | 1.56 | SY+Deb.* |
| Average | 108.94 | 144.46 | 7.85 | 10.66 | 12.03 | 1.13 | 1.53 | |
| SMM360S-1 | 129.00 | 134.50 | 9.69 | 12.89 | 13.11 | 1.02 | 1.35 | SY+Cov.S* |
| SMM360S-2 | 126.65 | 127.25 | 9.02 | 13.29 | 13.64 | 1.03 | 1.51 | SY+Cov.S* |
| Average | 127.83 | 130.88 | 9.36 | 13.09 | 13.38 | 1.02 | 1.43 | |

P_y : Yielding Load, P_u : Ultimate Load, δ_y : Yielding Deflections, δ_u : Ultimate Deflections, δ_f : Failure Deflections. * SY: Steel yielding, CC: Concrete crushing, Cov.S: Cover separation, Deb: Debonding.

Figure 33 shows the load-deflection response of RC beams after 360 days of sun exposure group. Thus, it can be observed that the SME strengthening system tested in this group showed the maximum increase in load carrying capacity over the other strengthening system, since it achieved almost 45.9% increase in its load carrying capacity when compared to the control un-strengthened beam. However, CFRP and SMM achieved only 36% and 32% increase in their load carrying capacity respectively.

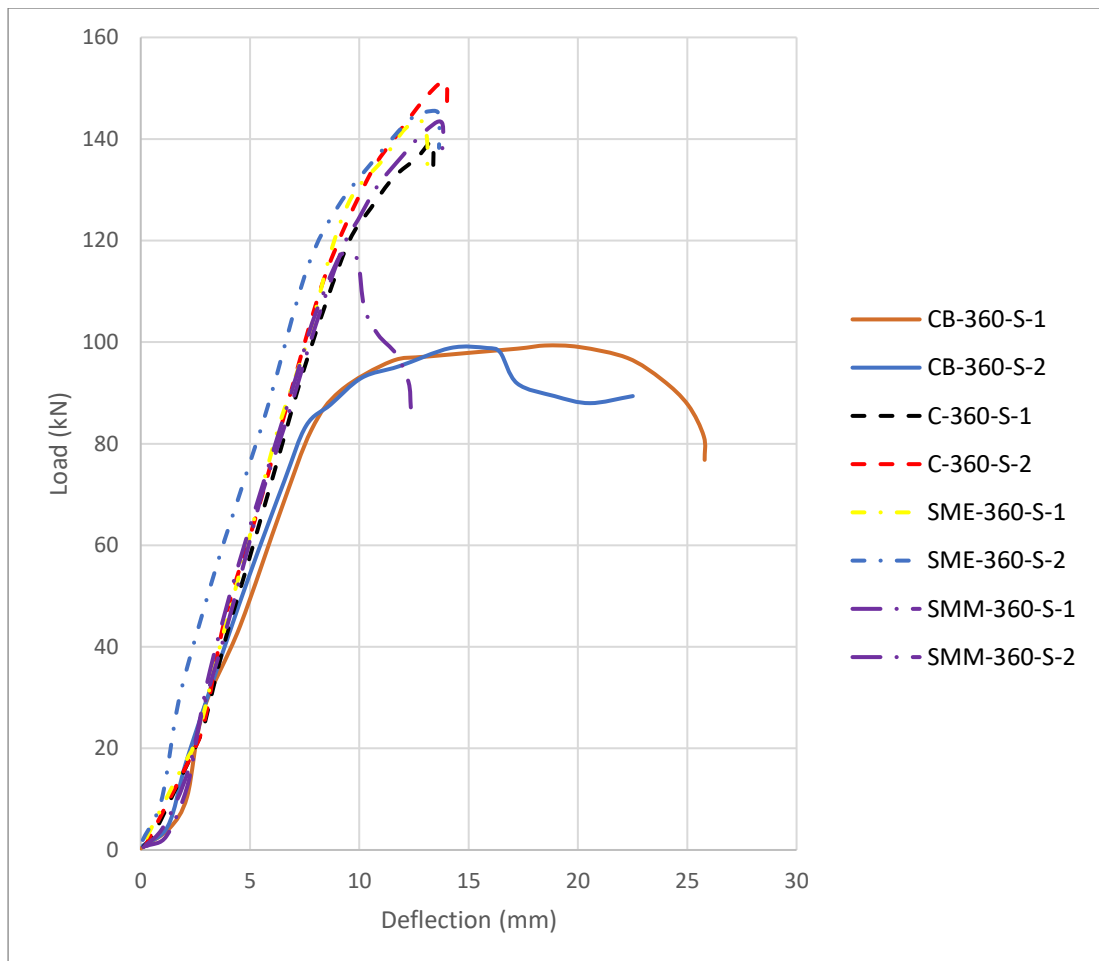


Figure 33: Summary results of the load-deflection curve response for RC beams after 360 days of sun exposure

Table 24 show the failure mode of the same experimental group. Strengthening system such as SMM had a debonding failure mode which indicates a weak bond strength, while SME and CFRP strengthening systems had a cover separation failure mode which indicates a strong bond strength between the interface and the substrate.

Table 24: Sample failure mode of RC beams after 360 days of sun exposure

| Specimen | Before Failure | After Failure |
|---|---|---|
| <p>CB360S-1 “Concrete crushing”</p> |  |  |
| <p>C360S-1 “Cover Separation failure”</p> |  |  |
| <p>SMM360S-1 “debonding failure”</p> |  |  |
| <p>SME360W-1 “Cover Separation failure”</p> |  |  |

4.4. RC Beams Degradation

In this section, the RC beams degradation summary is presented in Table 25, which summarizes the use of three different degradation equations. These equations could be used to accurately measure the degradation that the RC beams encountered during their exposure time periods. Degradation model's comparison of each strengthening systems is shown in the Appendix.

Table 25: RC Beams degradation summary

| Time Period | Exposure | Designation | P_u (kN) | LSR* | ESR* | ESR/LSR | R_n^* | R_b^* |
|-------------|----------|-------------|------------|------|------|---------|---------|---------|
| 28 Days | Lab | CB28L-1 | 87.4 | - | - | - | - | - |
| | | CB28L-2 | 85.6 | - | - | - | - | - |
| | | Average | 86.5 | 1.00 | - | - | - | - |
| | | C28L-1 | 128.5 | 1.49 | - | - | - | - |
| | | C28L-2 | 125.3 | 1.45 | - | - | - | - |
| | | Average | 126.9 | 1.47 | - | - | - | - |
| | | SME28L-1 | 130.7 | 1.51 | - | - | - | - |
| | | SME28L-2 | 137.9 | 1.59 | - | - | - | - |
| | | Average | 134.3 | 1.55 | - | - | - | - |
| | | SMM28L-1 | 132.4 | 1.53 | - | - | - | - |
| | | SMM28L-2 | 126.8 | 1.47 | - | - | - | - |
| | | Average | 129.6 | 1.50 | - | - | - | - |
| 6 Months | Saline | CB180W-1 | 101.2 | - | - | - | 1.17 | - |
| | | CB180W-2 | 100.8 | - | - | - | 1.17 | - |
| | | Average | 101 | - | 1.00 | 1.00 | 1.17 | - |
| | | C180W-1 | 136.1 | - | 1.35 | 0.91 | 1.07 | 0.87 |
| | | C180W-2 | 134.4 | - | 1.33 | 0.92 | 1.06 | 0.83 |
| | | Average | 135.25 | - | 1.34 | 0.91 | 1.07 | 0.85 |
| | | SME180W-1 | 141.9 | - | 1.40 | 0.93 | 1.06 | 0.86 |
| | | SME180W-2 | 149.1 | - | 1.48 | 0.93 | 1.11 | 1.01 |
| | | Average | 145.5 | - | 1.44 | 0.93 | 1.08 | 0.93 |
| | | SMM180W-1 | 144.8 | - | 1.43 | 0.94 | 1.12 | 1.02 |
| | | SMM180W-2 | 149.05 | - | 1.48 | 1.01 | 1.15 | 1.11 |
| | | Average | 146.925 | - | 1.45 | 0.97 | 1.13 | 1.07 |

Table 25 Continued: RC Beams degradation summary

| Time Period | Exposure | Designation | P _u (kN) | LSR* | ESR* | ESR/LSR | R _n * | R _b * |
|-------------|----------|-------------|---------------------|------|------|---------|------------------|------------------|
| 6 Months | Sun | CB180S-1 | 98.9 | - | - | - | 1.14 | - |
| | | CB180S-2 | 97.4 | - | - | - | 1.13 | - |
| | | Average | 98.15 | - | 1.00 | 1.00 | 1.13 | - |
| | | C180S-1 | 130.7 | - | 1.33 | 0.90 | 1.03 | 0.81 |
| | | C180S-2 | 145.3 | - | 1.48 | 1.02 | 1.14 | 1.17 |
| | | Average | 138 | - | 1.41 | 0.96 | 1.09 | 0.99 |
| | | SME180S-1 | 135.1 | - | 1.38 | 0.91 | 1.01 | 0.77 |
| | | SME180S-2 | 135.6 | - | 1.38 | 0.87 | 1.01 | 0.78 |
| | | Average | 135.35 | - | 1.38 | 0.89 | 1.01 | 0.78 |
| | | SMM180S-1 | 134.5 | - | 1.37 | 0.90 | 1.04 | 0.84 |
| | | SMM180S-2 | 129.2 | - | 1.32 | 0.90 | 1.00 | 0.72 |
| | | Average | 131.85 | - | 1.34 | 0.90 | 1.02 | 0.78 |
| 12 Months | Saline | CB360W-1 | 108.83 | - | - | - | 1.26 | - |
| | | CB360W-2 | 112.39 | - | - | - | 1.30 | - |
| | | Average | 110.61 | - | 1.00 | 1.00 | 1.28 | - |
| | | C360W-1 | 140.62 | - | 1.27 | 0.86 | 1.11 | 0.74 |
| | | C360W-2 | 141.39 | - | 1.28 | 0.88 | 1.11 | 0.76 |
| | | Average | 141.005 | - | 1.27 | 0.87 | 1.11 | 0.75 |
| | | SME360W-1 | 154 | - | 1.39 | 0.92 | 1.15 | 0.91 |
| | | SME360W-2 | 161.63 | - | 1.46 | 0.92 | 1.20 | 1.07 |
| | | Average | 157.815 | - | 1.43 | 0.92 | 1.18 | 0.99 |
| | | SMM360W-1 | 140.43 | - | 1.27 | 0.83 | 1.08 | 0.69 |
| | | SMM360W-2 | 142.15 | - | 1.29 | 0.88 | 1.10 | 0.73 |
| | | Average | 141.29 | - | 1.28 | 0.85 | 1.09 | 0.71 |
| | Sun | CB360S-1 | 99.3 | - | - | - | 1.15 | - |
| | | CB360S-2 | 98.84 | - | - | - | 1.14 | - |
| | | Average | 99.07 | - | 1.00 | 1.00 | 1.15 | - |
| | | C360S-1 | 139.48 | - | 1.41 | 0.95 | 1.10 | 1.00 |
| | | C360S-2 | 131.24 | - | 1.32 | 0.91 | 1.03 | 0.80 |
| | | Average | 135.36 | - | 1.37 | 0.93 | 1.07 | 0.90 |
| | | SME360S-1 | 143.41 | - | 1.45 | 0.96 | 1.07 | 0.93 |
| | | SME360S-2 | 145.5 | - | 1.47 | 0.92 | 1.08 | 0.97 |
| | | Average | 144.455 | - | 1.46 | 0.94 | 1.08 | 0.95 |
| | | SMM360S-1 | 134.50 | - | 1.36 | 0.89 | 1.04 | 0.82 |
| | | SMM360S-2 | 127.25 | - | 1.28 | 0.88 | 0.98 | 0.65 |
| | | Average | 130.88 | - | 1.32 | 0.88 | 1.01 | 0.74 |

$$* LSR = \frac{P_{nf}}{P_{nl}}$$

$$* R_n = \frac{P_{nfe}}{P_{nf}} / \frac{P_{ne}}{P_{nl}}$$

$$* ESR = \frac{P_{nfe}}{P_{ne}}$$

$$* R_b = \frac{P_{nfe} - P_{ne}}{P_{nf} - P_{nl}}$$

4.4.1. RC beams ESR/LSR degradation model. In the first model, the exposed specimens strengthening ratio (ESR) is divided by the lab specimens strengthening ratio (LSR), as previously defined by Equations (2 and 3) in section 3.4, so that we can obtain the exposure degradation ratio for the RC beams strengthening systems when compared with control unexposed strengthened specimens. Figures 34 and 35 show the results of all specimens' average degradation ratio for LSR/ESR model. Consequently, carbon fiber strengthened specimens retained 87% of its strength after 360 days of saline exposure, while it retained 93% of its strength after 360 days of sun exposure. SME strengthened specimens retained 92% of its strength after 360 days of saline exposure, while it retained 96% of its strength after 360 days of sun exposure. While, SMM strengthened specimens retained 85% of its strength after 360 days of saline exposure, while it retained 85% of its strength after 360 days of sun exposure.

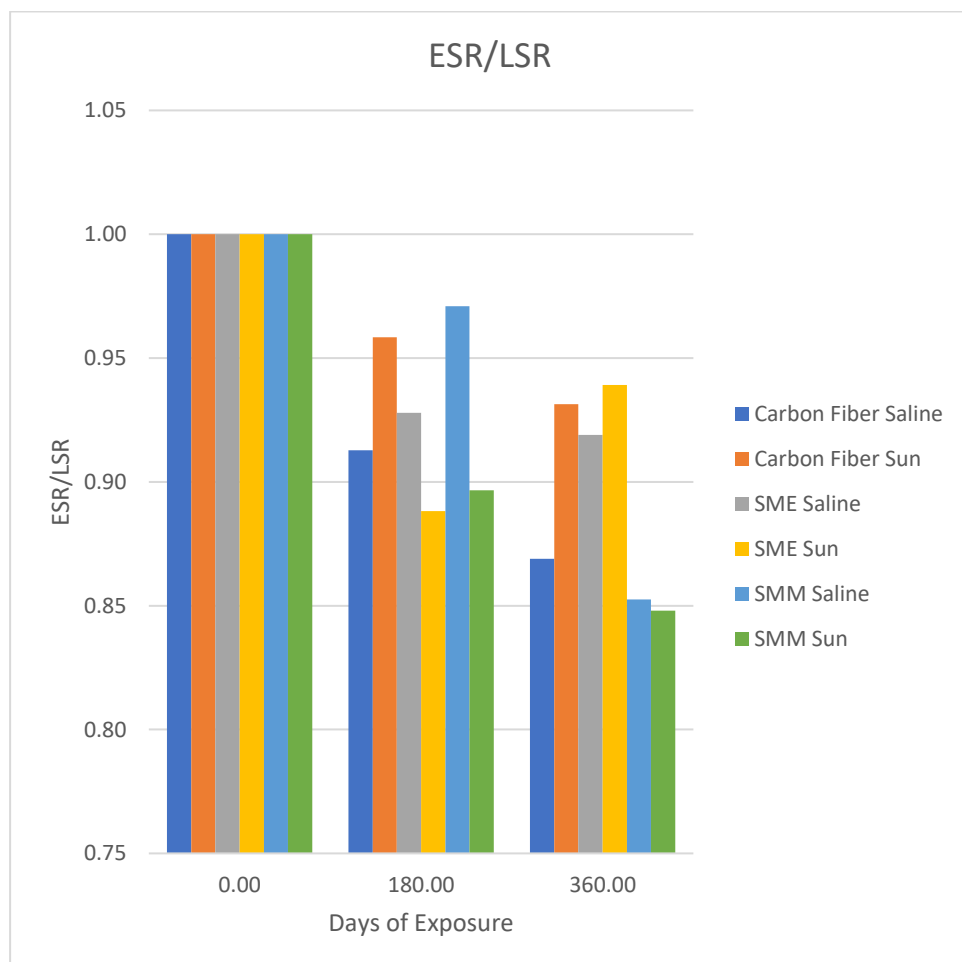


Figure 34: Bar Graph of RC beams ESR/LSR degradation model

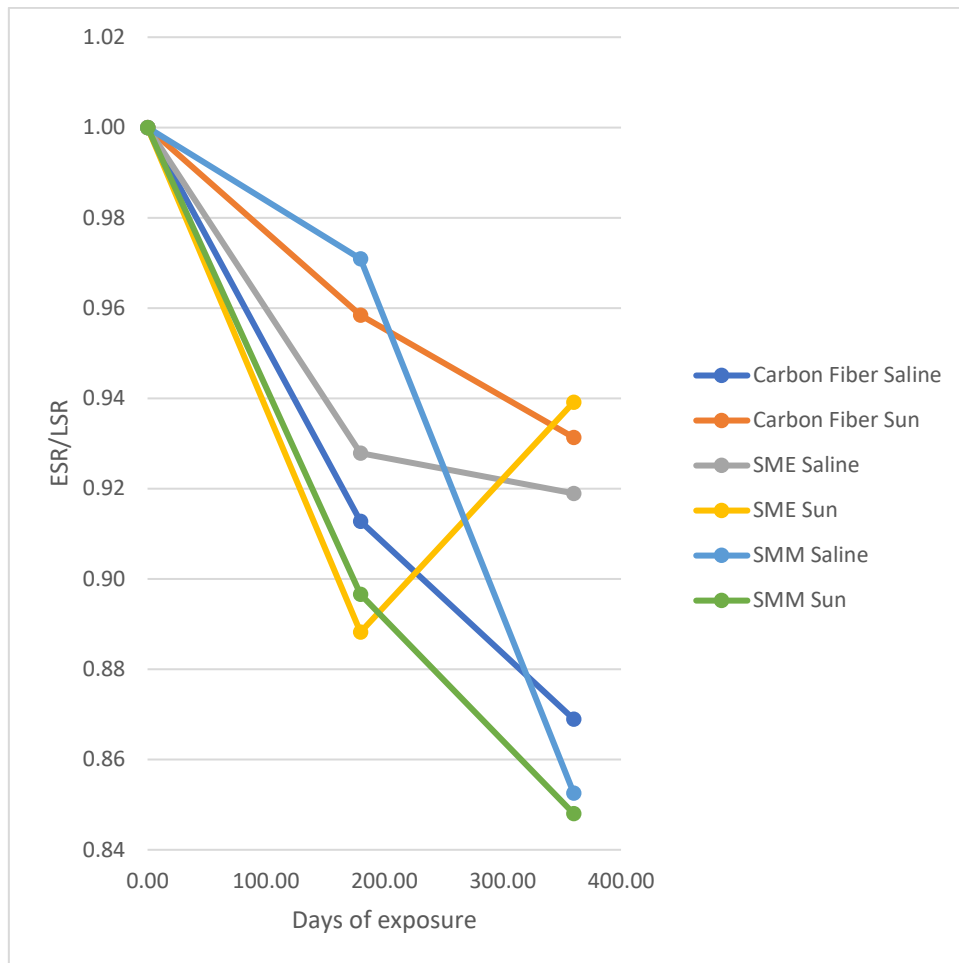


Figure 35: Line Chart of RC beams ESR/LSR degradation model

4.4.2. RC beams R_n degradation model. The second model defines the Retention ratio of the different strengthening systems, as previously defined by Equation (4) in section 3.4, so that we can obtain the exposure degradation ratio for the RC beams strengthening systems when compared with control unexposed strengthened specimens. Figures 36 and 37 show the results of all specimens' average degradation ratio for R_n model. Moreover, carbon fiber strengthened specimens retained 111% of its strength after 360 days of saline exposure, while it retained 107% of its strength after 360 days of sun exposure. SME strengthened specimens retained 118% of its strength after 360 days of saline exposure, while it retained 108% of its strength after 360 days of sun exposure. While, SMM strengthened specimens retained 109% of its strength after 360 days of saline exposure, while it retained 101% of its strength after 360 days of sun exposure.

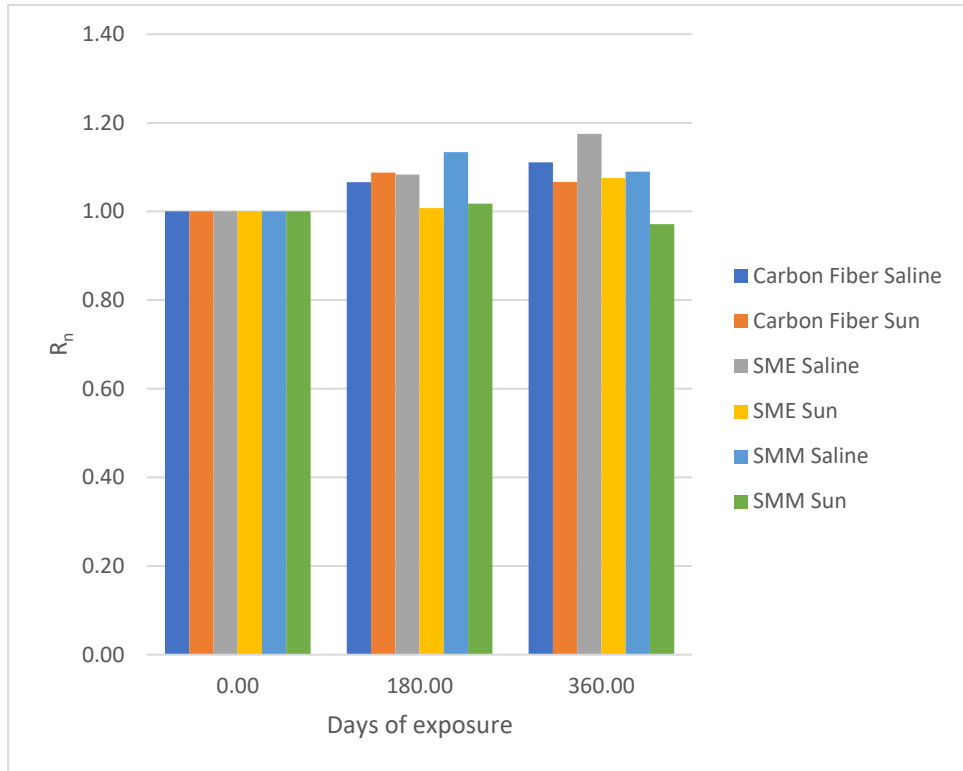


Figure 36: Bar Graph of RC beams R_n degradation model

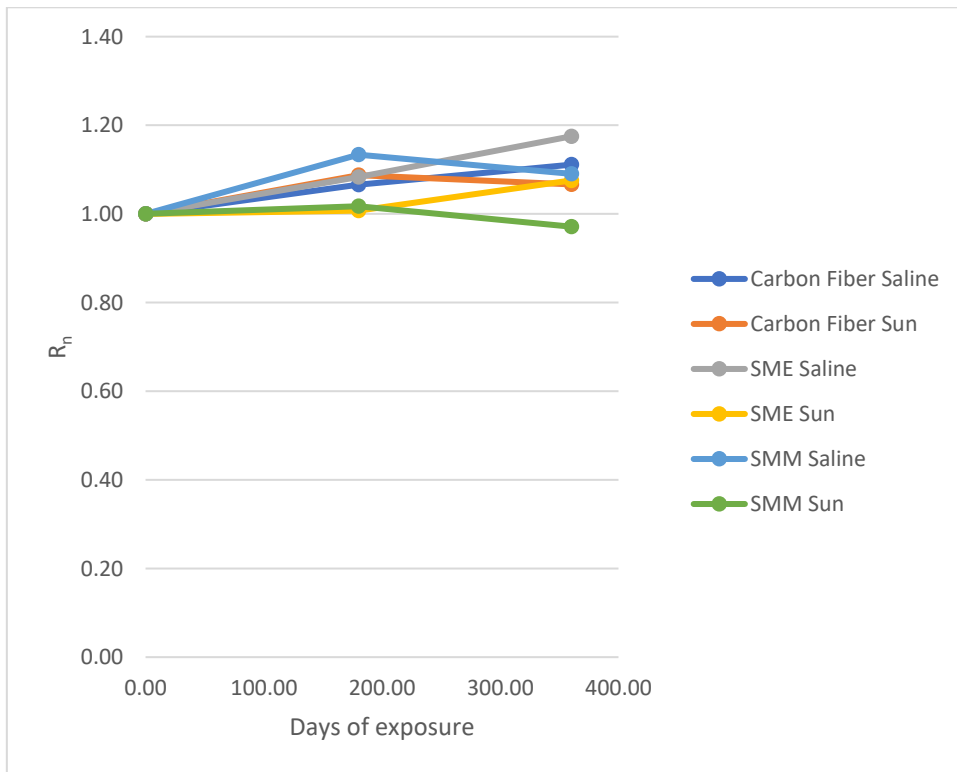


Figure 37: Line Chart of RC beams R_n degradation model

4.4.3. RC beams R_b degradation model. The third model defines the Retention ratio of the different strengthening systems bond strength, as previously defined by Equation (5) in section 3.4, so that we can obtain the exposure degradation ratio for the RC beams strengthening systems when compared with control unexposed strengthened specimens. Figure 38 and 39 show the results of all specimens' average degradation ratio for R_b model. Moreover, carbon fiber strengthened specimens retained 75% of its strength after 360 days of saline exposure, while it retained 90% of its strength after 360 days of sun exposure. SME strengthened specimens retained 99% of its strength after 360 days of saline exposure, while it retained 95% of its strength after 360 days of sun exposure. While, SMM strengthened specimens retained 71% of its strength after 360 days of saline exposure, while it retained 74% of its strength after 360 days of sun exposure.

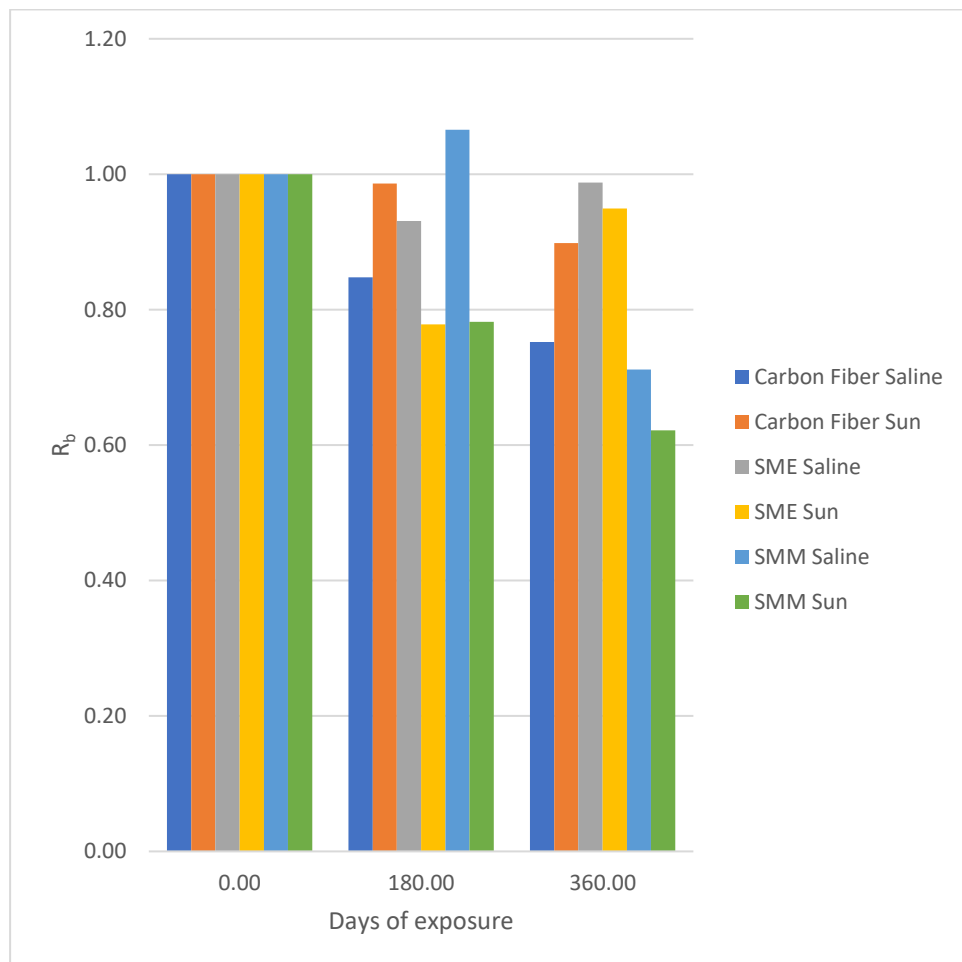


Figure 38: Bar Graph of RC beams R_b degradation model

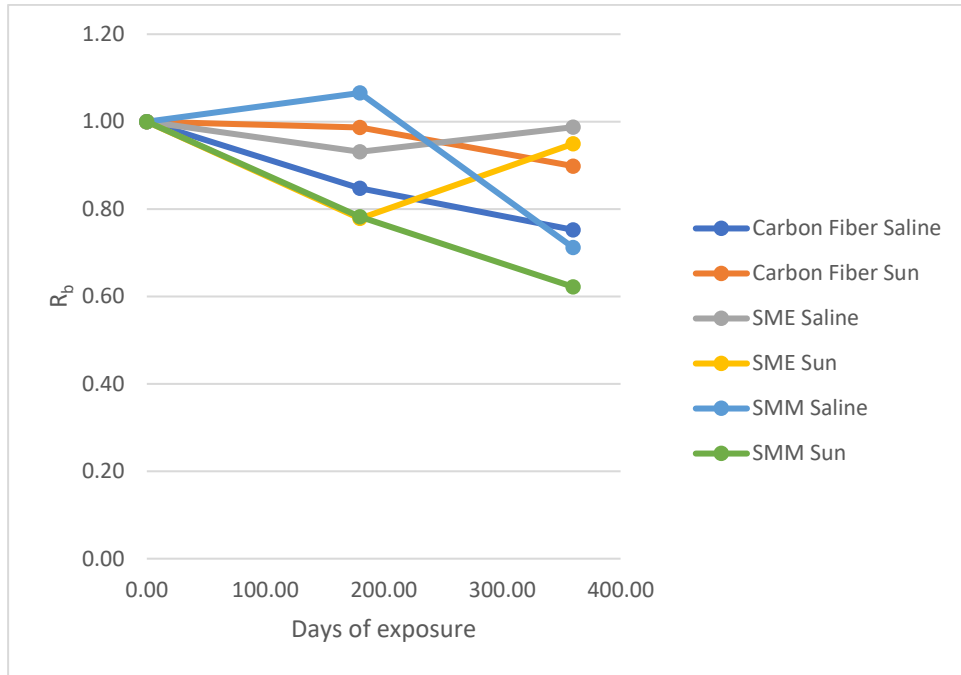


Figure 39: Line Chart of RC beams R_b degradation model

4.4.4. CFRP RC beams sun light exposure. The load-deflection responses of RC beams strengthened with CFRP and exposed to direct sun light are shown in Figure 40. The CFRP RC beams strength decreased by 10% after 360 days of exposure, and the RC beams' ductility increased over time as shown in Table 25 and Figure 40.

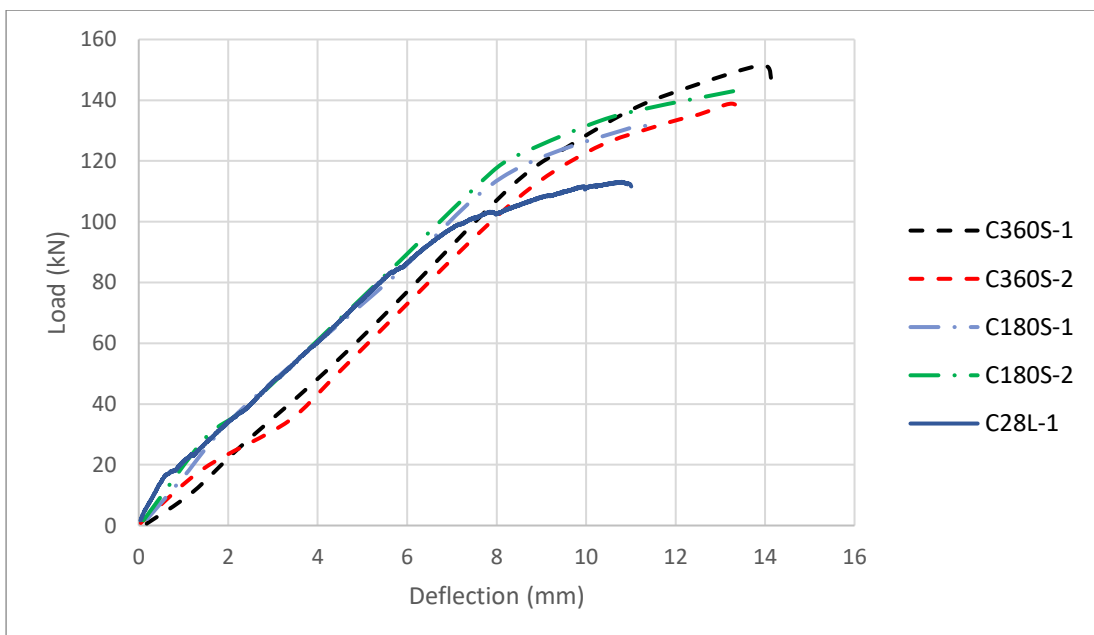


Figure 40: CFRP RC beams exposed to direct sun light

4.4.5. CFRP beams saline water exposure. The load-deflection responses of RC beams strengthened with CFRP and exposed to saline water are shown in Figure 41. The CFRP RC beams strength decreased by 25% after 360 days of exposure, and the RC beams' ductility increased over time as shown in Table 25 and Figure 41.

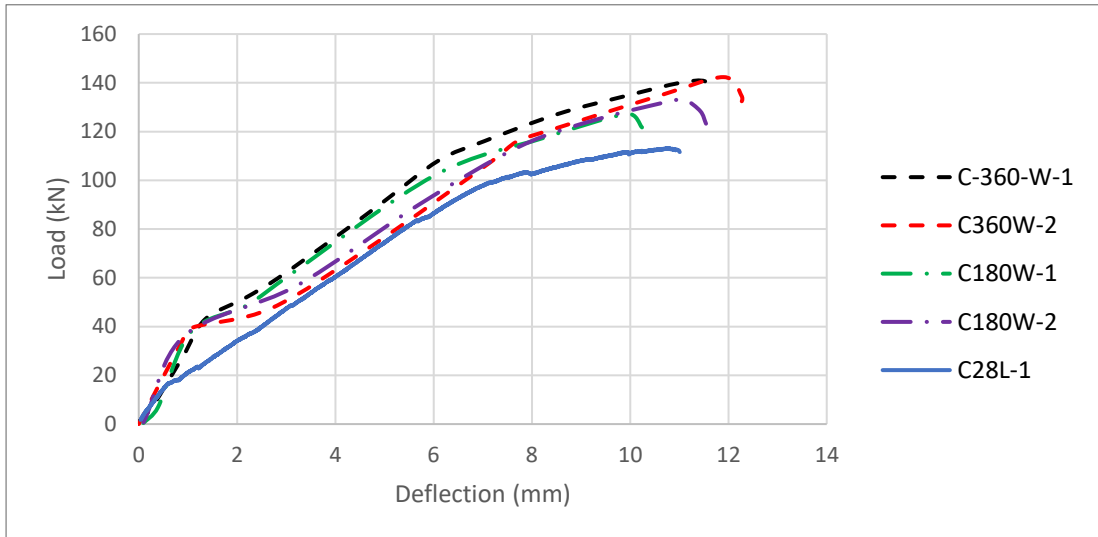


Figure 41: CFRP RC beams exposed to saline water

4.4.6. SME RC beams sun light exposure. The load-deflection responses of RC beams strengthened with SME and exposed to direct sun are shown in Figure 42. The SME RC beams strength decreased by 5% after 360 days of exposure, and the RC beams' ductility increased over time as shown in Table 25 and Figure 42.

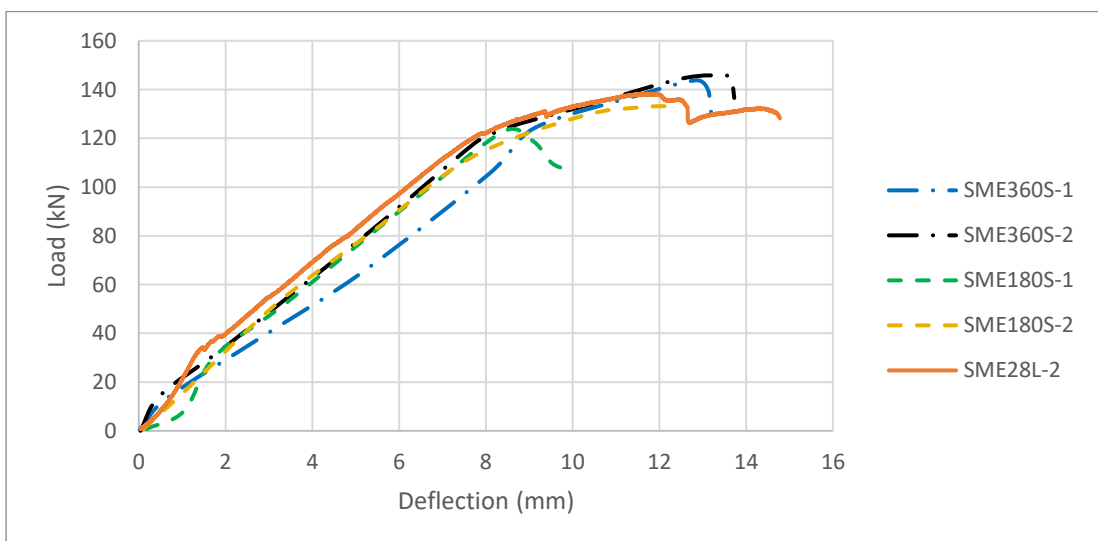


Figure 42: SME RC beams exposed to direct sun light

4.4.7. SME RC beams saline water exposure. The load-deflection responses of RC beams strengthened with SME and exposed to saline water are shown in Figure 43. The SME RC beams strength decreased by 1% after 360 days of exposure, and the RC beams' ductility increased over time as shown in Table 25 and Figure 43.

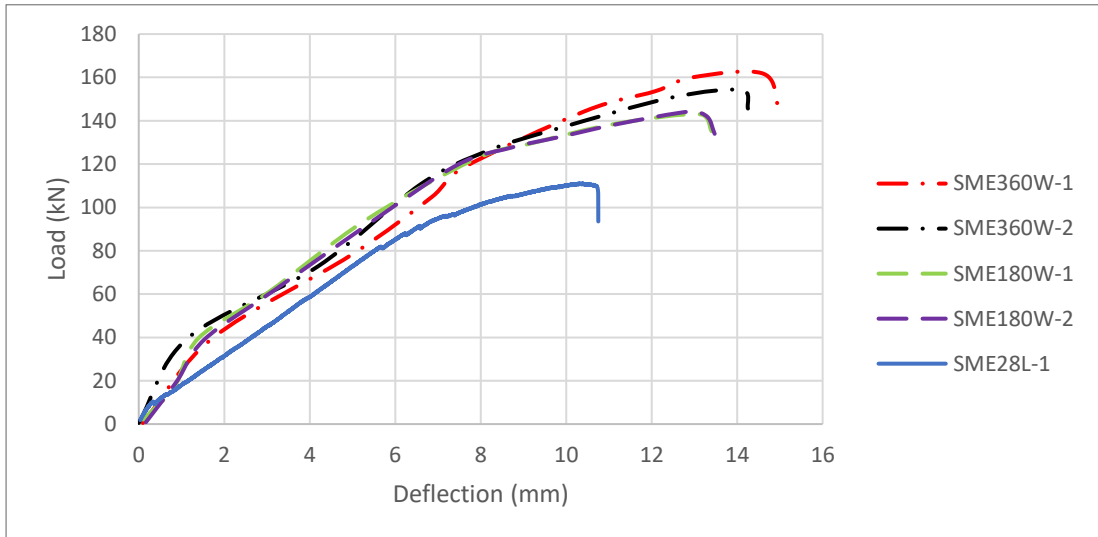


Figure 43: SME RC beams exposed to saline water

4.4.8. SMM RC beams sun light exposure. The load-deflection responses of RC beams strengthened with SMM and exposed to direct sun light are shown in Figure 44. The SMM RC beams strength decreased by 26% after 360 days of exposure, and the RC beams' ductility decreased over time as shown in Table 25 and Figure 44.

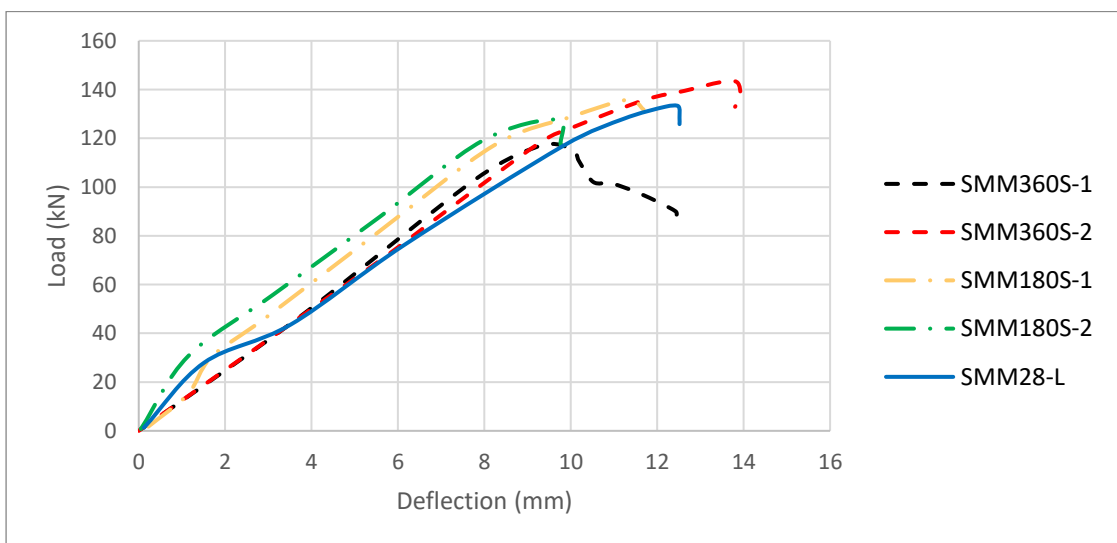


Figure 44: SMM RC beams exposed to direct sun light

4.4.9. SMM RC beams saline water exposure. The load-deflection responses of RC beams strengthened with SMM and exposed to saline water are shown in Figure 45. The SMM RC beams strength decreased by 29% after 360 days of exposure, and the RC beams' ductility did not change over time as shown in Table 25 and Figure 45.

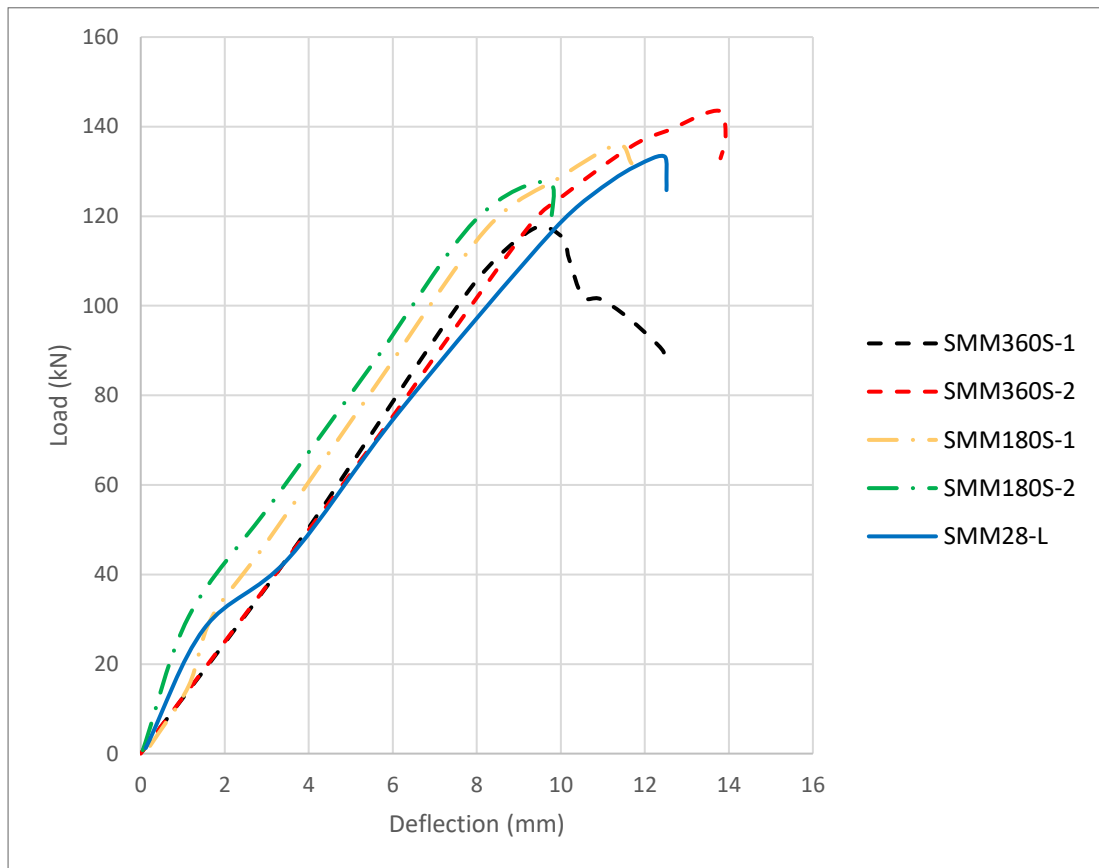


Figure 45: SMM RC beams exposed to saline water

4.5. Flexure Prisms Results

In this section, the flexure prism degradation report summary is presented in Table 26, which summarizes the use of flexure prism retention ratio (R_P). Moreover, Figures 46 and 47 show the results of all specimens' average degradation ratio for the R_P model. Consequently, carbon fiber strengthened specimens retained 61% of its strength after 540 days of saline exposure, while it retained 66% of its strength after 540 days of sun exposure. SME strengthened specimens retained 97% of its strength after 540 days of saline exposure, while it retained 67% of its strength after 540 days of sun exposure. While, SMM strengthened specimens retained 97% of its strength after

540 days of saline exposure, while it retained 89% of its strength after 540 days of sun exposure.

Table 26: Flexure prism degradation summary

| Time Period | Exposure | Strengthening system | Designation | Pu (kN) | Average bond stress (Mpa) | Rp |
|-------------|----------|-------------------------------|-------------|---------|---------------------------|------|
| 28 days | Lab | Carbon Fiber | C28L-1 | 15.07 | 5.43 | - |
| | | | C28L-2 | 17.13 | 6.17 | - |
| | | | Average | 16.10 | 5.80 | - |
| | | Steel mesh bonded with Epoxy | SME28L-1 | 15.45 | 5.56 | - |
| | | | SME28L-2 | 15.13 | 5.45 | - |
| | | | Average | 15.29 | 5.50 | - |
| | | Steel mesh bonded with Mortar | SMM28L-1 | 5.83 | 2.10 | - |
| | | | SMM28L-2 | 6.10 | 2.20 | - |
| | | | Average | 5.97 | 2.15 | - |
| 18 Months | Saline | Carbon Fiber | C180W-1 | 10.06 | 3.62 | 0.62 |
| | | | C180W-2 | 9.65 | 3.47 | 0.60 |
| | | | Average | 9.86 | 3.55 | 0.61 |
| | | Steel mesh bonded with Epoxy | SME180W-1 | 13.87 | 4.99 | 0.91 |
| | | | SME180W-2 | 15.78 | 5.68 | 1.03 |
| | | | Average | 14.83 | 5.34 | 0.97 |
| | | Steel mesh bonded with Mortar | SMM180W-1 | 6.16 | 2.22 | 1.03 |
| | | | SMM180W-2 | 5.45 | 1.96 | 0.91 |
| | | | Average | 5.81 | 2.09 | 0.97 |
| | Sun | Carbon Fiber | C180S-1 | 10.28 | 3.70 | 0.64 |
| | | | C180S-2 | 10.99 | 3.96 | 0.68 |
| | | | Average | 10.64 | 3.83 | 0.66 |
| | | Steel mesh bonded with Epoxy | SME180S-1 | 10.47 | 3.77 | 0.68 |
| | | | SME180S-2 | 9.99 | 3.60 | 0.65 |
| | | | Average | 10.23 | 3.68 | 0.67 |
| | | Steel mesh bonded with Mortar | SMM180S-1 | 5.36 | 1.93 | 0.90 |
| | | | SMM180S-2 | 5.30 | 1.91 | 0.89 |
| | | | Average | 5.33 | 1.92 | 0.89 |

The CFRP flexure prism specimens experienced the most degradation in both saline water and sun light environments. Thus, it could be deduced that the bond strength of the CFRP strengthening system degraded the most. However, the SME specimens experienced a lower bond strength degradation in saline water environment and a similar degradation in sun light environment, when compared to CFRP

specimens, as shown in Figures 46 and 47. Although the least amount of degradation was experienced by SMM specimens, but it attained the lowest bond strength out of the three strengthening systems.

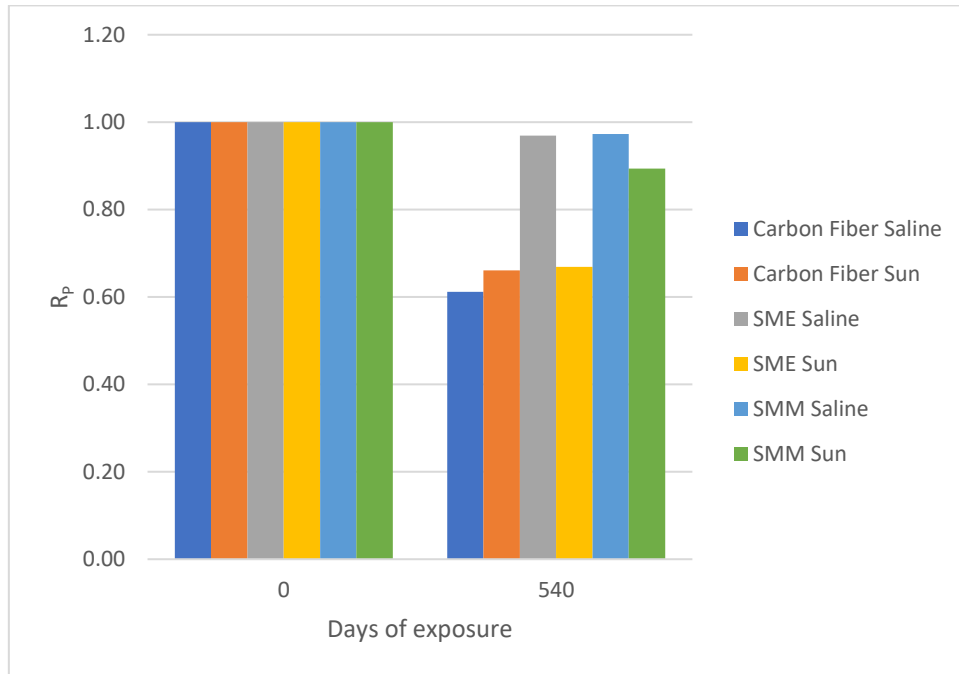


Figure 46: Bar graph of flexure prism R_P degradation model

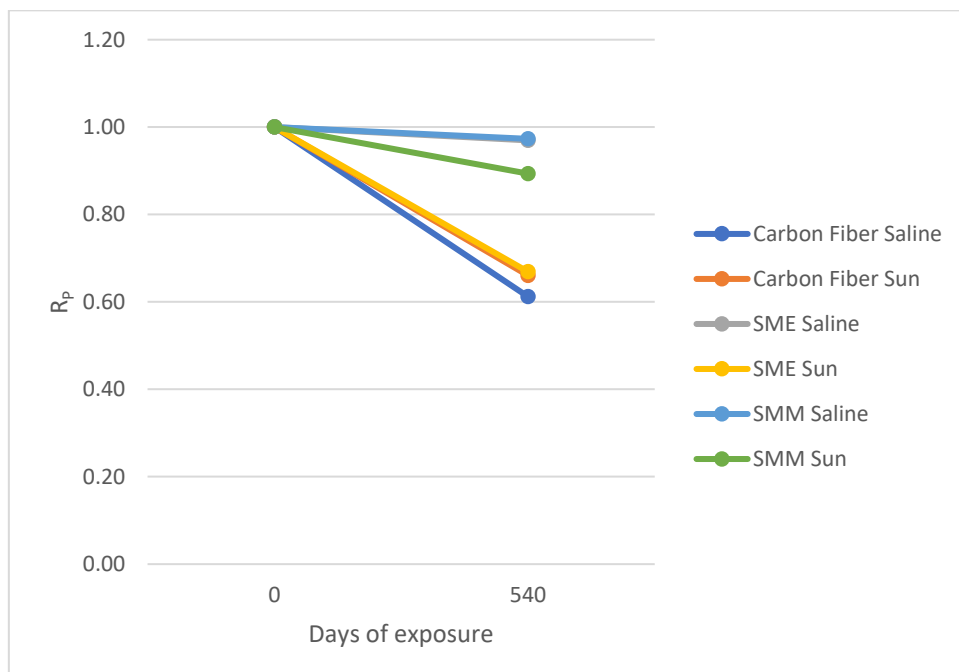


Figure 47: Line chart of flexure prism R_P degradation model

Almost all CFRP and SME specimens had an adhesive failure mode, such that the strengthening system debonded from the concrete surface in a clean manner without breaking the concrete aggregates while debonding. however, SMM specimens broke completely because of an oxidation action that occurs in the galvanized steel cords. The oxidation of these cords in SMM specimens occurred due to the mortar's high porosity that allowed the saline water to interact with the galvanized steel cords, as shown in Table 27.

Table 27: Flexure prisms failure mode

| Specimen | Failure mode | |
|----------------------------|---|---|
| CFRP “Adhesive failure” |  |  |
| SMM “Adhesive failure” |  |  |
| SME “Adhesive failure” |  |  |

4.6. Coupon Results

In this section, the coupon degradation report summary is presented in Table 28, which summarizes the use of coupon retention ratio (R_c). Moreover, Figure 48 and 49 show the results of all specimens' average degradation ratio for R_c model. Consequently, carbon fiber strengthened specimens retained 96% of its strength after 360 days of saline exposure, while it retained 94% of its strength after 360 days of sun exposure. SME strengthened specimens retained 74% of its strength after 360 days of saline exposure, while it retained 78% of its strength after 360 days of sun exposure. While, SMM strengthened specimens retained 97% of its strength after 360 days of saline exposure, while it retained 102% of its strength after 360 days of sun exposure.

Table 28: Coupon degradation summary

| Time Period | Exposure | Strengthening system | Designation | Tensile Strength (kN) | E | Unit | R_c |
|-------------|----------|-------------------------------|-------------|-----------------------|-------|---------|-------|
| 28 days | Lab | Carbon Fiber | C28L-1 | 31.00 | 69.6 | GPa | - |
| | | | C28L-2 | 32.40 | 72.36 | GPa | - |
| | | | Average | 31.70 | 70.98 | GPa | - |
| | | Steel mesh bonded with Epoxy | SME28L-1 | 12.20 | 29.08 | GPa | - |
| | | | SME28L-2 | 11.50 | 28.45 | GPa | - |
| | | | Average | 11.85 | 28.76 | GPa | - |
| | | Steel mesh bonded with Mortar | SMM28L-1 | 14.20 | 14.2 | kN/cord | - |
| | | | SMM28L-2 | 14.70 | 14.70 | kN/cord | - |
| | | | Average | 14.45 | 14.45 | kN/cord | - |
| 6 Months | Saline | Carbon Fiber | C180W-1 | 30.3 | 69.70 | GPa | 0.98 |
| | | | C180W-2 | 31.2 | 69.00 | GPa | 0.97 |
| | | | Average | 30.75 | 69.35 | GPa | 0.98 |
| | | Steel mesh bonded with Epoxy | SME180W-1 | 11.2 | 28.58 | GPa | 0.99 |
| | | | SME180W-2 | 10.8 | 22.00 | GPa | 0.76 |
| | | | Average | 11 | 25.29 | GPa | 0.88 |
| | | Steel mesh bonded with Mortar | SMM180W-1 | 14.5 | 14.48 | kN/cord | 1.00 |
| | | | SMM180W-2 | 14.7 | 14.65 | kN/cord | 1.01 |
| | | | Average | 14.6 | 14.56 | kN/cord | 1.01 |

Table 28 Continued: Coupon degradation summary

| Time Period | Exposure | Strengthening system | Designation | Tensile Strength (kN) | E | Unit | Rc |
|-------------------------------|-----------|-------------------------------|-------------|-----------------------|-------|---------|------|
| 6 Months | Sun | Carbon Fiber | C180S-1 | 28.3 | 69.36 | GPa | 0.98 |
| | | | C180S-2 | 30.60 | 71.90 | GPa | 1.01 |
| | | | Average | 29.45 | 70.63 | GPa | 1.00 |
| | | Steel mesh bonded with Epoxy | SME180S-1 | 11.80 | 29.78 | GPa | 1.04 |
| | | | SME180S-2 | 12.10 | 21.35 | GPa | 0.74 |
| | | | Average | 11.95 | 25.56 | GPa | 0.89 |
| | | Steel mesh bonded with Mortar | SMM180S-1 | 15.10 | 15.14 | kN/cord | 1.05 |
| | | | SMM180S-2 | 15.20 | 15.24 | kN/cord | 1.05 |
| | | | Average | 15.15 | 15.19 | kN/cord | 1.05 |
| 12 Months | Saline | Carbon Fiber | C360W-1 | 27.66 | 65.82 | GPa | 0.93 |
| | | | C360W-2 | 29.55 | 70.33 | GPa | 0.99 |
| | | | Average | 28.60 | 68.07 | GPa | 0.96 |
| | | Steel mesh bonded with Epoxy | SME360W-1 | 8.03 | 19.10 | GPa | 0.66 |
| | | | SME360W-2 | 9.96 | 23.70 | GPa | 0.82 |
| | | | Average | 8.99 | 21.40 | GPa | 0.74 |
| | | Steel mesh bonded with Mortar | SMM360W-1 | 14.21 | 14.21 | kN/cord | 0.98 |
| | | | SMM360W-2 | 13.75 | 13.75 | kN/cord | 0.95 |
| | | | Average | 13.98 | 13.98 | kN/cord | 0.97 |
| | Sun | Carbon Fiber | C360S-1 | 28.83 | 68.62 | GPa | 0.97 |
| | | | C360S-2 | 26.99 | 64.23 | GPa | 0.90 |
| | | | Average | 27.91 | 66.42 | GPa | 0.94 |
| | | Steel mesh bonded with Epoxy | SME360S-1 | 8.12 | 19.32 | GPa | 0.67 |
| | | | SME360S-2 | 10.81 | 25.73 | GPa | 0.89 |
| | | | Average | 9.46 | 22.52 | GPa | 0.78 |
| Steel mesh bonded with Mortar | SMM360S-1 | 14.97 | 14.97 | kN/cord | 1.04 | | |
| | SMM360S-2 | 14.44 | 14.44 | kN/cord | 1.00 | | |
| | Average | 14.71 | 14.70 | kN/cord | 1.02 | | |

The CFRP and SMM coupon specimens almost experienced no degradation in both saline water and sun light environments. Thus, it can be deduced that the material of both strengthening systems experienced little to no degradation. However, the SME coupon specimens experienced degradation, which means that the material properties of this strengthening system have degraded in both environments, as shown in Figures 48 and 49.

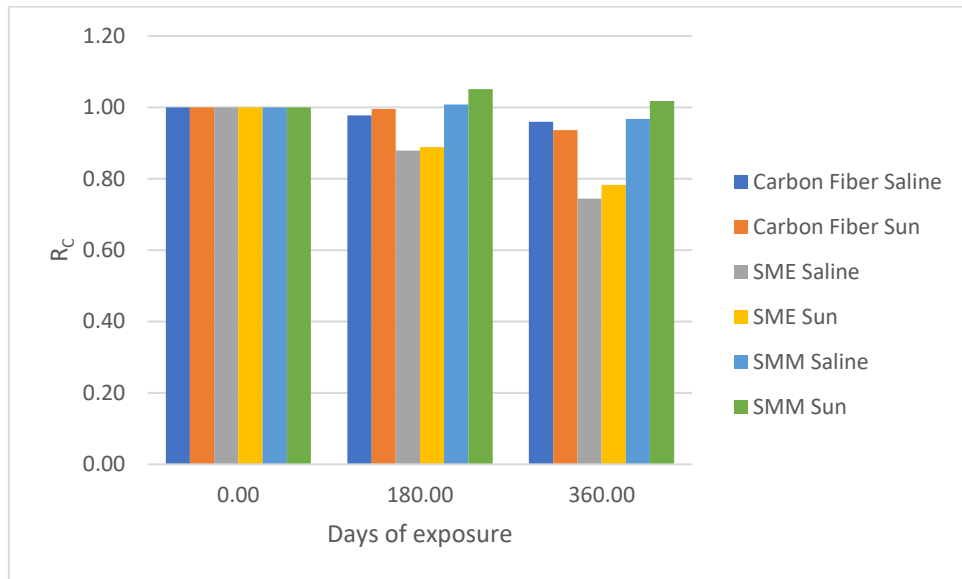


Figure 48: Bar graph of coupon R_C degradation model

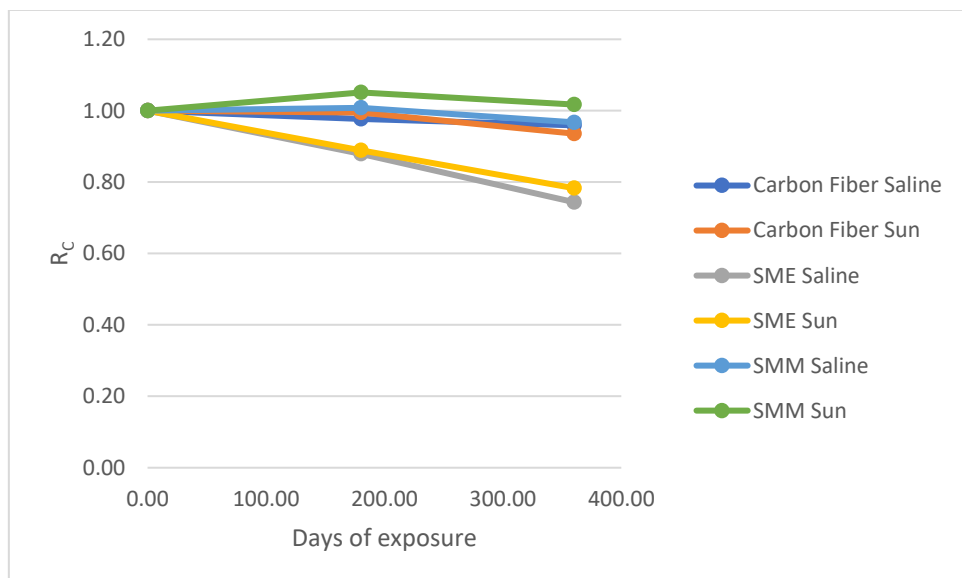








Figure 49: Line chart of coupon R_C degradation model

The SME and CFRP coupons failed at almost one-third of their length, which was highly expected. However, due to the large scale of the SMM coupons obtained from the manufacturer, the SMM coupons failed due to the individual tearing of the steel galvanized cords, as shown in Table 29.

Table 29: Coupons failure mode

| Specimen | Failure mode | |
|----------|---|---|
| CFRP |  |  |
| SMM |  |  |
| SME |  |  |

4.7. Pullout Results

In this section the pullout degradation report summary is presented in Table 30, which summarizes the use of coupon retention ratio (R_{PO}). Moreover, Figures 50 and 51 show the results of all specimens' average degradation ratio for R_{PO} model. Consequently, carbon fiber strengthened specimens retained 113% of its strength after 360 days of saline exposure, while it retained 115% of its strength after 360 days of sun exposure. SME strengthened specimens retained 114% of its strength after 360 days of saline exposure, while it retained 108% of its strength after 360 days of sun exposure. While, SMM strengthened specimens retained 138% of its strength after 360 days of saline exposure, while it retained 151% of its strength after 360 days of sun exposure.

Table 30: Pullout degradation summary

| Time Period | Exposure | Strengthening system | Designation | Pu (kN) | Bond Shear Stress (MPa) | Rpo |
|-------------------------------|-----------|-------------------------------|-------------|--------------|-------------------------|-------|
| 28 days | Lab | Carbon Fiber | C28L-1 | 18.20 | 1.94 | 1.00 |
| | | | C28L-2 | 16.83 | 1.80 | 1.00 |
| | | | Average | 17.52 | 1.87 | 1.00 |
| | | Steel mesh bonded with Epoxy | SME28L-1 | 15.88 | 1.69 | 1.00 |
| | | | SME28L-2 | 12.84 | 1.37 | 1.00 |
| | | | Average | 14.36 | 1.53 | 1.00 |
| | | Steel mesh bonded with Mortar | SMM28L-1 | 4.08 | 0.44 | 1.00 |
| | | | SMM28L-2 | 5.34 | 0.57 | 1.00 |
| | | | Average | 4.71 | 0.5 | 1.00 |
| | | 6 Months | Saline | Carbon Fiber | C180W-1 | 20.36 |
| C180W-2 | 16.63 | | | | 1.77 | 0.95 |
| Average | 18.5 | | | | 1.97 | 1.06 |
| Steel mesh bonded with Epoxy | SME180W-1 | | | 12.09 | 1.29 | 0.84 |
| | SME180W-2 | | | 18.00 | 1.92 | 1.25 |
| | Average | | | 15.05 | 1.6 | 1.05 |
| Steel mesh bonded with Mortar | SMM180W-1 | | | 6.63 | 0.71 | 1.41 |
| | SMM180W-2 | | | 6.42 | 0.68 | 1.36 |
| | Average | | | 6.53 | 0.7 | 1.39 |

Table 30 Continued: Pullout degradation summary

| Time Period | Exposure | Strengthening system | Designation | Pu (kN) | Bond Shear Stress (MPa) | Rpo |
|-------------|----------|-------------------------------|-------------|---------|-------------------------|------|
| 6 Months | Sun | Carbon Fiber | C180S-1 | 16.20 | 1.73 | 0.92 |
| | | | C180S-2 | 21.00 | 2.24 | 1.20 |
| | | | Average | 18.6 | 1.98 | 1.06 |
| | | Steel mesh bonded with Epoxy | SME180S-1 | 14.58 | 1.56 | 1.02 |
| | | | SME180S-2 | 16.87 | 1.80 | 1.17 |
| | | | Average | 15.73 | 1.68 | 1.10 |
| | | Steel mesh bonded with Mortar | SMM180S-1 | 4.73 | 0.5 | 1.00 |
| | | | SMM180S-2 | 4.16 | 0.44 | 0.88 |
| | | | Average | 4.45 | 0.47 | 0.94 |
| 12 Months | Saline | Carbon Fiber | C360W-1 | 20.34 | 2.17 | 1.16 |
| | | | C360W-2 | 19.24 | 2.05 | 1.10 |
| | | | Average | 19.79 | 2.11 | 1.13 |
| | | Steel mesh bonded with Epoxy | SME360W-1 | 16.5 | 1.76 | 1.15 |
| | | | SME360W-2 | 16.31 | 1.74 | 1.14 |
| | | | Average | 16.41 | 1.75 | 1.14 |
| | | Steel mesh bonded with Mortar | SMM360W-1 | 6.21 | 0.66 | 1.32 |
| | | | SMM360W-2 | 6.82 | 0.73 | 1.45 |
| | | | Average | 6.52 | 0.69 | 1.38 |
| | Sun | Carbon Fiber | C360S-1 | 20.51 | 2.19 | 1.17 |
| | | | C360S-2 | 19.65 | 2.1 | 1.12 |
| | | | Average | 20.08 | 2.14 | 1.15 |
| | | Steel mesh bonded with Epoxy | SME360S-1 | 14.65 | 1.56 | 1.02 |
| | | | SME360S-2 | 16.31 | 1.74 | 1.14 |
| | | | Average | 15.48 | 1.65 | 1.08 |
| | | Steel mesh bonded with Mortar | SMM360S-1 | 6.63 | 0.71 | 1.41 |
| | | | SMM360S-2 | 7.63 | 0.81 | 1.62 |
| | | | Average | 7.13 | 0.76 | 1.51 |

Almost all pullout specimens did not experience degradation in both exposures, saline water, and sun light environments, as shown in Figures 50 and 51. However, the SMM specimens failed at much lower ultimate load when compared with CFRP and

SME specimens. Thus, it can be deduced that the SMM system has the weakest bond strength when compared with CFRP and SME systems.

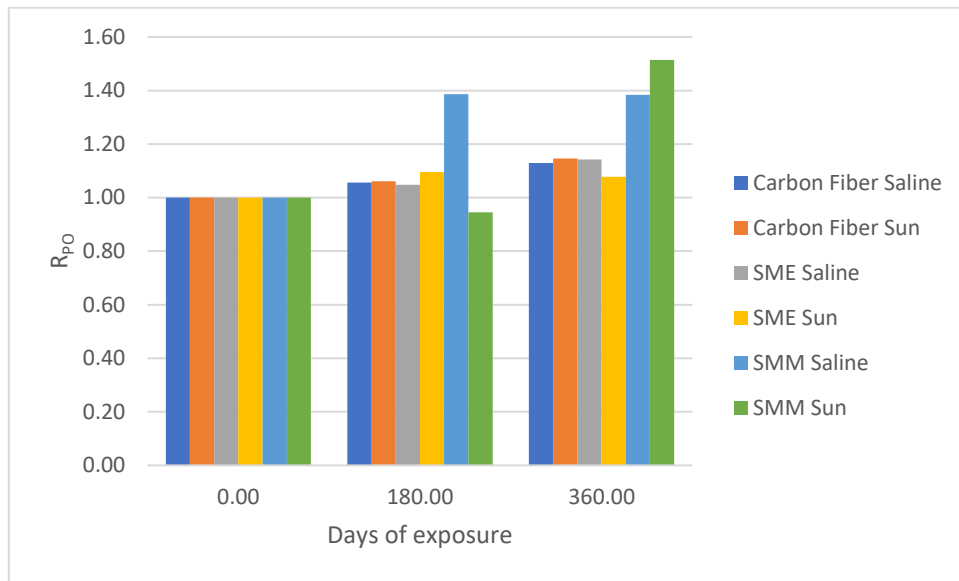


Figure 50: Bar graph of pullout R_{PO} degradation model

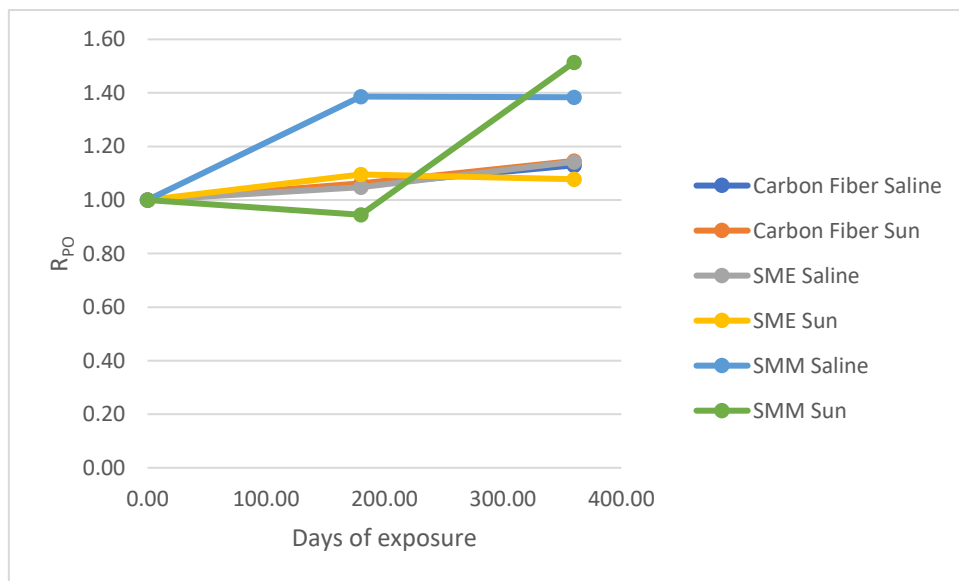








Figure 51: Line chart of pullout R_{PO} degradation model

The SMM and CFRP specimens experienced an adhesive debonding failure. However, the SME specimens experienced a cohesive failure, where the system detached from the substrate while breaking some of the concrete surfaces, as shown in Table 31.

Table 31: Pullout failure mode

| Specimen | Failure mode | |
|------------------------------------|---|--|
| <p>CFRP “Adhesive failure”</p> |  |  |
| <p>SMM “Adhesive failure”</p> |  |  |
| <p>SME “Cohesive failure”</p> |  |  |

4.8. Proposed Environmental Factor for U.A.E. Harsh Environments

Table 32 shows the comparable environmental effect between all the tests conducted for each strengthening system, and in both environments, saline and sun exposures.

Table 32: Summary of the specimen's environmental factor

| | Strengthening System | Saline Water (C_E) | Sun Light (C_E) |
|---------------------------------|-----------------------------|-------------------------------------|----------------------------------|
| ACI440.2R-17 | Carbon Fiber | 0.85 | 0.85 |
| RC Beams | Carbon Fiber | 0.75 | 0.90 |
| | GSM bonded with epoxy | 0.99 | 0.97 |
| | GSM bonded with mortar | 0.71 | 0.62 |
| Coupons | Carbon Fiber | 0.96 | 0.94 |
| | GSM bonded with epoxy | 0.74 | 0.78 |
| | GSM bonded with mortar | 0.97 | 1.00 |
| Flexure Prism | Carbon Fiber | 0.61 | 0.66 |
| | GSM bonded with epoxy | 0.97 | 0.67 |
| | GSM bonded with mortar | 0.97 | 0.89 |
| Pullout Single-Lap Shear | Carbon Fiber | 1.00 | 1.00 |
| | GSM bonded with epoxy | 1.00 | 1.00 |
| | GSM bonded with mortar | 1.00 | 1.00 |

However, to compute the flexural strength for externally strengthened members as previously illustrated in Equation (12) for such composite materials, the environmental factors (C_E) in both saline water and direct sun light exposures in the UAE are provided in Table 33.

Table 33: Recommended environmental factor (CE) in the UAE

| | Strengthening System | Saline Water (C_E) | Sun Light (C_E) |
|--------------------|-----------------------------|-------------------------------------|----------------------------------|
| Recommended | Carbon Fiber | 0.75 | 0.90 |
| | GSM bonded with epoxy | 0.95 | 0.95 |
| | GSM bonded with mortar | 0.70 | 0.60 |

Chapter 5: Summary and Conclusion

Strengthening RC structures has been the major interest in recent researches. Thus, causing the development of new strengthening materials other than CFRP, such as GSM sheets that could be bonded with both cement mortar or epoxy adhesive. The objective of this research is to study the behavior CFRP and GSM strengthened concrete specimens when exposed to harsh environments in the U.A.E., such as saline water and direct sun light. Accordingly, a total of 40 RC beams, 30 coupons, and 30 pull-out specimens have been tested on three-time intervals, before exposure, after 180 days of exposure, and finally after 360 days of exposure, while 16 flexure prisms were tested after 28 days and 540 days. The test results of the specimens have been analyzed to develop an environmental factor for the U.A.E different harsh environment, which showed that the SME strengthening system experienced the least degradation and exhibited the largest ultimate load-carrying capacity.

Based on the obtained results the following conclusion and observations may be drawn:

- The average load carrying capacity of carbon fiber strengthened RC beams has increased by 47% after 28 days of curing, which is indicated by the LSR ratio.
- The average load carrying capacity of SME strengthened RC beams has increased by 55% after 28 days of curing, which is indicated by the LSR ratio.
- The average load carrying capacity of SMM strengthened RC beams has increased by 50% after 28 days of curing, which is indicated by the LSR ratio.
- Carbon fiber strengthened RC beams were able to retain more strength while exposed to direct sun light (90%), when compared to RC beams with similar strengthening system and exposed to saline water (75%).
- GSM sheets bonded with epoxy was the most efficient strengthening system utilized on RC beams, since it was able to retain most of its strength when exposed to both environments, saline water (99%) and sun light (97%).
- GSM sheet bonded with mortar was the least efficient strengthening system utilized on RC beams, since it was able to retain only 71% of its load carrying capacity when exposed to saline water, and that phenomena could be explained

by the porosity of mortar that is used as a bonding agent, which allowed the saline water to reach the GSM sheets.

- GSM sheet bonded with mortar was the least efficient strengthening system utilized on RC beams, since it was able to retain only 62% of its load carrying capacity when exposed to direct sun light, and that phenomena could be explained by the developing of micro cracks in mortar substrate that is used as a bonding agent, which tremendously decreased the bond strength of this strengthening system.
- Although SMM flexure prisms experienced the least degradation after 540 days, but it also exhibited the least ultimate load-carrying capacity.
- Almost no degradation was noticed in pullout specimens. However, SMM specimens experienced a lower failure load when compared with CFRP and SME specimens. Therefore, the SMM system has the weakest bond strength when compared with CFRP and SME systems.
- Although the SME RC beams retained most of its strength, the SME mechanical properties of this strengthening system have degraded in both environments.
- The recommended environmental factor for CFRP in saline water exposure and sun light exposure is 0.75 and 0.90 respectively.
- The recommended environmental factor for SME in saline water exposure and sun light exposure is 0.95 and 0.95 respectively.
- The recommended environmental factor for SME in saline water exposure and sun light exposure is 0.70 and 0.60 respectively.

Further investigation could be done to observe the development of micro-cracks in the interface and to further investigate the mortar's porosity issue throughout the exposure period. A more detailed study should be conducted to study the behavior of GSM sheets bonded with mortar over shorter time periods

References

- [1] M.A. Aiello, M. Frigione, and D. Acierno, "Effects of environmental conditions on performance of polymeric adhesives for restoration of concrete structures." *Journal of Materials in Civil Engineering*, vol. 14, no. 2, pp. 185-189, 2002.
- [2] J. Abdalla, F. Hraib, R. Hawileh and A. Mirghani, "Experimental investigation of bond-slip behavior of aluminum plates adhesively bonded to concrete", *Journal of Adhesion Science and Technology*, vol. 31, no. 1, pp. 82-99, 2016.
- [3] J.A. Abdalla, A. Abu-Obeidah and R. A.Hawileh, R. A. "Behaviour of Shear Deficient Reinforced Concrete Beams with Externally Bonded Aluminum Alloy Plates." in *2011 Int. Conf. World Congress on Advances in Structural Engineering and Mechanics (ASEM)*, September 2011, pp. 18-23.
- [4] W. Nawaz, R. Hawileh, E.I. Saqan, and J.A. Abdalla, "Effect of Longitudinal CFRP Plates on the Shear Strength of RC Beams." *ACI Structural Journal, American Concrete Institute*, vol. 113, no. 3, pp. 577-586, 2016.
- [5] Teng J., Smith S., Yao J., and Chen J., "Intermediate crack-induced debonding in RC beams and slabs," *Construction and Building Materials*, vol. 17, pp. 357–62, 2003.
- [6] Qeshta, I.M.I., Shafigh, P., and Jumaat, M.Z., "Flexural behaviour of RC beams strengthened with wire mesh-epoxy." *Construction and Building Materials*, vol. 79, pp. 104-114, 2015.
- [7] R. Hawileh, J. Abdalla, and M. Naser, "Modeling the Shear Strength of Concrete Beams Reinforced with CFRP Bars under Unsymmetrical Loading." *Mechanics of Advanced Materials and Structures*, pp. 1-8, 2018.
- [8] H. Rasheed, J. Abdalla, R. Hawileh, and A. Al-Tamimi, "Flexural Behavior of Reinforced Concrete Beams Strengthened with Externally Bonded Aluminum Alloy Plates." *Engineering Structures, Elsevier*, vol. 147, no. 15, pp. 473-485, 2017.
- [9] E. Karam, R. Hawileh, T.A. El-Maaddawy and J.A. Abdalla, "Experimental Investigations of Repair of pre-damaged steel-concrete composite beams using CFRP laminates and mechanical anchors" *Thin-Walled Structures, Elsevier*, Vol. 112, pp. 107-117, 2017.
- [10] J. Abdalla, A. Abu-Obeidah, R. Hawileh and H. Rasheed, "Shear strengthening of reinforced concrete beams using externally-bonded aluminum alloy plates: An experimental study", *Construction and Building Materials*, vol. 128, pp. 24-37, 2016.
- [11] S. Smith and J. Teng, "FRP-strengthened RC beams. I: review of debonding strength models", *Engineering Structures*, vol. 24, no. 4, pp. 385-395, 2002.
- [12] A. Al-Tamimi, R. Hawileh, J. Abdalla, H. Rasheed and R. Al-Mahaidi, "Durability of the Bond between CFRP Plates and Concrete Exposed to Harsh Environments", *Journal of Materials in Civil Engineering*, vol. 27, no. 9, pp. 42-52, 2015.
- [13] L. De Lorenzis and J. Teng, "Near-surface mounted FRP reinforcement: An emerging technique for strengthening structures", *Composites Part B: Engineering*, vol. 38, no. 2, pp. 119-143, 2007.

- [14] R. Hawileh, A. Al Tamimi and J.A. Abdalla, "Influence of bond length on FRP concrete shear strength," in *2010 Int. Conf. Application of Traditional and High Performance Materials in Harsh Environments (4th IMS)*, March 2010, pp. 1-5.
- [15] J.A. Abdalla, R.A. Hawileh, W. Nawaz, A. Mohammed, "Reinforced concrete beams externally strengthened in flexure using hybrid systems," in *2018 Science and Engineering Technology Int. Conf. (ASET)*, April 2018.
- [16] A.S.D. Salama, R.A. Hawileh, J.A. Abdalla. "Performance of externally strengthened RC beams with side-bonded CFRP sheets," *Composite Structures* vol. 212, pp. 281-290, 2019.
- [17] R. Hawileh, A. Salama and J. Abdalla. "Strengthening of reinforced concrete beams in flexure with side-bonded CFRP laminates." In *2017 5th Int. Conf. on Durability of Fiber Reinforced Polymer (FRP) Composites for Construction and Rehabilitation of Structures (CDCC)*, July 2017, pp. 19-21.
- [18] C. Triantafillou, G. Papanicolaou, P. Zissimopoulos, and T. Laourdekis, "Concrete confinement with textile-reinforced mortar jackets." *ACI Structural Journal*, vol. 103, no. 1, pp. 28-37, 2006.
- [19] M. Naser, "Bond Behavior of CFRP Cured Laminates: Experimental and Numerical Investigation", *Journal of Engineering Materials and Technology*, vol. 134, no. 2, pp. 1-9, 2012.
- [20] R. Hawileh, T. El-Maaddawy and M. Naser, "Nonlinear finite element modeling of concrete deep beams with openings strengthened with externally-bonded composites", *Materials & Design*, vol. 42, pp. 378-387, 2012.
- [21] A. K. Al-Tamimi et al., "Effects of Ratio of CFRP Plate Length to Shear Span and End Anchorage on Flexural Behavior of SCC RC Beams," *Journal of Composites for Construction*, vol. 15, no. 6, pp. 908–919, 2011.
- [22] K. Mohamed, J. A. Abdalla, R. Hawileh, and W. Nawaz, "Using bore-epoxy anchorage to delay debonding of CFRP plates strengthened concrete beams," in *2018 First Multi Conf. on Advances in Science and Engineering Technology-Advanced Materials, Design and Manufacturing Int. Conf. (ASET)*, February 2018.
- [23] A. Mohammed, J. A. Abdalla, R. Hawileh, and W. Nawaz, "Reinforced Concrete Beams Externally Strengthened In Flexure Using Hybrid Systems," in *2018 First Multi Conf. on Advances in Science and Engineering Technology-Advanced Materials, Design and Manufacturing Int. Conf. (ASET)*, February 2018.
- [24] Y. Al-Salloum, N. Siddiqui, H. Elsanadedy, A. Abadel and M. Aqel, "Textile-Reinforced Mortar versus FRP as Strengthening Material for Seismically Deficient RC Beam-Column Joints", *Journal of Composites for Construction*, vol. 15, no. 6, pp. 920-933, 2011.
- [25] R. Hawileh, M. Naser and J. Abdalla, "Finite element simulation of reinforced concrete beams externally strengthened with short-length CFRP plates", *Composites Part B: Engineering*, vol. 45, no. 1, pp. 1722-1730, 2013.
- [26] A. Ali, J. Abdalla, R. Hawileh and K. Galal, "CFRP Mechanical Anchorage for Externally Strengthened RC Beams under Flexure", *Physics Procedia*, vol. 55, pp. 10-16, 2014.
- [27] H. Elsanadedy, T. Almusallam, S. Alsayed and Y. Al-Salloum, "Flexural strengthening of RC beams using textile reinforced mortar – Experimental and numerical study", *Composite Structures*, vol. 97, pp. 40-55, 2013.

- [28] Z. Tetta, L. Koutas and D. Bournas, "Textile-reinforced mortar (TRM) versus fiber-reinforced polymers (FRP) in shear strengthening of concrete beams", *Composites Part B: Engineering*, vol. 77, pp. 338-348, 2015.
- [29] R. Hawileh, A. Al-Tamimi, J. Abdalla and M. Wehbi, "Retrofitting Pre-Cracked RC Beams Using CFRP and Epoxy Injections", *Key Engineering Materials*, vol. 471-472, pp. 692-696, 2011.
- [30] R. Hawileh, J. Abdalla, M. Tanarlan and M. Naser, "Modeling of nonlinear cyclic response of shear-deficient RC T-beams strengthened with side bonded CFRP fabric strips", *Computers & concrete*, vol. 8, no. 2, pp. 193-206, 2011.
- [31] KeraKoll GeoSteel, Design specifications for G1200 Hardwire unidirectional ultra-high strength galvanized steel micro-cords for structural strengthening. www.kerakoll.com. 2014. [Accessed: 5-may-2019].
- [32] C. Au and O. Büyüköztürk, "Peel and Shear Fracture Characterization of Debonding in FRP Plated Concrete Affected by Moisture", *Journal of Composites for Construction*, vol. 10, no. 1, pp. 35-47, 2006.
- [33] K. A. Douier, R. Hawileh, J. A. Abdalla, and W. Nawaz, "Bond behavior of Galvanized Steel Mesh to Concrete." in *2018 First Multi Conf. on Advances in Science and Engineering Technology-Advanced Materials, Design and Manufacturing Int. Conf. (ASET)*, February 2018.
- [34] ACI Committee 440. Guide for the design and construction of externally bonded FRP systems for strengthening concrete structures (ACI 440. 2R-17). American Concrete Institute 2017, Farmington Hills, Mich, ISBN: 978-1-945487-59-0.
- [35] E. Saqan, H. Rasheed and R. Hawileh, "An efficient design procedure for flexural strengthening of RC beams based on ACI 440.2R-08", *Composites Part B: Engineering*, vol. 49, pp. 71-79, 2013.
- [36] G. Al-Bayati, R. Al-Mahaidi, M. Hashemi and R. Kalfat, "Torsional strengthening of RC beams using NSM CFRP rope and innovative adhesives", *Composite Structures*, vol. 187, pp. 190-202, 2018.
- [37] L. Wang, J. Zhang, J. Xu and Q. Han, "Anchorage systems of CFRP cables in cable structures—A review", *Construction and Building Materials*, vol. 160, pp. 82-99, 2018.
- [38] S. Tibhe and V. Rathi, "Comparative Experimental Study on Torsional Behavior of RC Beam Using CFRP and GFRP Fabric Wrapping", *Procedia Technology*, vol. 24, pp. 140-147, 2016.
- [39] M. Hosen, M. Jumaat, U. Alengaram and N. Ramli Sulong, "CFRP strips for enhancing flexural performance of RC beams by SNSM strengthening technique", *Construction and Building Materials*, vol. 165, pp. 28-44, 2018.
- [40] S. Babatunde, "Review of strengthening techniques for masonry using fiber reinforced polymers", *Composite Structures*, vol. 161, pp. 246-255, 2017.
- [41] F. Ascione, M. Lamberti, A. Napoli, G. Razaqpur and R. Realfonzo, "An experimental investigation on the bond behavior of steel reinforced polymers on concrete substrate", *Composite Structures*, vol. 181, pp. 58-72, 2017.
- [42] R. Krzywoń, M. Górski and S. Dawczyński, "Features of SRP Tapes against CFRP Composites Used for Strengthening of Concrete Structures", *Procedia Engineering*, vol. 193, pp. 289-296, 2017.
- [43] A. Napoli and R. Realfonzo, "Reinforced concrete beams strengthened with SRP/SRG systems: Experimental investigation", *Construction and Building Materials*, vol. 93, pp. 654-677, 2015.

- [44] R. Hawileh, W. Nawaz and J. Abdalla, "Flexural behavior of reinforced concrete beams externally strengthened with Hardwire Steel-Fiber sheets", *Construction and Building Materials*, vol. 172, pp. 562-573, 2018.
- [45] B. Ray and D. Rathore, "Durability and integrity studies of environmentally conditioned interfaces in fibrous polymeric composites: Critical concepts and comments", *Advances in Colloid and Interface Science*, vol. 209, pp. 68-83, 2014.
- [46] T. Nguyen, Y. Bai, X. Zhao and R. Al-Mahaidi, "Durability of steel/CFRP double strap joints exposed to sea water, cyclic temperature and humidity", *Composite Structures*, vol. 94, no. 5, pp. 1834-1845, 2012.
- [47] R. Woo, Y. Chen, H. Zhu, J. Li, J. Kim and C. Leung, "Environmental degradation of epoxy–organoclay nanocomposites due to UV exposure. Part I: Photo-degradation", *Composites Science and Technology*, vol. 67, no. 15-16, pp. 3448-3456, 2007.
- [48] T. Xu, G. Li and S. Pang, "Effects of ultraviolet radiation on morphology and thermo-mechanical properties of shape memory polymer based syntactic foam", *Composites Part A: Applied Science and Manufacturing*, vol. 42, no. 10, pp. 1525-1533, 2011.
- [49] F. Larsson, "The Effect of Ultraviolet Light on Mechanical Properties of Kevlar 49 Composites", *Journal of Reinforced Plastics and Composites*, vol. 5, no. 1, pp. 19-22, 1986.
- [50] I. Nishizaki and Y. Kato, "Durability of the adhesive bond between continuous fibre sheet reinforcements and concrete in an outdoor environment", *Construction and Building Materials*, vol. 25, no. 2, pp. 515-522, 2011.
- [51] Pizzi A, Mittal KL. *Handbook of adhesive technology*. New York: Marcel Dekker; 2003.
- [52] D. Borrie, H. Liu, X. Zhao, R. Singh Raman and Y. Bai, "Bond durability of fatigued CFRP-steel double-lap joints pre-exposed to marine environment", *Composite Structures*, vol. 131, pp. 799-809, 2015.
- [53] M. Li and H. Li, "Effects of Strain Rate on Reinforced Concrete Structure under Seismic Loading", *Advances in Structural Engineering*, vol. 15, no. 3, pp. 461-475, 2012.
- [54] A. Gartner, E. Douglas, C. Dolan and H. Hamilton, "Small Beam Bond Test Method for CFRP Composites Applied to Concrete", *Journal of Composites for Construction*, vol. 15, no. 1, pp. 52-61, 2011.
- [55] T. D'Antino, L. Sneed, C. Carloni and C. Pellegrino, "Effect of the inherent eccentricity in single-lap direct-shear tests of PBO FRCM-concrete joints", *Composite Structures*, vol. 142, pp. 117-129, 2016.
- [56] L. Sneed, T. D'Antino, C. Carloni and C. Pellegrino, "A comparison of the bond behavior of PBO-FRCM composites determined by double-lap and single-lap shear tests", *Cement and Concrete Composites*, vol. 64, pp. 37-48, 2015.
- [57] Y. Huang and B. Young, "The art of coupon tests", *Journal of Constructional Steel Research*, vol. 96, pp. 159-175, 2014.
- [58] Y. Koda, S. Minakawa and I. Iwaki, "Influence of ambient temperature and moisture conditions on fatigue resistance of concrete and RC beam", *Journal of Japan Society of Civil Engineers*, vol. 74, no. 1, pp. 35-52, 2018.
- [59] J. Tatar, C. Torrence, J. Mecholsky, C. Taylor and H. Hamilton, "Effects of silane surface functionalization on interfacial fracture energy and durability of

adhesive bond between cement paste and epoxy", *International Journal of Adhesion and Adhesives*, vol. 84, pp. 132-142, 2018.

- [60] J. Tatar, N. Brenkus, G. Subhash, C. Taylor and H. Hamilton, "Characterization of adhesive interphase between epoxy and cement paste via Raman spectroscopy and mercury intrusion porosimetry", *Cement and Concrete Composites*, vol. 88, pp. 187-199, 2018.
- [61] B. Blackburn, J. Tatar, E. Douglas and H. Hamilton, "Effects of hygrothermal conditioning on epoxy adhesives used in FRP composites", *Construction and Building Materials*, vol. 96, pp. 679-689, 2015.
- [62] A. Al-Abdwais and R. Al-Mahaidi, "Bond properties between carbon fibre reinforced polymer (CFRP) textile and concrete using modified cement-based adhesive", *Construction and Building Materials*, vol. 154, pp. 983-992, 2017.
- [63] A. Al-Abdwais and R. Al-Mahaidi, "Modified cement-based adhesive for near-surface mounted CFRP strengthening system", *Construction and Building Materials*, vol. 124, pp. 794-800, 2016.
- [64] A. Al-Abdwais, R. Al-Mahaidi and A. Al-Tamimi, "Performance of NSM CFRP strengthened concrete using modified cement-based adhesive at elevated temperature", *Construction and Building Materials*, vol. 132, pp. 296-302, 2017.
- [65] ASTM D3039 / D3039M-17, Standard Test Method for Tensile Properties of Polymer Matrix Composite Materials, ASTM International, West Conshohocken, PA, 2017.
- [66] J. Tatar and H. Hamilton, "Implementation of Bond Durability in the Design of Flexural Members with Externally Bonded FRP", *Journal of Composites for Construction*, vol. 20, no. 3, pp. 401-507, 2016.
- [67] C. Carloni, S. Verre, L. Sneed and L. Ombres, "Loading rate effect on the debonding phenomenon in fiber reinforced cementitious matrix-concrete joints", *Composites Part B: Engineering*, vol. 108, pp. 301-314, 2017.
- [68] KeraKoll GeoLite Gel. Design specifications for GeoLite Gel Epoxy mineral adhesive. www.kerakoll.com. 2014. [Accessed: 5-may-2019].
- [69] KeraKoll GeoLite. Design specifications for GeoLite geo-mortar with a crystalline geo-binder based. www.kerakoll.com. 2014. [Accessed: 5-may-2019].
- [70] Structural Technologies. TD-VWRAP-C200H. High strength carbon fiber fabric. www.structuraltechnologies.com, 2014. [Accessed: 5-may-2019].
- [71] Structural Technologies. TD-VWRAP-700. Epoxy Adhesive. www.structuraltechnologies.com, 2014. [Accessed: 5-may-2019].

Appendix

Figures 52 and 53 show the degradation models comparison of CFRP strengthened RC beams exposed to saline water.

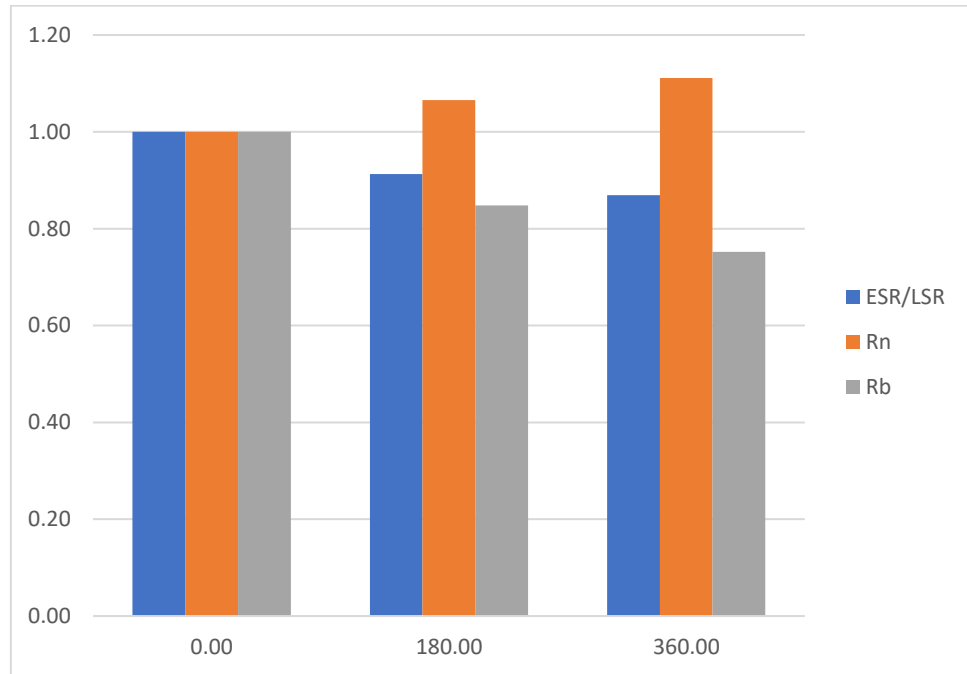


Figure 52: Bar graph of CFRP RC beams in saline exposure

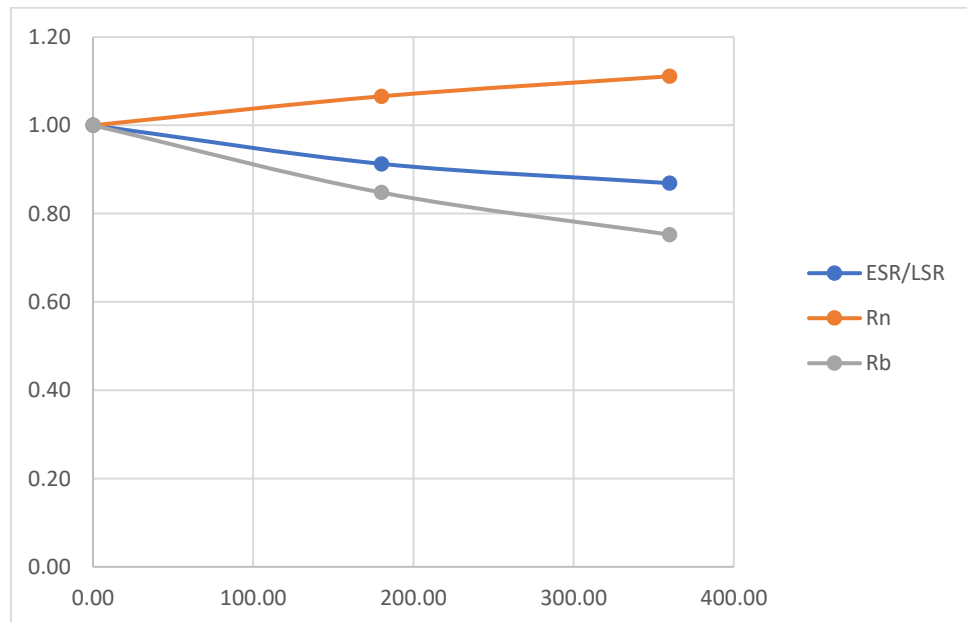


Figure 53: Line graph of CFRP RC beams in saline exposure

Figures 54 and 55 show the degradation model's comparison of CFRP strengthened RC beams exposed to direct sun light.

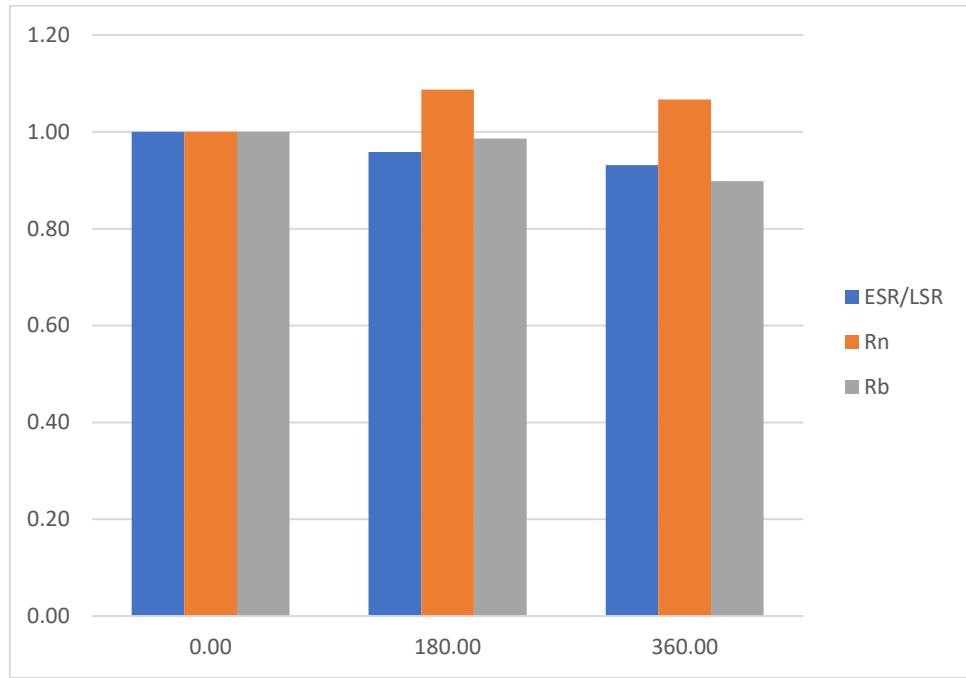


Figure 54: Bar graph of CFRP RC beams in sun exposure

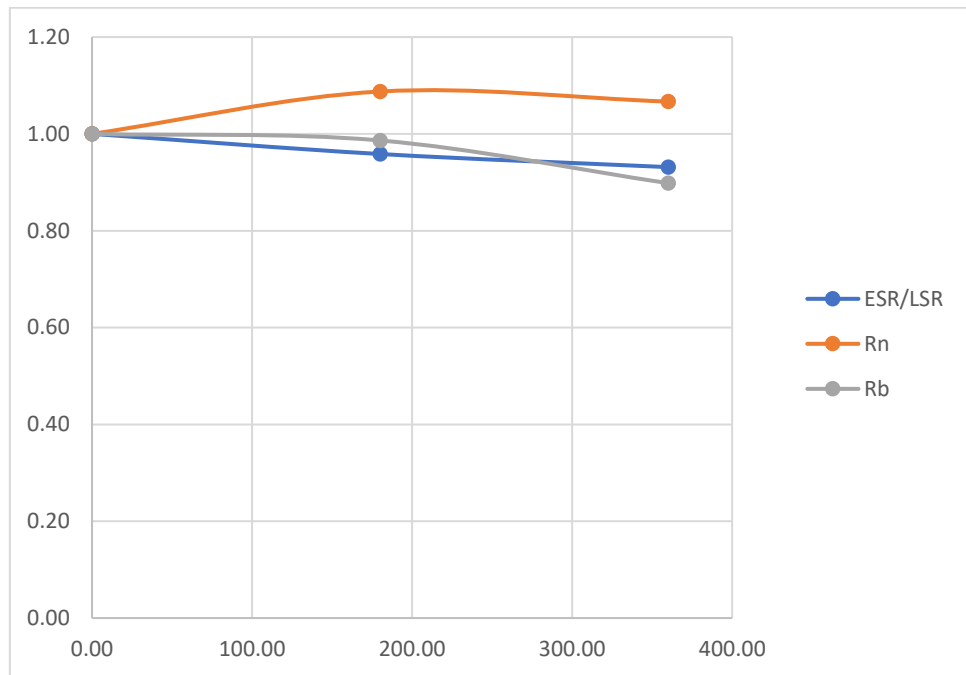


Figure 55: Line graph of CFRP RC beams in sun exposure

Figures 56 and 57 show the degradation model's comparison of SME strengthened RC beams exposed to saline water.

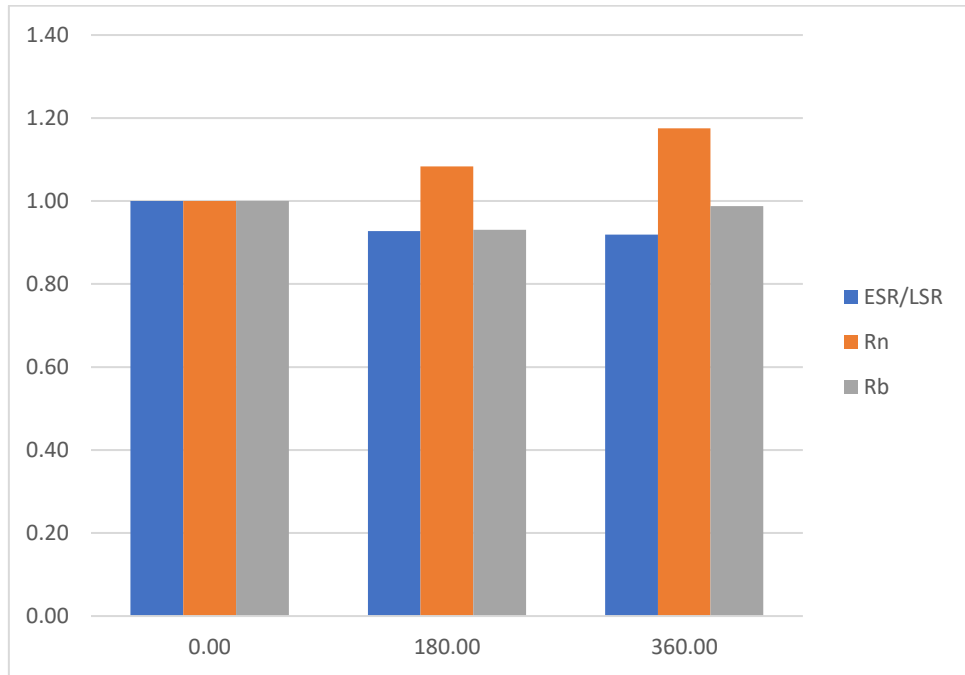


Figure 56: Bar graph of SME RC beams in saline exposure

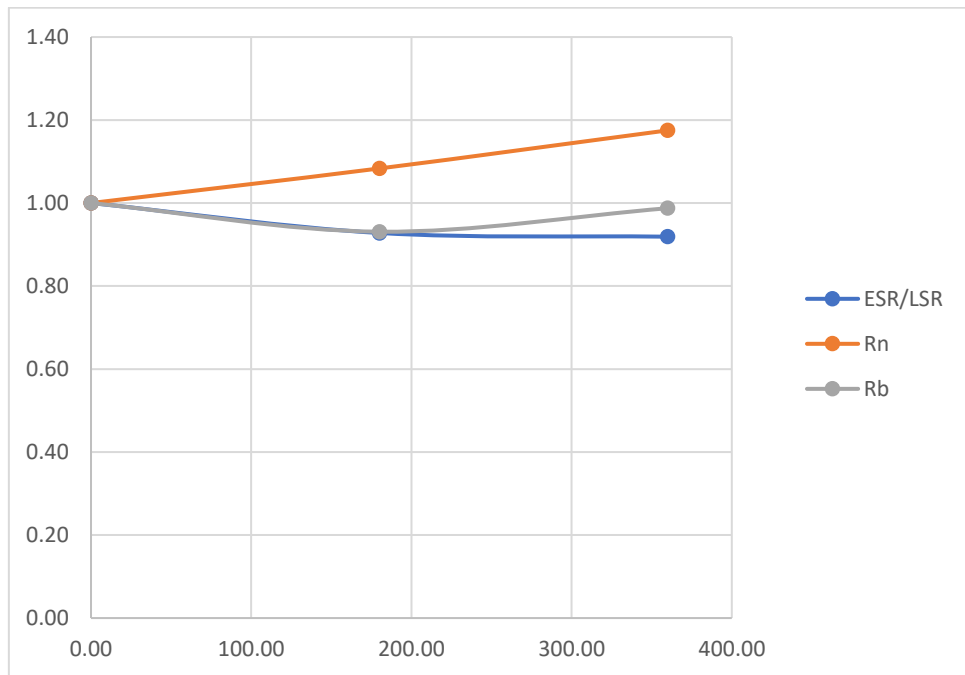


Figure 57: Line graph of SME RC beams in saline exposure

Figures 58 and 59 show the degradation model's comparison of SME strengthened RC beams exposed to direct sun light.

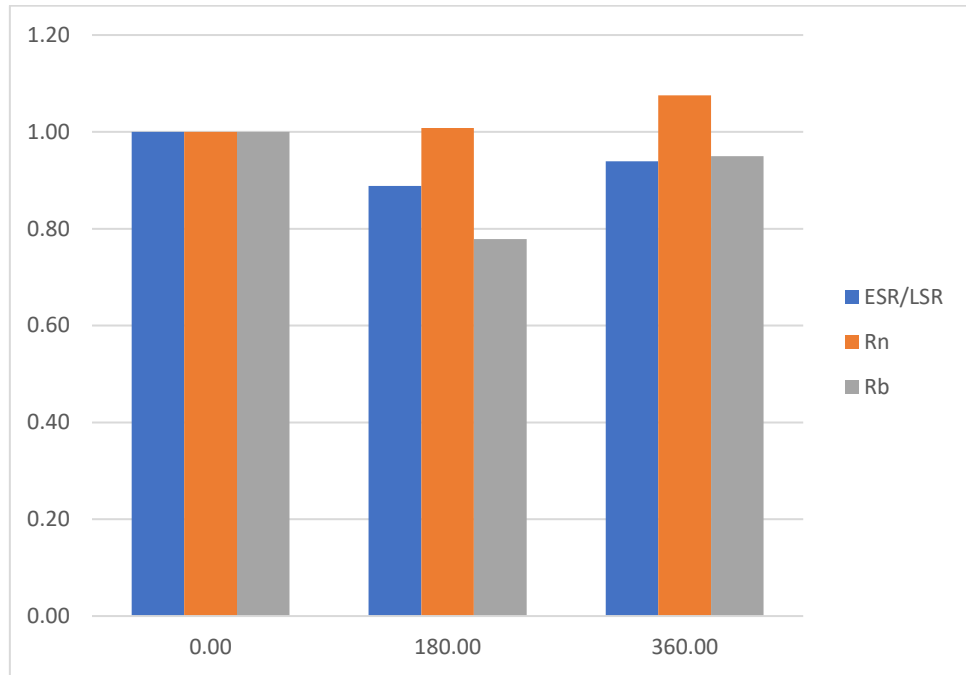


Figure 58: Bar graph of SME RC beams in sun exposure

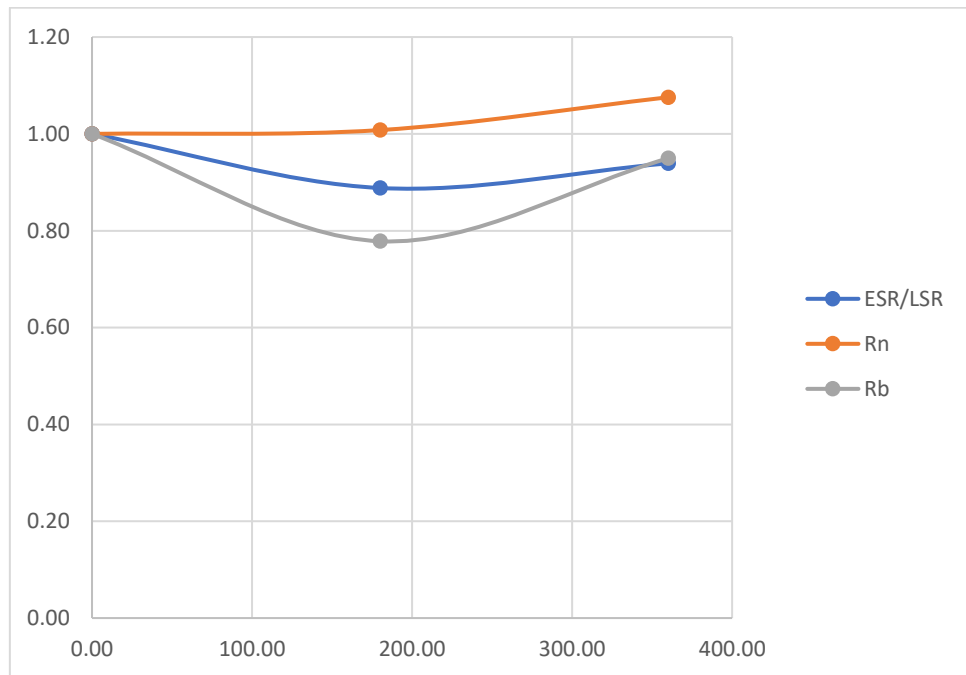


Figure 59: Line graph of SME RC beams in sun exposure

Figures 60 and 61 show the degradation model's comparison of SMM strengthened RC beams exposed to saline water.

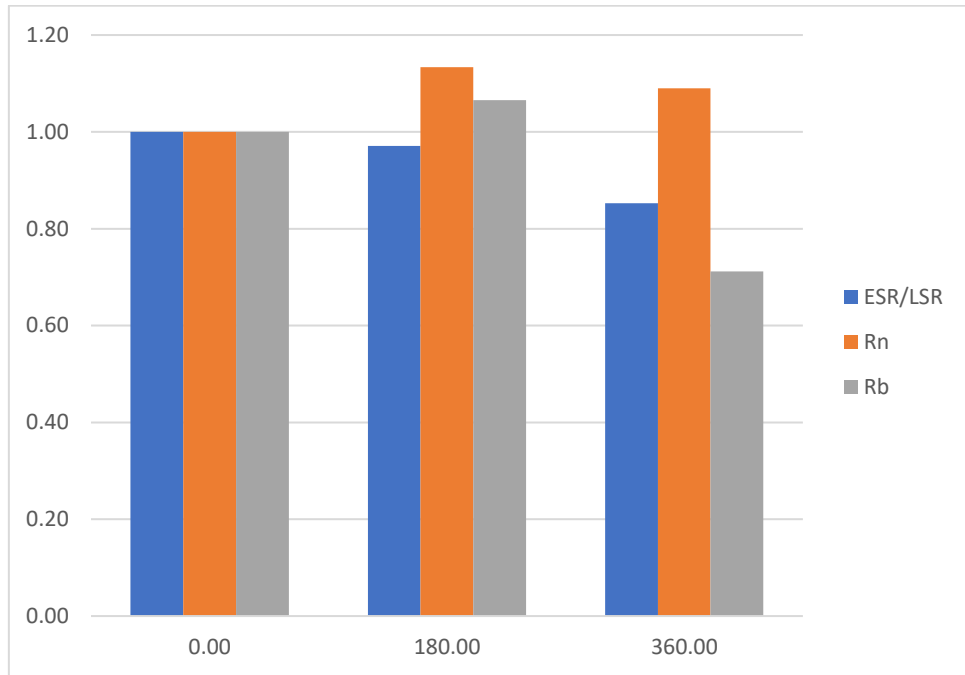


Figure 60: Bar graph of SMM RC beams in saline exposure

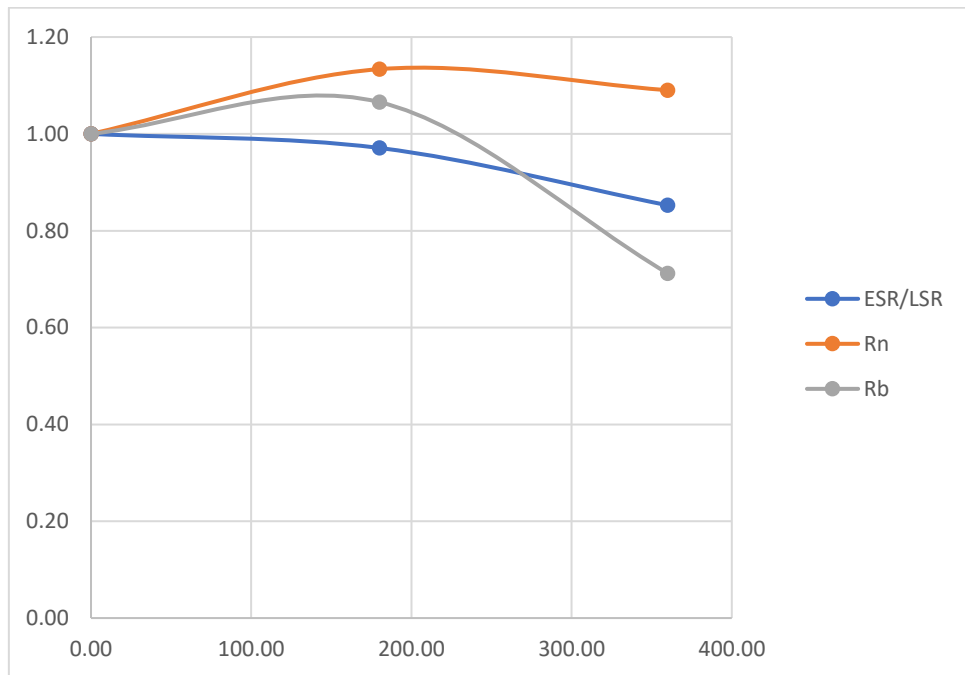


Figure 61: Line graph of SMM RC beams in saline exposure

Figures 62 and 63 show the degradation model's comparison of SMM strengthened RC beams exposed to direct sun light.

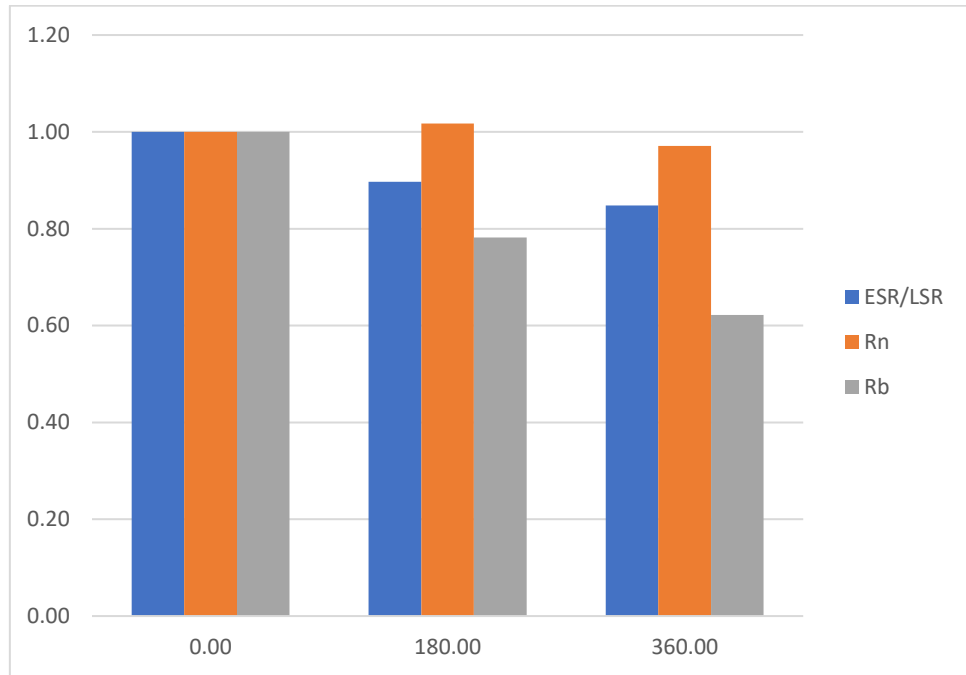


Figure 62: Bar graph of SMM RC beams in sun exposure

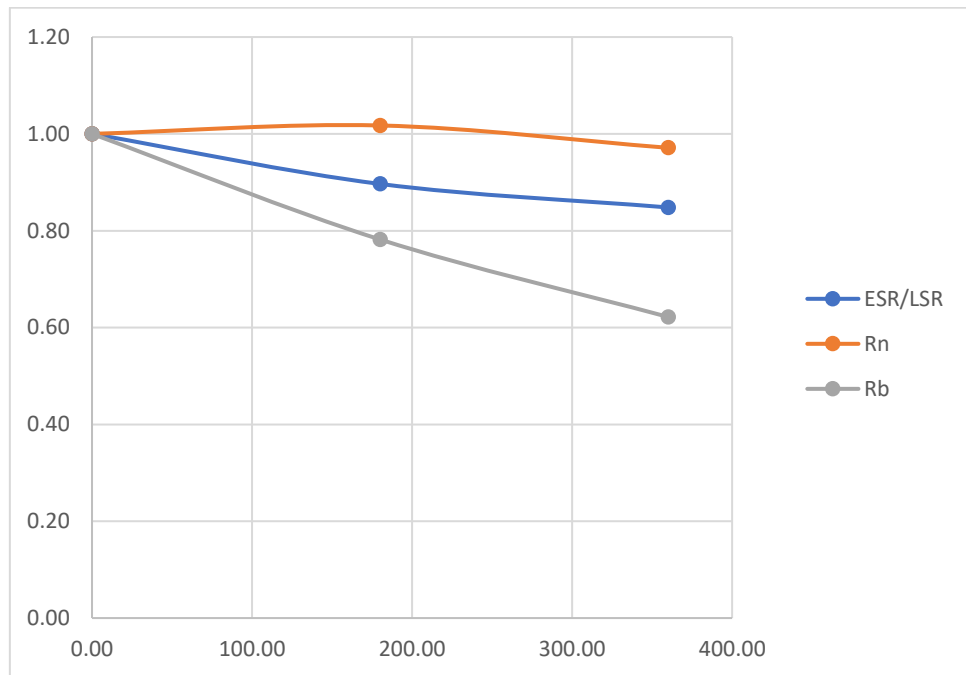


Figure 63: Line graph of SMM RC beams in sun exposure

Vita

Kais Aiman Douier was born in 1995, in Swida, Syria. He was educated in local private schools and graduated from Global Academy International. He received a Merit Scholarship to the American University of Sharjah, United Arab Emirates, from which he graduated, in 2016. His degree was a Bachelor of Science in Civil Engineering.

Kais Douier joined the Civil Engineering program in the American University of Sharjah as a graduate teaching assistant in fall of 2017. His research interests are in design, construction, and analysis of strengthening reinforced concrete structures.